AD-778 770

TECHNOLOGY DEVELOPMENT REPORT-MODEL 301 HLH/ATC CARGO HANDLING SYSTEM COUPLING

W. Nutley

Boeing Vertol Company

Prepared for:

Army Aviation Systems Command

January 1974

DISCLAIMERS

The findings in this report are not to be construed as an official Department of the Army position unless so designated by other authorized documents.

When Government drawings, specifications, or other data are used for any purpose other than in connection with a definitely related Government procurement operation, the United States Government thereby incurs no responsibility nor any obligation whatsoever; and the fact that the Government may have formulated, furnished, or in any way supplied the said drawings, specifications, or other data is not to be regarded by implication or otherwise as in any manner licensing the holder or any other person or corporation, or conveying any rights or permission, to manufacture, use, or sell any patented invention that may in any way be related thereto.

Trade names cited in this report do not constitute an official endorsement or approval of the use of such commercial hardware or software.

DISPOSITION INSTRUCTIONS

Destroy this report when no longer needed. Do not return it to the originator.

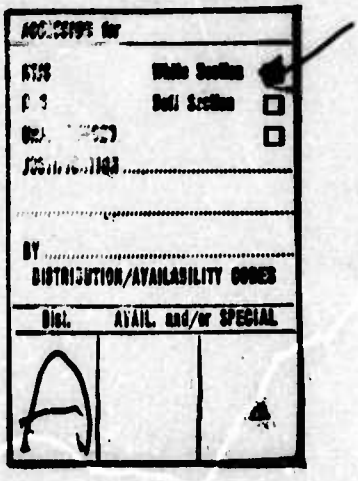

III

Unclassified

Security Classification

AD 778 770

DOCUMENT CONTROL DATA - R & D

(Security classification of title, body of abstract and indexing annotation must be entered when the overall report is classified)

1. ORIGINATING ACTIVITY (Corporate author) The Boeing Company Vertol Division Philadelphia, Pennsylvania	2a. REPORT SECURITY CLASSIFICATION Unclassisied 2b. GROUP

3. REPORT TITLE

TECHNOLOGY DEVELOPMENT REPORT - MODEL 301 HLH/ATC CARGO HANDLING SYSTEM COUPLING

4. DESCRIPTIVE NOTES (Type of report and inclusive dates)

Final Report

5. AUTHOR(S) (First name, middle initial, last name)

W. Nutley

6. REPORT DATE	7a. TOTAL NO. OF PAGES	7b. NO. OF REFS
January 1974	85	9

8a. CONTRACT OR GRANT NO.	9a. ORIGINATOR'S REPORT NUMBER(S)
DAAJ01-71-C-0840(P40) b. PROJECT NO. 1X163203D156 c. d.	USAAMRDL Technical Report 73-88 9b. OTHER REPORT NO(S) (Any other numbers that may be assigned this report) T301-10131-1

10. DISTRIBUTION STATEMENT

Approved for public release; distribution unlimited.

11. SUPPLEMENTARY NOTES	12. SPONSORING MILITARY ACTIVITY
	U. S. Army Aviation Systems Command St. Louis, Missouri

13. ABSTRACT

This report contains the results of a two-part Heavy Lift Helicopter (HLH) coupling development program. Part I was a stress analysis of photoelastic epoxy models of two HLH cargo load beam configurations. The "L" shape proved to be more efficient than the "C" shape in minimizing the weight of the coupling; and high-strength steel proved to be a more efficient material for this application than titanium. In Part II, a complete load beam was instrumented and tested in order to evaluate stress levels through ultimate failure. During testing, the load beam met the limit load requirement, but ultimate failure was premature due to the brittle nature of the material. Corrective measures, including more stringent material specifications and processes and redesign of the load beam trunnion, were recommended to overcome the discrepancy. Part III contains the results of the ultimate test on the improved load beam.

I

DD FORM 1 NOV 68 1473 REPLACES DD FORM 1473, 1 JAN 64, WHICH IS OBSOLETE FOR ARMY USE.

Unclassified

Security Classification

14. KEY WORDS	LINK A		LINK B		LINK C	
	ROLE	WT	ROLE	WT	ROLE	WT
Coupling						
Epoxy model						
Heavy Lift Helicopter (HLH)						
Load beam						
Photoelastic						
Ultimate test						

II

DEPARTMENT OF THE ARMY
U. S. ARMY AIR MOBILITY RESEARCH & DEVELOPMENT LABORATORY
EUSTIS DIRECTORATE
FORT EUSTIS, VIRGINIA 23604

This report was prepared by the Boeing Company, Vertol Division, under the terms of Contract DAAJ01-71-C-0840(P40). The objective of this effort was to define the design criteria and to design, fabricate, and test the load-carrying component of a large-capacity cargo coupling to obtain the optimum in materials, design configuration, and fabrication processes for use in the HLH aircraft. Analytical model testing was performed to establish the beam configuration. Full-scale hardware was tested to failure to establish physical and mechanical characteristics of the beam.

The results showed that for large-capacity couplings, an "L" beam configuration with a separate shaft in the trunnion area to minimize stress concentration is optimum for HLH applications. In addition, it is of extreme importance that close control of the material be maintained throughout all phases of manufacture and fabrication.

This directorate concurs with the conclusions presented herein.

The technical monitor for this effort was Mr. Jules A. Vichness, Heavy Lift Helicopter Project Office.

Project 1X163203D156
Contract DAAJ01-71-C-0840(P40)
USAAMRDL Technical Report 73-88
January 1974

TECHNOLOGY DEVELOPMENT REPORT - MODEL 301 HLH/ATC CARGO HANDLING SYSTEM COUPLING

T301-10131-1

by

W. Nutley

Prepared by

The Boeing Vertol Company
(A Division of The Boeing Company)
Philadelphia, Pennsylvania

for

U. S. ARMY AVIATION SYSTEMS COMMAND
ST. LOUIS, MISSOURI

iii b

SUMMARY

Photoelastic models of two HLH cargo load beam configurations were fabricated and tested to determine the most efficient geometry and to minimize the weight of the coupling load beam. Stress intensities across critical sections were evaluated for both specimens. A study of these intensities, in conjunction with an analysis, resulted in the conclusion that the "L" shape is more efficient than the "C" shape and that the high-strength steel (HT 250 KSI) is more efficient than 6Al-4V titanium for this particular application.

Based on this conclusion, the first HLH coupling load beam was designed and manufactured. The limit load requirement of the load beam (without yielding) was 140,000 pounds, and the ultimate load requirement (without rupturing) was 210,000 pounds. The beam was made from Carpenter Custom 455 stainless steel under specification AMS 5617 with the following required "longitudinal" properties: ultimate tensile strength, 220,000 psi; yield strength, 205,000 psi; percent elongation, 10% minimum; and percent reduction in area, 40% minimum.

During testing the load beam met the limit load requirement, but ultimate failure occurred at 190,000 pounds. Three tensile test specimens taken from the same forged billet as the load beam and three specimens cut from the remains of the fractured load beam all showed similar characteristics. All had satisfactory yield and ultimate strengths but showed low percentage elongation and low percentage reduction in area.

The cause of the premature failure was shown to be the brittle nature of the material. This characteristic was traced to improper forging techniques used during manufacture of the load beam. As a result of this investigation into the failure, Carpenter 455 was concluded to be an appropriate material if the correct component manufacturing procedures are followed. Several corrective measures were also recommended to guard against a repetition of the discrepancy:

a. Better material properties obtained by use of a more stringent material specification (BMS 7-213 instead of AMS 5617)

b. A separate shaft pressed into the load beam, instead of an integral trunnion

A second beam which incorporated these changes was manufactured and tested. The results were satisfactory, as the beam did not yield under limit load and ultimate failure occurred at 243,500 pounds.

TABLE OF CONTENTS

		Page
SUMMARY		iii
LIST OF ILLUSTRATIONS		vi
LIST OF TABLES		viii
LIST OF SYMBOLS		ix
INTRODUCTION		1
PART I.	TESTING AND ANALYSIS OF PHOTOELASTIC MODELS OF COUPLING	2
	Discussion	2
	Test Program	13
	Task Conclusions and Recommendations	19
PART II.	FIRST ULTIMATE TEST OF COUPLING LOAD BEAM.	28
	Discussion	28
	Test Program	33
	Task Conclusions and Recommendations	54
PART III.	SECOND ULTIMATE TEST OF COUPLING LOAD BEAM	57
	Discussion	57
	Test Program	59
	Task Conclusions and Recommendations	73
LITERATURE CITED		74
DISTRIBUTION		75

LIST OF ILLUSTRATIONS

Figure		Page
1	HLH Load Beam Coupling Model (SK301-10235)	3
2	HLH Load Beam Configuration Study (SK301-10250, Sheet 1 of 3)	7
3	HLH Load Beam Configuration Study (SK301-10250, Sheet 2 of 3)	9
4	HLH Load Beam Configuration Study (SK301-10250, Sheet 3 of 3)	11
5	Test Schematic	14
6	"L" Shaped Coupler Under 30-Pound Load	15
7	"C" Shaped Coupler Under 30-Pound Load	16
8	Stress Intensity Curves at a Section From Hook Throat Through Pivot Pin for "L" Shaped Load Beam Coupling Model	20
9	Stress Intensity Curves and Stress Trajectories for "L" Shaped Load Beam Coupling Model	21
10	Stress Intensity Curve at a Section From Hook Throat Through Center of Pivot Pin for "C" Shaped Load Beam Coupling Model	22
11	Stress Intensity Curves and Stress Trajectories for "C" Shaped Load Beam Coupling Model	23
12	Photoelastic Model of HLH Cargo System Hook	24
13	Photoelastic Model of HLH Cargo System Hook	25
14	Photoelastic Model of HLH Cargo System Hook	27
15	Section C-C	32
16	HLH Coupling Load Beam No. 1 and Tensile Specimens.	34
17	Strain Gage Location	36
18	Load Beam Fractures	39
19	Load Beam Fractures	40

Figure		Page
20	Load Beam Fractures	41
21	Test Specimen Load-Strain Curves for Specimens No. 1, 2 and 3	46
22	Test Specimen Load-Strain Curves for Specimens No. 4, 7 and 8	47
23	Necking Down at Failure	49
24	Load Versus Strain (Gage No. 3)	50
25	Load Versus Strain (Gage No. 4)	51
26	Load Versus Strain (Gage No. 11).	52
27	Fracture Points	53
28	Section at Trunnion	55
29	Load Beam Assembly - Second Ultimate Test . . .	60
30	Location of Load Beam and Tensile Specimens in Forged Billet - Second Ultimate Test . .	61
31	HLH Load Beam Fixture and Specimen	63
32	Load Versus Strain - Second Ultimate Test . . .	70
33	Load Beam Fracture - Second Ultimate Test . . .	71
34	Load Beam Fracture - Second Ultimate Test . . .	72

LIST OF TABLES

Table		Page
I	"L" Shaped Coupler Test Data	17
II	"C" Shaped Coupler Test Data	18
III	Mechanical Properties	30
IV	Strain Gage Reading in Microinches per Inch . . .	42
V	Results in Tensile Specimen Testing	45
VI	Comparison of Physical Properties - Specifications AMS 5617 and BMS 7-213	58
VII	Results in Tensile Specimen Testing - Second Ultimate Test	65
VIII	Strain Gage and Dial Gage Readings - Load Run to Failure	67

LIST OF SYMBOLS

C	distance from neutral axis to extreme fiber, in.
E	modulus of elasticity, psi
f_b	actual bending stress, psi
F_{t_u}	allowable ultimate tensile strength, psi
F_{t_y}	allowable tensile yield strength at .2% offset, psi
I	moment of inertia, $in.^4$
K_{iscc}	measurement of resistance to stress corrosion
K_t	stress concentration factor at a change in section or surface irregularity
M	bending moment, in.-lb
Y.T.S.	yield tensile strength
U.T.S.	ultimate tensile strength
ε	strain, in./in.
σ	stress

INTRODUCTION

Each of the dual hoists of the Heavy Lift Helicopter (HLH) cargo handling system incorporates cargo coupling devices at the lower end of paired cable systems attached to the hoists. These coupling devices, which raise and lower as required, contain load beams (also called cargo hooks) which attach to the cargo to be transported by the HLH.

This report contains the results of an evaluation of a photoelastic stress model of the load beam portion of the coupling device.

Part I describes the tests of two-dimensional plastic stress models of the cargo load beam to determine the most efficient configuration and material to be used.

Since the plastic model is only of value in the elastic stress range, a complete load beam was instrumented and tested in order to evaluate stress levels through ultimate failure. Parts II and III describe this latter portion of the program, which determined the yield and ultimate capabilities of the part and evaluated the material to be used in the final HLH design.

PART I. TESTING AND ANALYSIS OF PHOTOELASTIC MODELS OF COUPLING

DISCUSSION

Task Objectives and Approach

The primary objective was to establish a design-weight differential between an "L" shaped and a "C" shaped load beam.

The selected approach was to employ a two-dimensional photoelastic plastic modeling technique which uses a constant thickness model to provide geometric profile information.

A three-dimensional model analysis permits more complete determination of the stress distribution in the load beam; however, a two-dimensional model was felt to be adequate for this investigation since the most highly stressed plane would be on the centerline of symmetry and this could be satisfactorily represented by a flat plastic model. The overall stress distribution throughout the model would also be readily apparent.

Reviews and Trade-Offs

The throat opening and major load beam area were defined to accommodate a 2½-x-2½-x-5-inch load sling envelope.

Starting with this established area, the required pin size, and the general overall shape requirements, a layout was constructed showing various positions of the pivot pin in relation to the throat area. See Specimen Design Details.

A nominal 20-degree sling slide angle was established. That is, when the beam opened to a 20-degree slope to the horizontal, the sling would begin to move. Its minimum full open angle was established at 60 degrees and the maximum at 90 degrees.

Specimen Selection

The transparent photoelastic model is made of elastic material and must have contours geometrically similar to those of the member in which the stress field is desired. Since the representation required was at the centerline of symmetry of both types of beams, full-scale models at these planes were manufactured from 1/4-inch-thick plastic. The geometry of both models is shown on Figure 1.

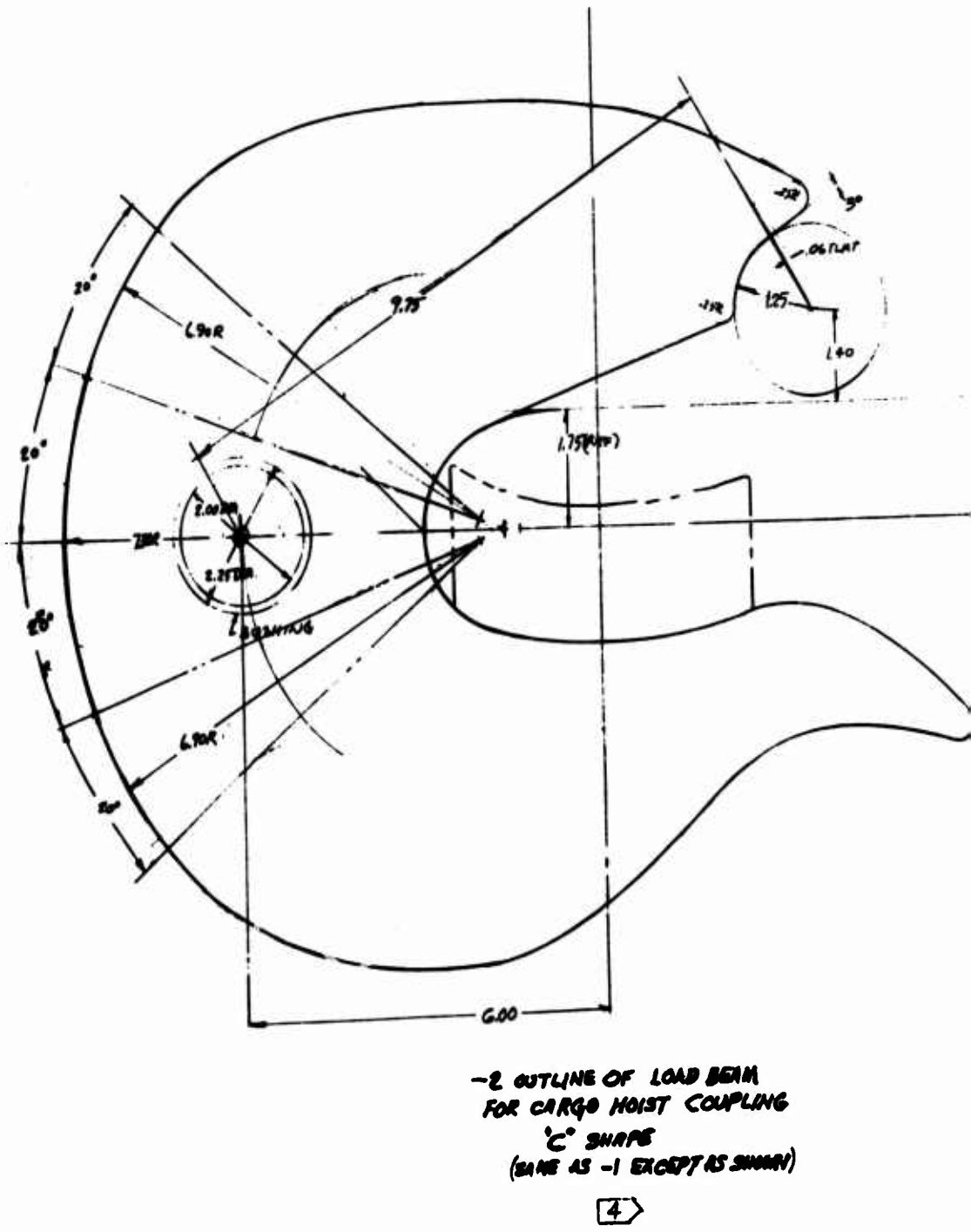

SHEET 3

Figure 1. HLH Load Beam Coupling Model (SK301-10235).

NOTES:

1. -1 & -2 PATTERNS TO BE USED
   PHOTOELASTIC MODEL FOR SI
2. LOAD TO BE SIMULATED IS
3. THE LOAD AREA IS NOTED AS
   INCHES OR TWO (2) NYLON SLIN
   TWO 2 1/4 DIA STEEL SHACKLE
4. MATERIAL & THICKNESS TO BE
   LAB REF FRED SACHS

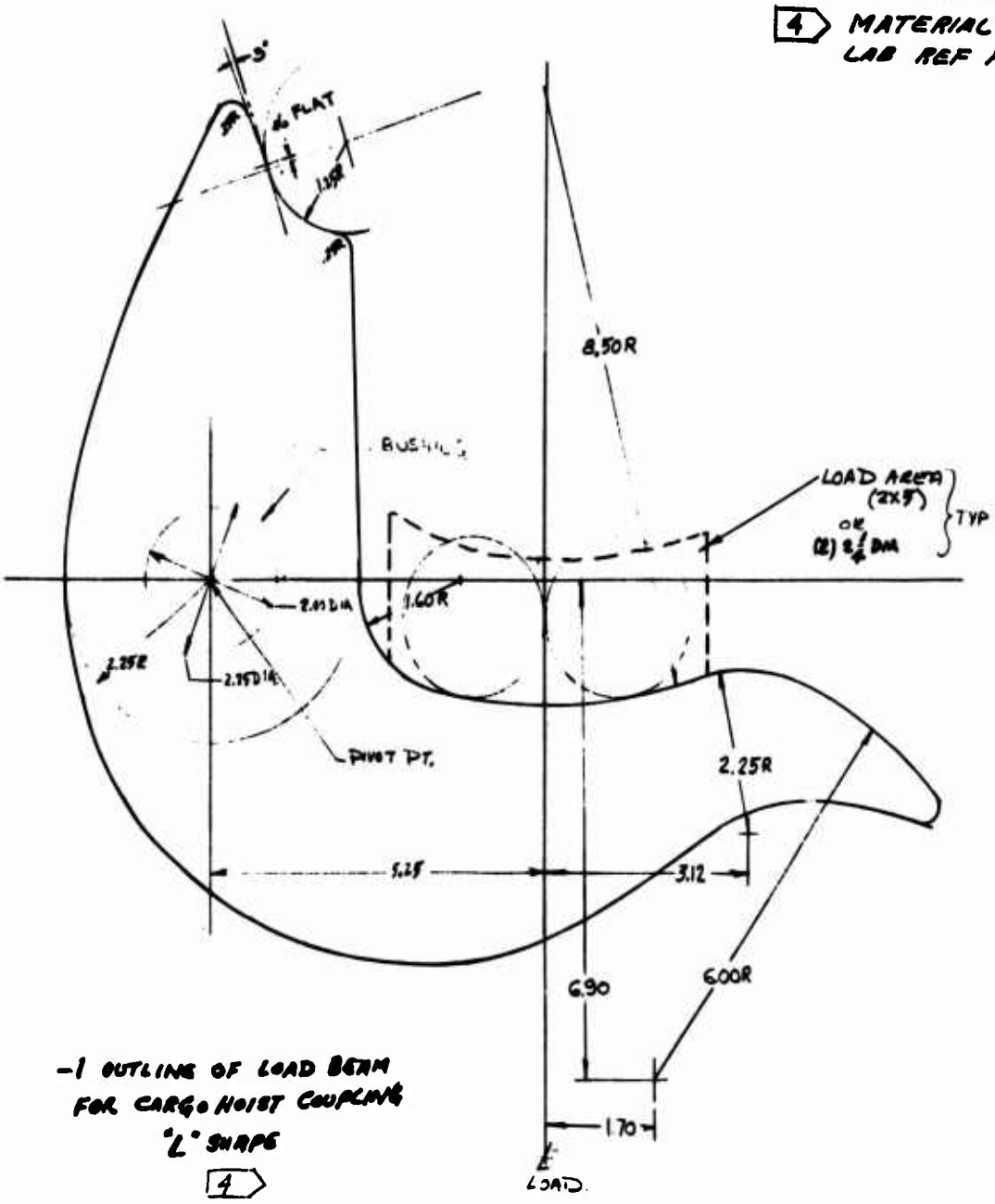

-1 OUTLINE OF LOAD BEAM
FOR CARGO HOIST COUPLING
"L" SHAPE
4

NOTES:

1. -1 & -2 PATTERNS TO BE USED TO MAKE A TWO DIMENSIONAL PHOTOELASTIC MODEL FOR SIMULATED LOAD TESTS.
2. LOAD TO BE SIMULATED IS 56,000 LB WKG LOAD
3. THE LOAD AREA IS NOTED AS A NYLON SLING · 2×5 INCHES OR TWO (2) NYLON SLINGS 2×2½ INCHES OR TWO 2¼ DIA STEEL SHACKLES.
4. MATERIAL & THICKNESS TO BE DETERMINED BY TEST LAB REF FRED SACHS

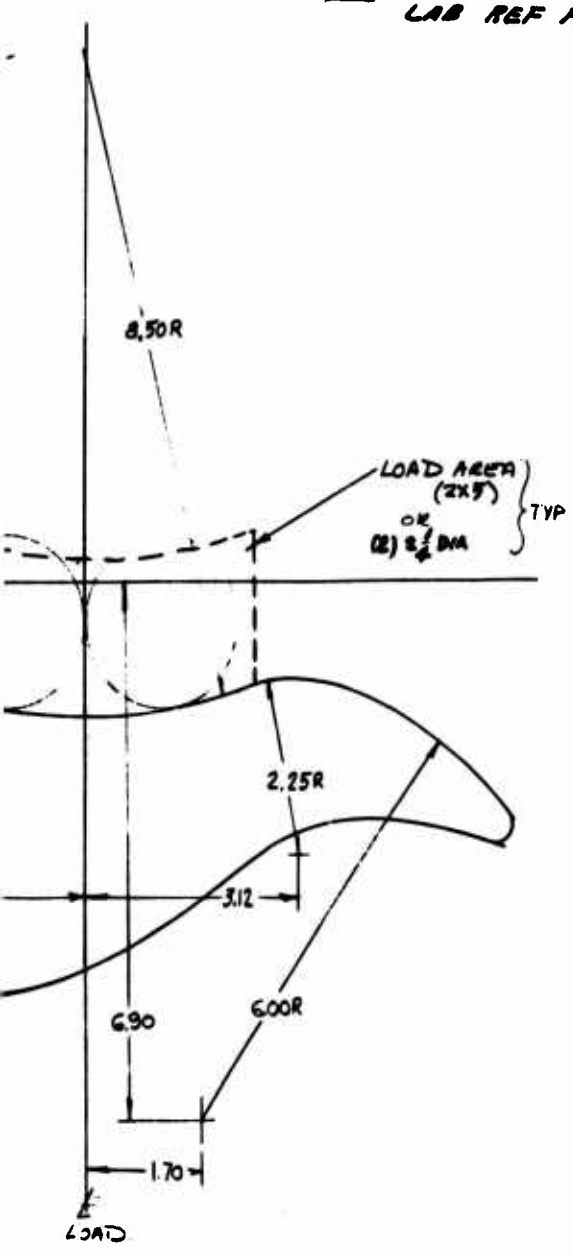

Specimen Design Details

A load beam study is depicted on Figures 2, 3 and 4. The study objective was to provide the most efficient location for the pivot point, in terms of reaction magnitude and reliability of operation.

Figure 2 is an overlay of the throat configuration per requirement of the Reference 1 drawing. Point A is the back of the load beam throat contour, Point L is the center of the load or center of the load beam, and Point P is the pivot point.

Figures 3 and 4 show both the L shape and the C shape, respectively, with the pivot point in several different locations. Configurations marked "upper" indicate that the pivot point is above the throat centerline. Those marked "lower" indicate that the pivot point is below the throat centerline. R_1 and R_2 are the reactions on the "L" and "C" shapes, respectively.

Figure 2B presents the results of these studies in chart form. Values of reaction forces R_1 and R_2 are plotted against pivot point locations as follows:

Reaction Force Value	Plotted Between Points
R_1 upper	B and C
R_1 lower	C and D
R_2 upper	E and F
R_2 lower	G and F

Line J-J defines the boundary of acceptability of the pivot point location. The area to the left of J-J denotes pivot point locations which will cause the system to malfunction. Either the hook will not open at all or the load sling will not slide off the load beam. The latter will happen if the opening angle is too small for the load weight to overcome the friction. Experience on the CH-47 helicopter has indicated that the load beam slope should be greater than 17-20 degrees from the horizontal centerline for the fabric sling to slide on the metal load beam.

To provide reliability of operation, and minimal size and magnitude of reaction, the optimum pivot point (location H) should therefore be in the shaded area between C and F.

SHEET 5

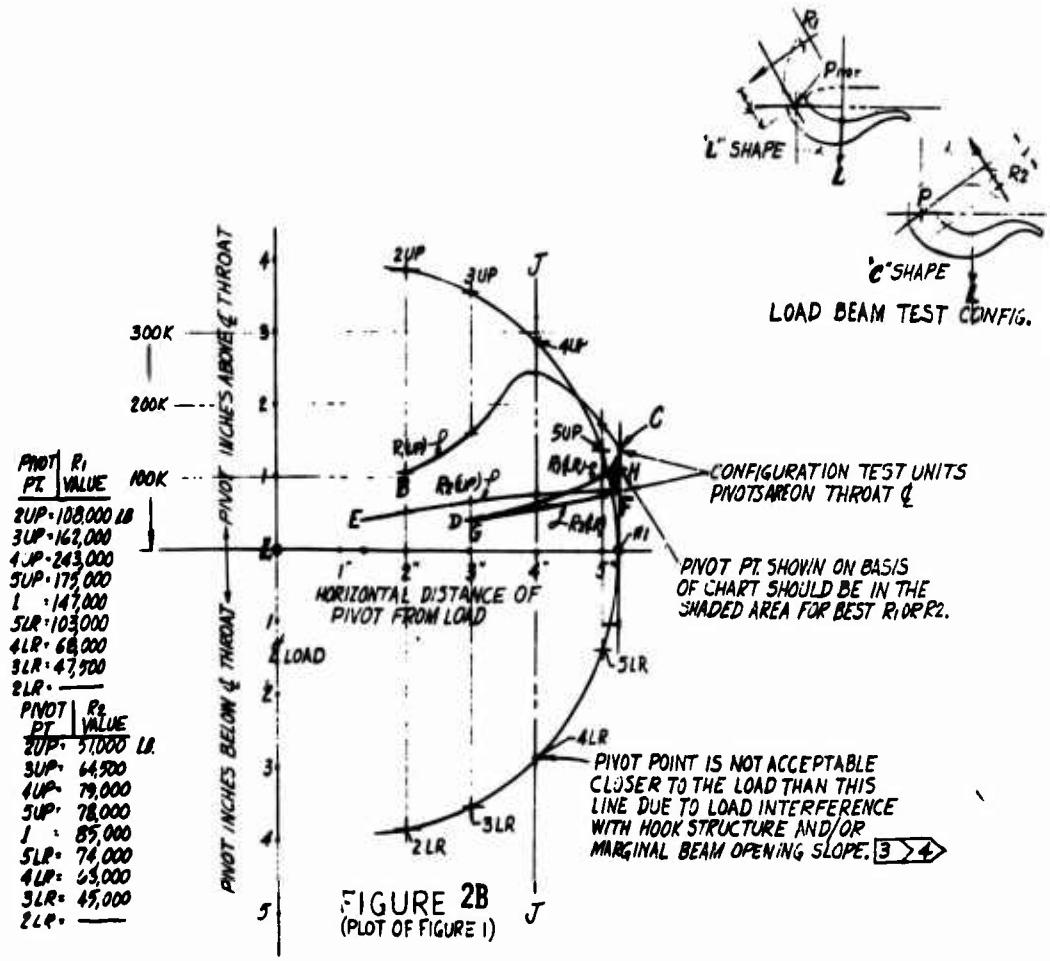

FIGURE 2B
(PLOT OF FIGURE 1)

Figure 2. HLH Load Beam Configuration Study (SK301-10250, Sheet 1 of 3).

Preceding page blank

NOTES:

1. LAST 2.0 INCHES OF BEAM OPEN MOVEMENT IS DUE TO THE LOAD SLIDING ON BEAM TO CONTINUE BEAM OPENING
2. 2.6 INCHES PER NOTE 1
3. LOAD WILL NOT PROGRESS BEYOND THIS POINT. COEF. OF FRICTION IS .2 - .36 AND THE TANGENT OF THE 3° OPEN ANGLE IS ONLY .05 (REF FIG 1)
4. OPENING IS TOO MARGINAL TO BE ACCEPTABLE.

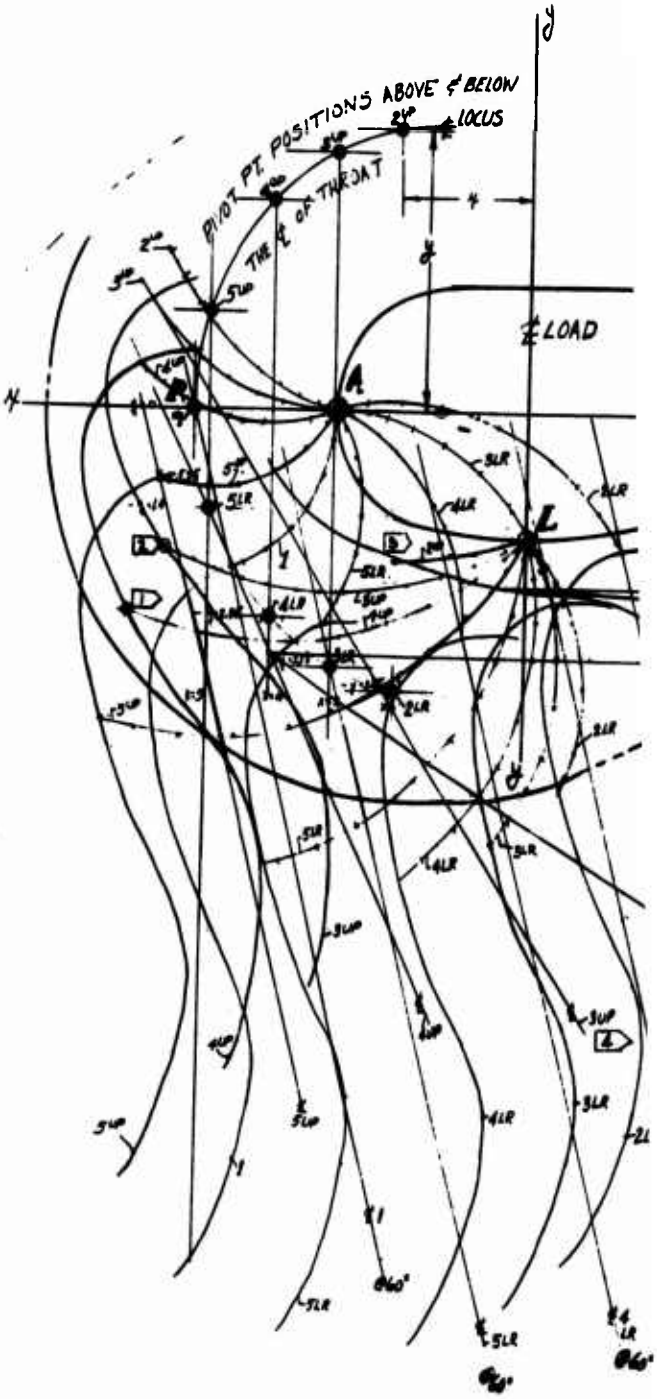

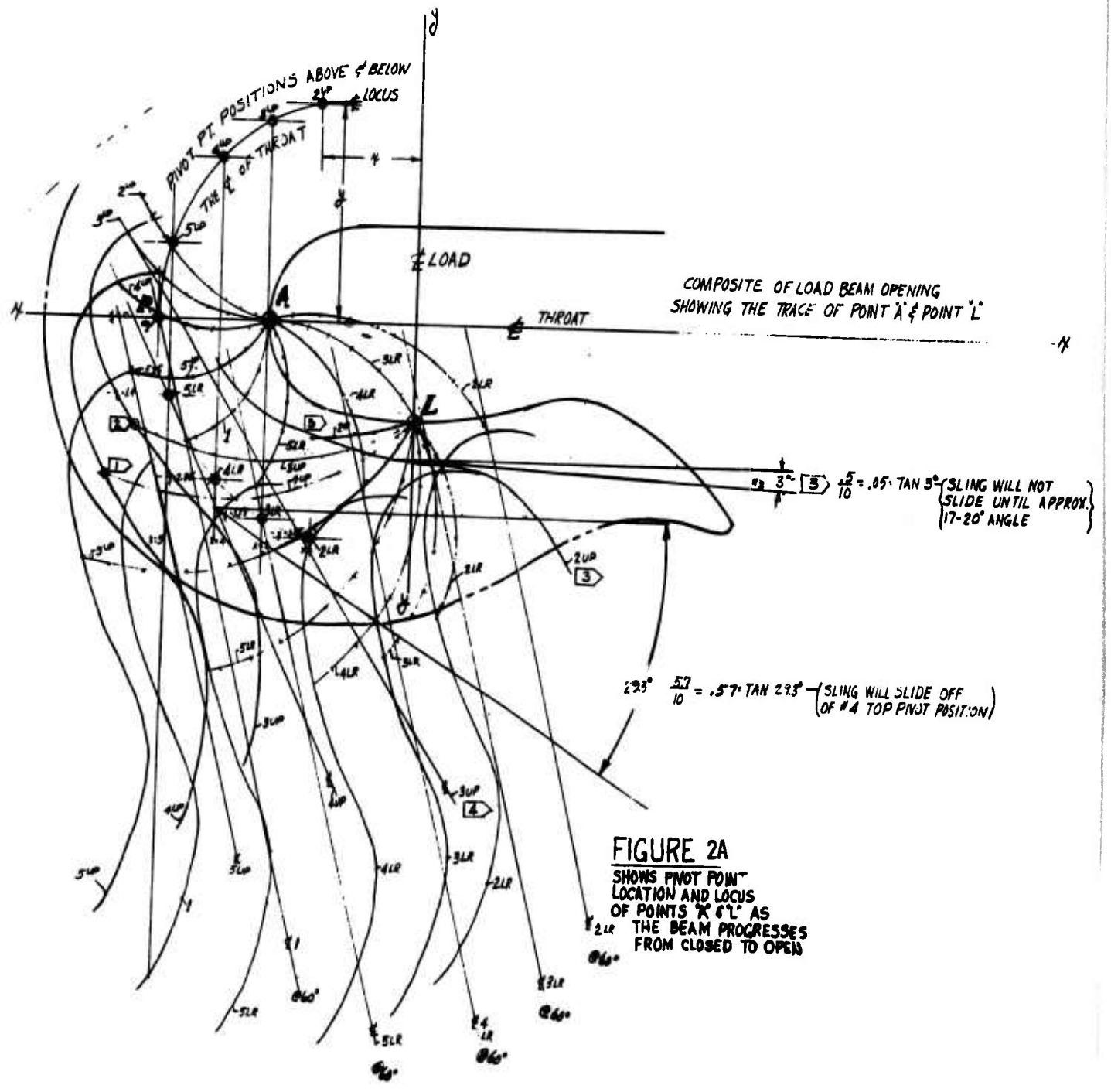

FIGURE 2A

SHOWS PIVOT POINT LOCATION AND LOCUS OF POINTS "A" & "L" AS THE BEAM PROGRESSES FROM CLOSED TO OPEN

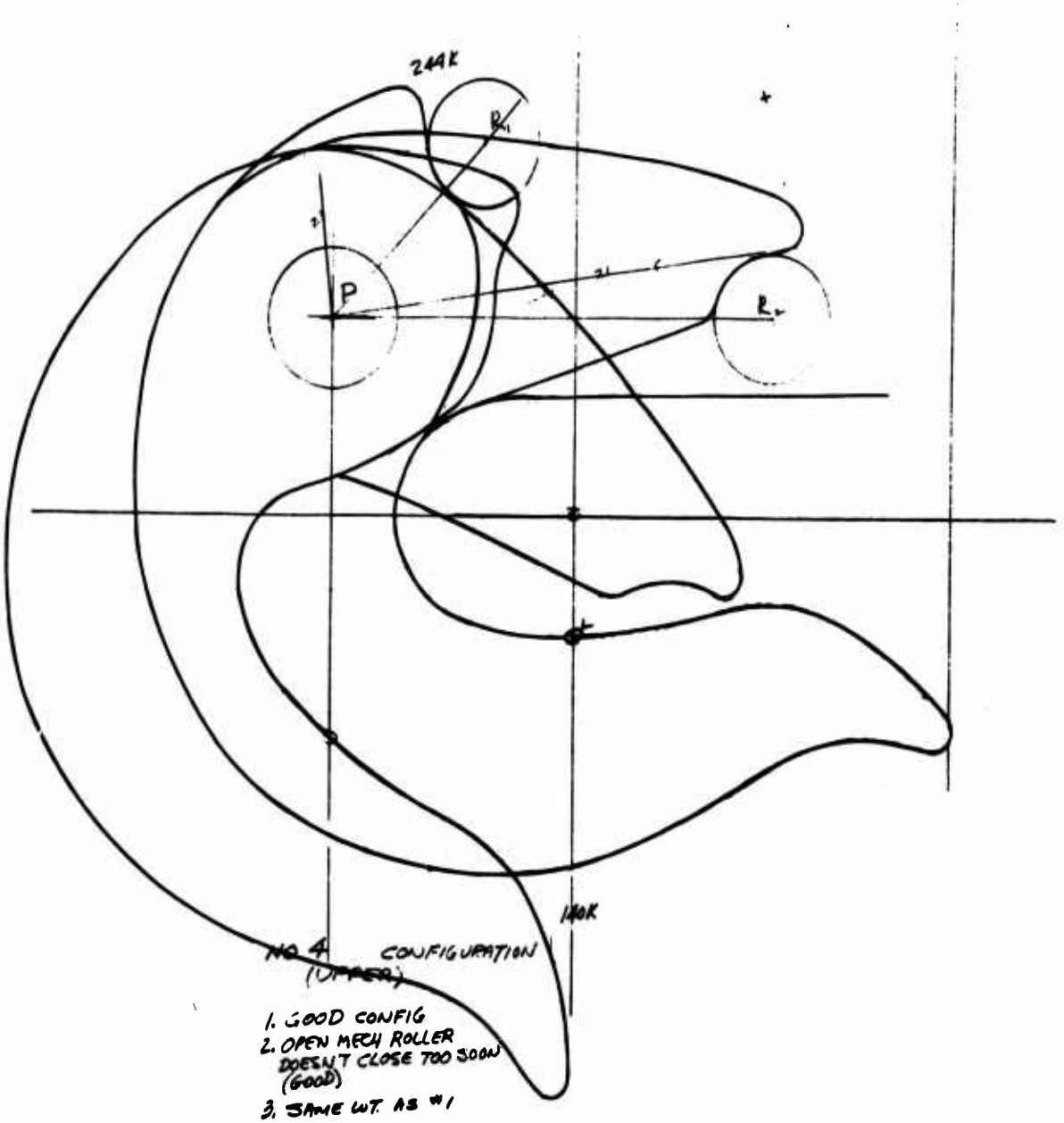

SHEET 6

Figure 3. HLH Load Beam Configuration Study (SK301-10250, Sheet 2 of 3).

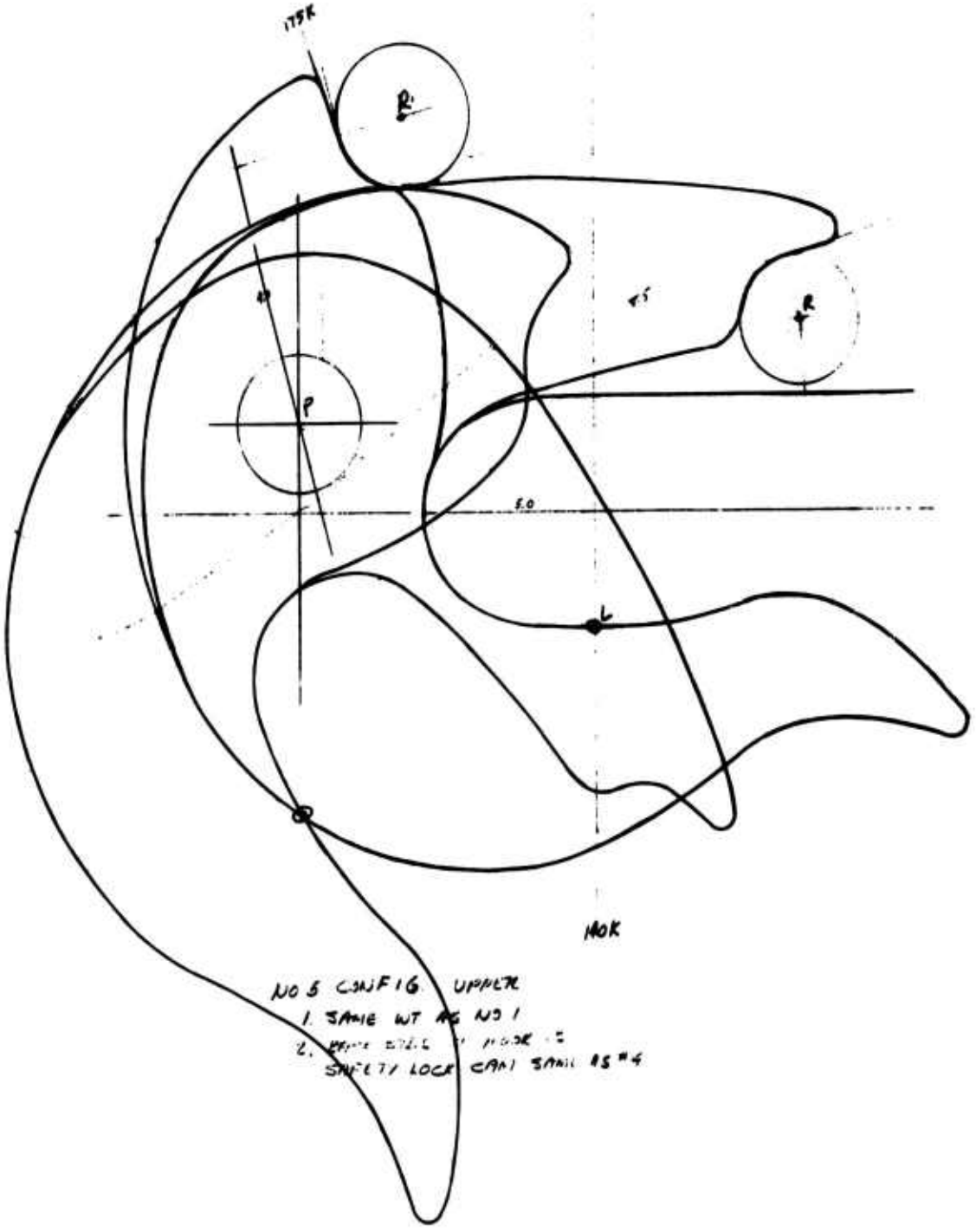

NO 5 CONFIG UPPER
1 SAME WT AS NO 1
2. [illegible]
SAFETY LOCK CAN SAME AS #4

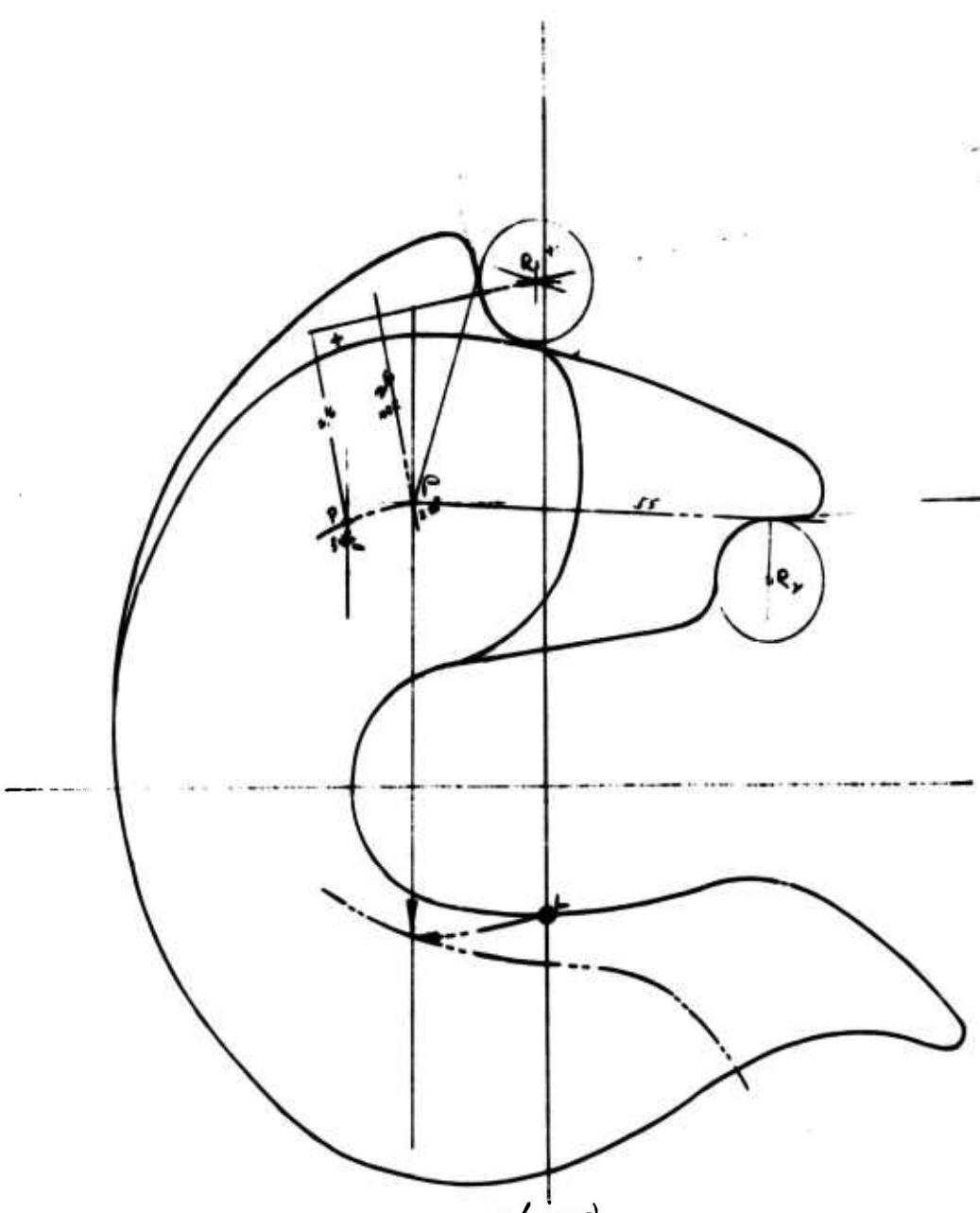

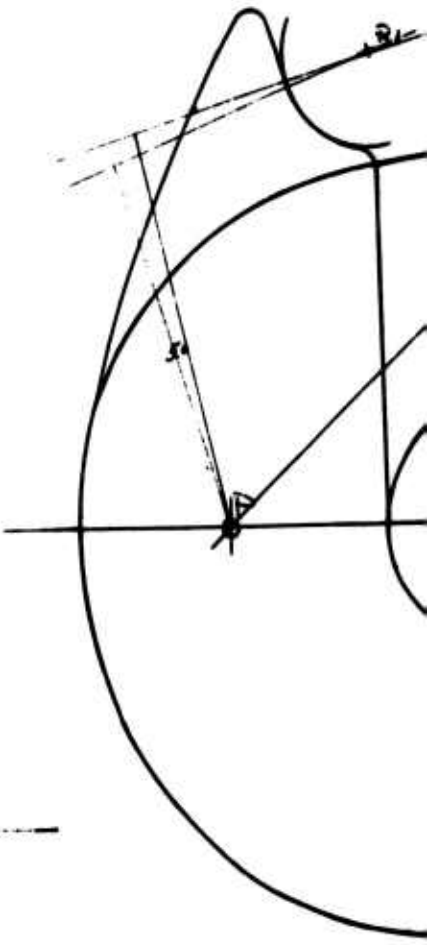

NO 2 CONFIG (UPPER)
UNACCEPTABLE
1. TOO LARGE
2. WILL NOT DUMP
NO 3 CONFIG IS SIMILAR (UPPER
UNACCEPTABLE
1. MARGIN DUMP 2. TOO LARGE

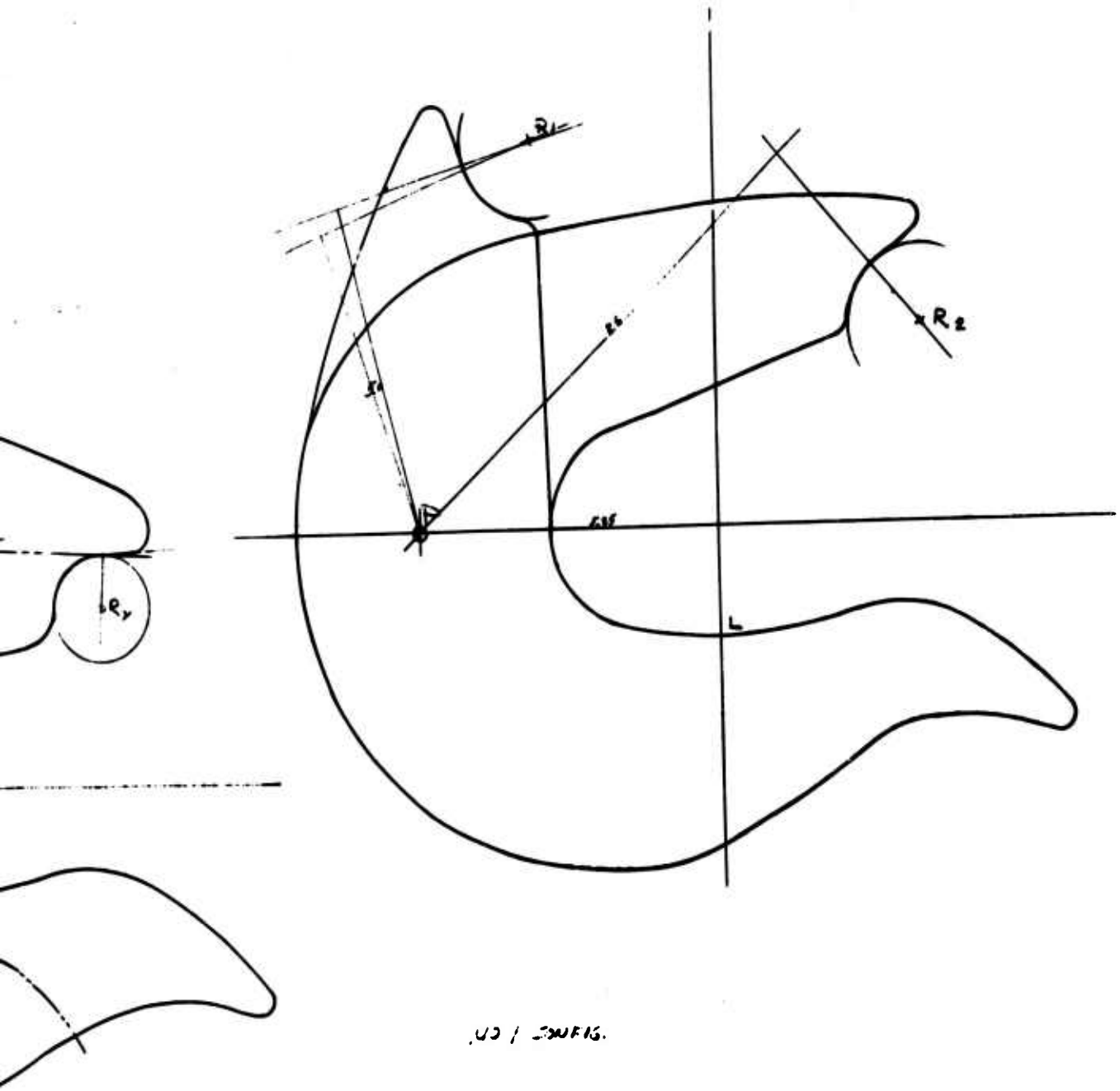

.03 / .030 FIG.

UPPER
TOO LARGE

9b

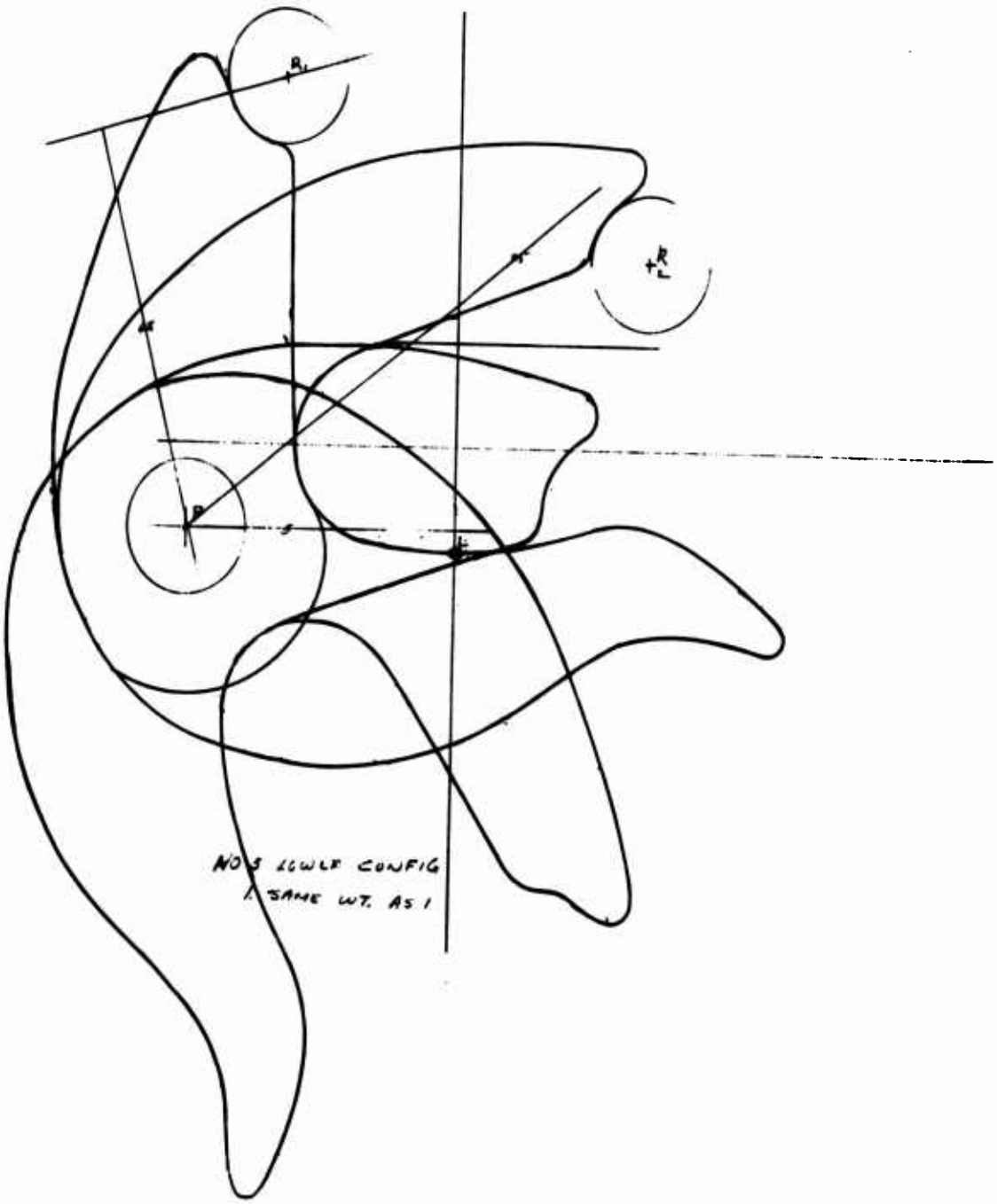

SHEET 7

Figure 4. HLH Load Beam Configuration Study (SK301-10250, Sheet 3 of 3).

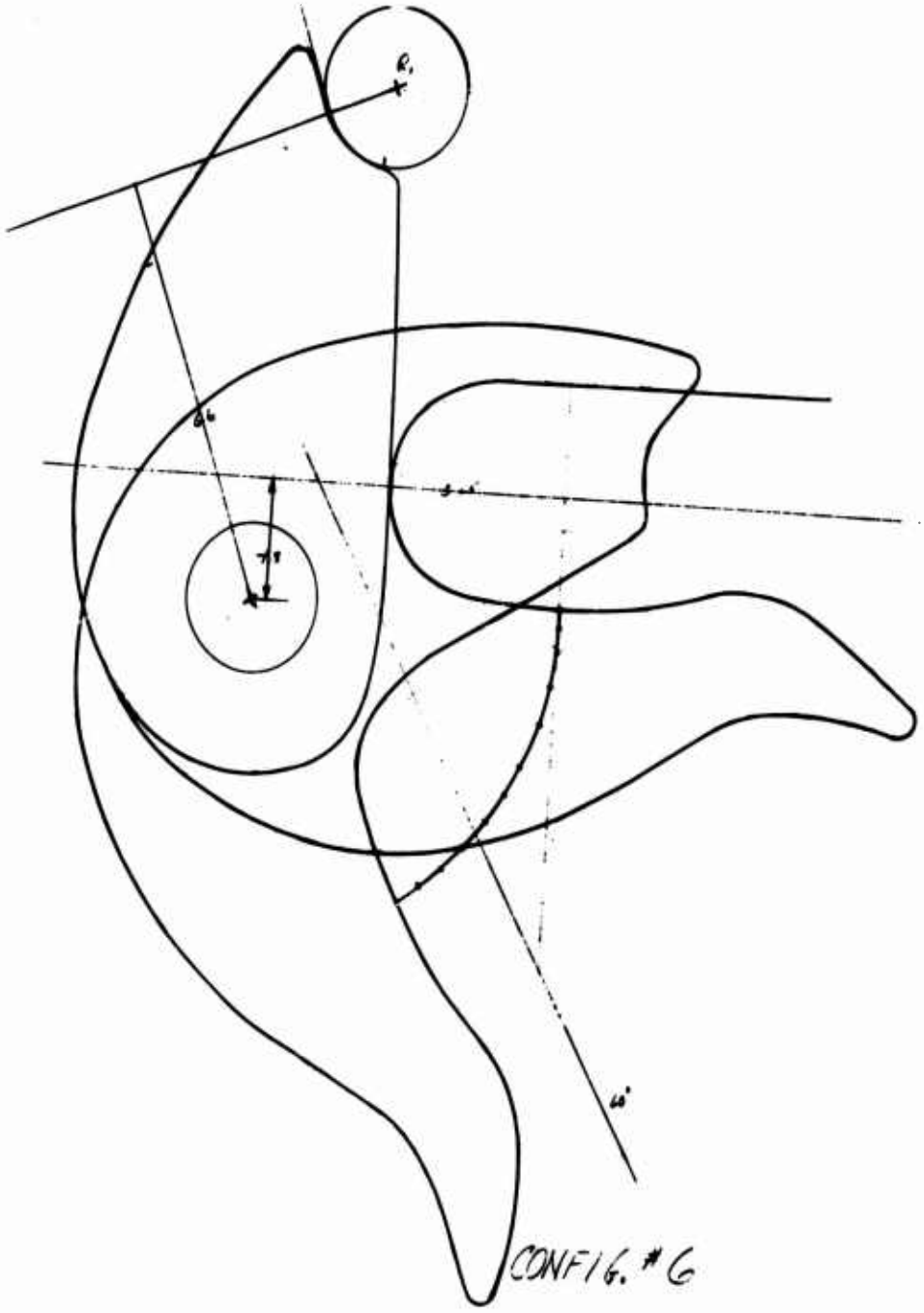
CONFIG. #6

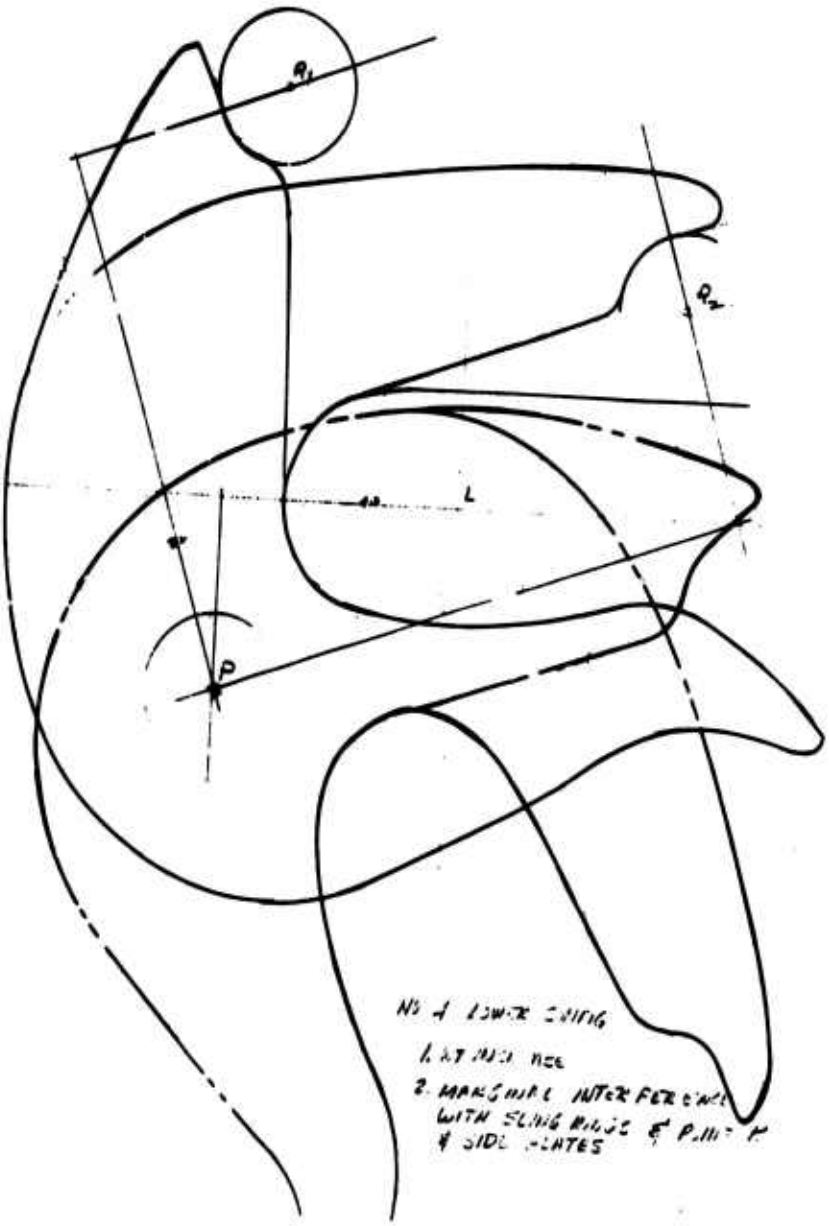

NO 4 LOWER SLING

1. NOT ACCEPTABLE

2. MARGINAL INTERFERENCE WITH SLING RINGS & PITCH & SIDE PLATES

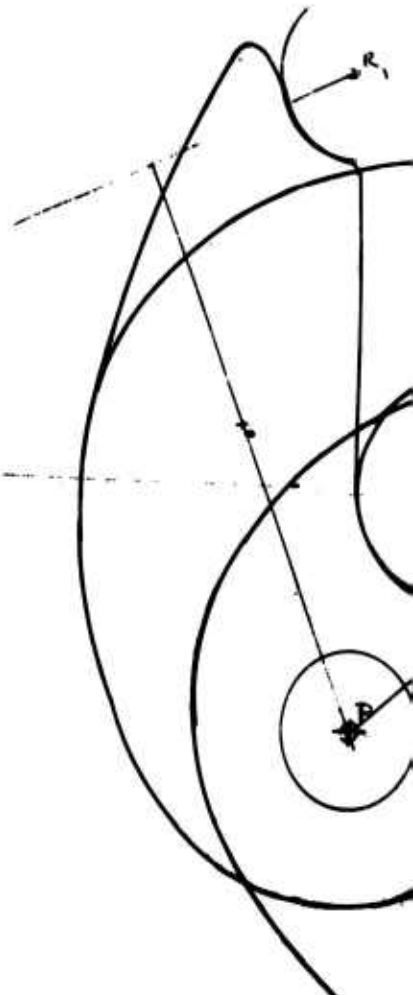

NO 3 CONFIG

NOT ACCEPTA

1. P MECHANISM

TO INTERFERE

SLING RINGS.

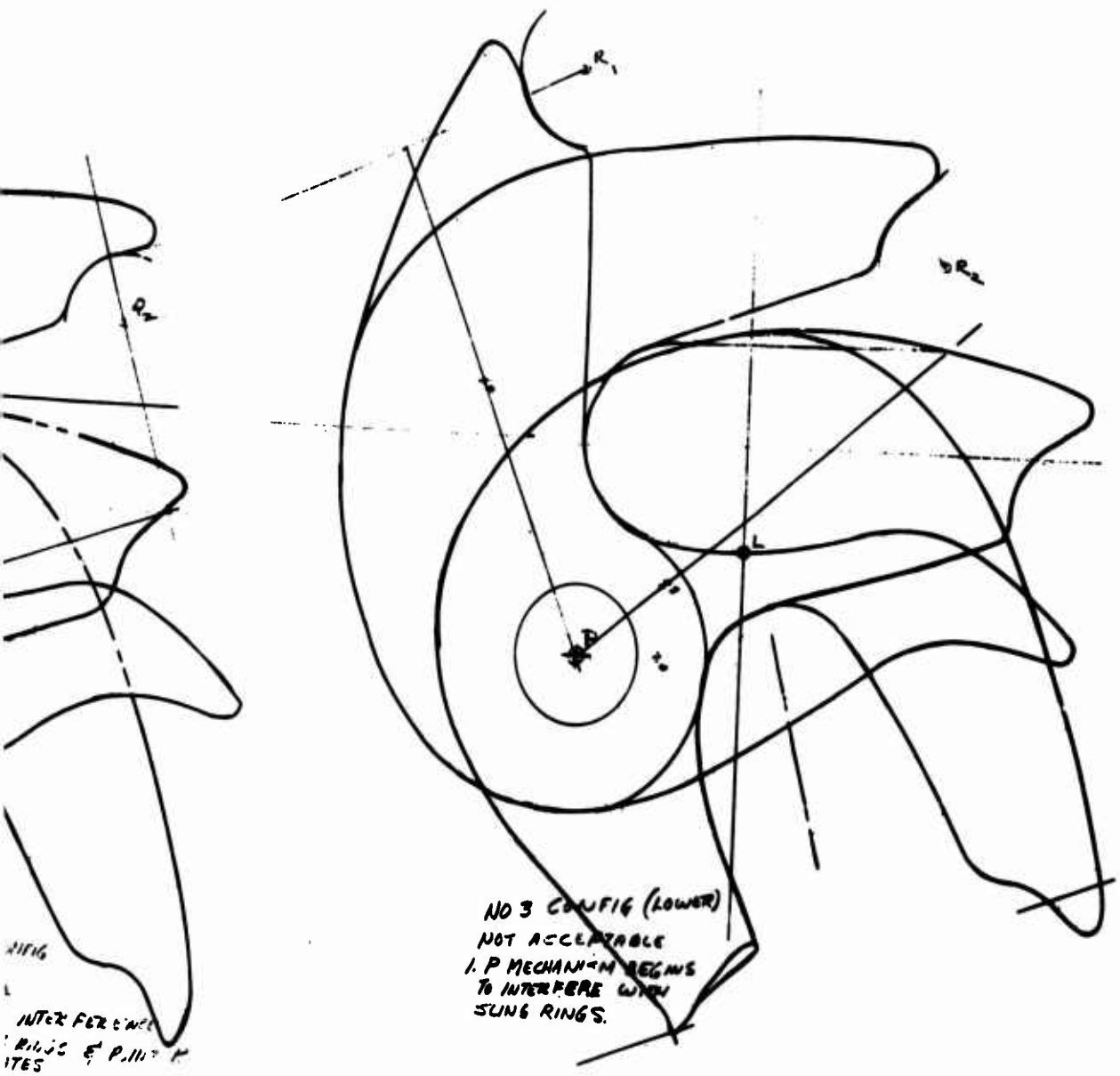
R_1
R_2
L
NO 3 CONFIG (LOWER)
NOT ACCEPTABLE
I. P MECHANISM BEGINS
TO INTERFERE WITH
SUNG RINGS.

Fabrication

Templates of .050-inch aluminum were made to the dimensional requirements of Figure 1. The templates were bonded to the plastic material and the general shapes of the models cut out on a band saw. The finish machining was done with a router.

TEST PROGRAM

Test Plans and Approach

The model is examined in a field of polarized light under applied loads similar to those to be experienced on the actual load beam. Under these conditions, a series of brilliantly colored tint bands can be observed. The optical effects of this graphic presentation may be readily interpreted in terms of stress distribution.

Since it is desirable to have a fringe pattern which will clearly show areas of high stress but which will not "wash out" some fringes or interfere with graphic clarity, a series of loads were applied to each specimen to determine the best condition. A model load of 30 pounds was found to be optimum.

Test Facilities and Instrumentation

The models were mounted in a test fixture as shown in the schematic, Figure 5. The fixture consisted of a 1-inch-thick aluminum back plate and pins of appropriate diameter to act as pivot points and points of load reaction for two model configurations. A silver coating was sprayed on one side of the model so that a reflective polariscope could be used to view the model under load. With this instrument, polarized light is reflected from the surface of the coating, traversing twice through the model. The model then exhibits a pattern of bifringence which disappears upon removal of the load. The bifringence or fringe order can be converted to stress following plastic calibration.

Test Data Collection, Processing and Analysis

A grid was drawn on each model to provide points for taking data. Lines were drawn at .20-inch intervals parallel to the inner contour to a distance 1 inch inboard of the contour (see Figures 6 and 7). Lines were then drawn radially from and perpendicular to the edge of the contour and spaced at approximately .30 inch apart. Photoelastic measurements, in fringe orders, were taken at each point as shown in Tables I and II. From this data, stress intensity curves were plotted to show stress levels at various points around the contour

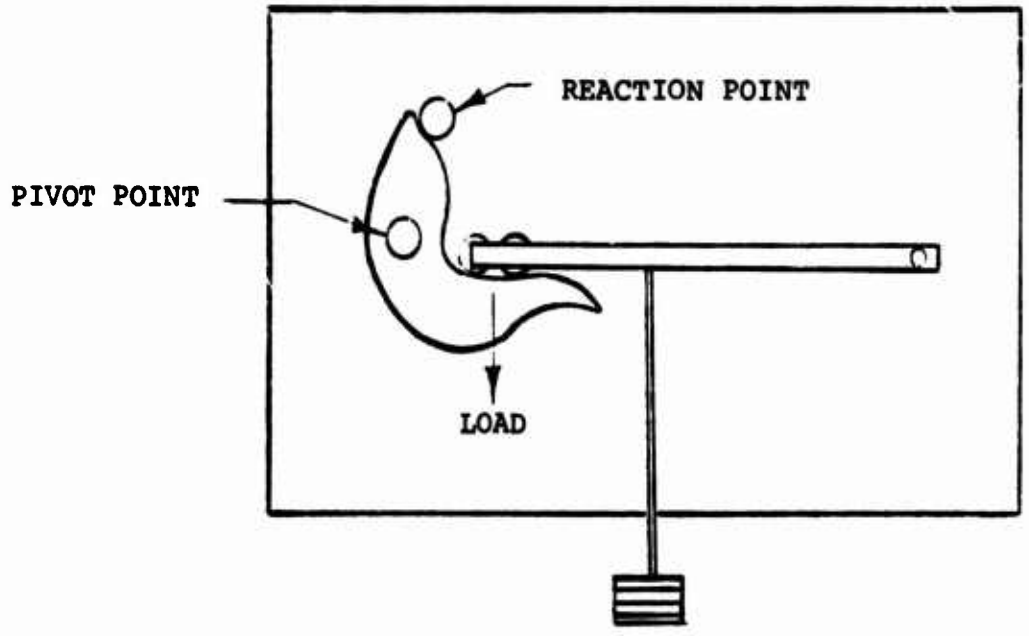

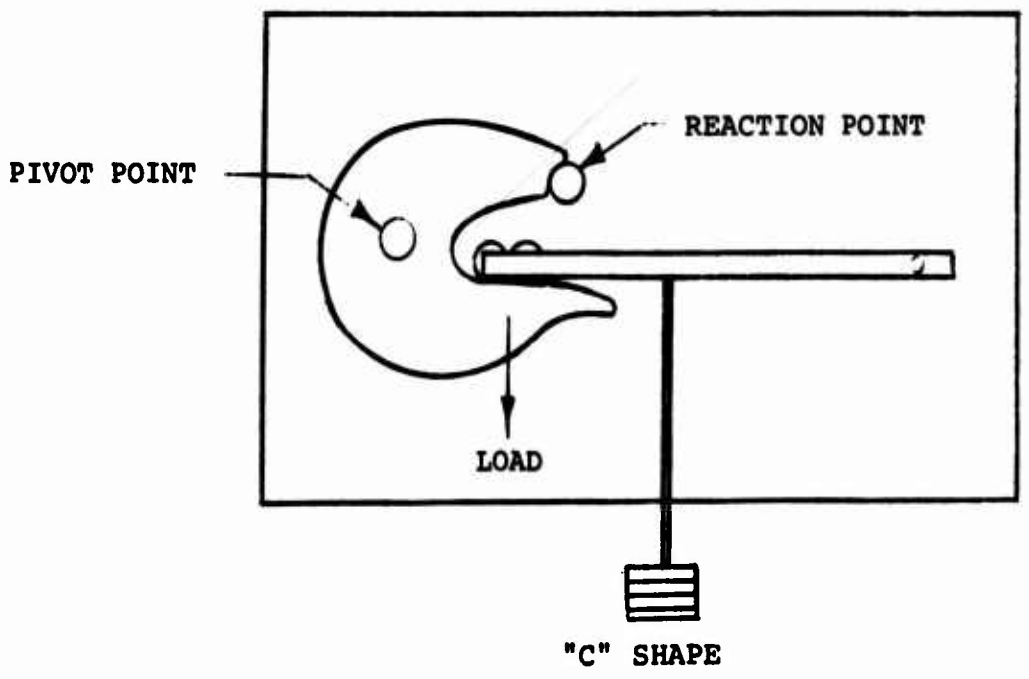

Figure 5. Test Schematic.

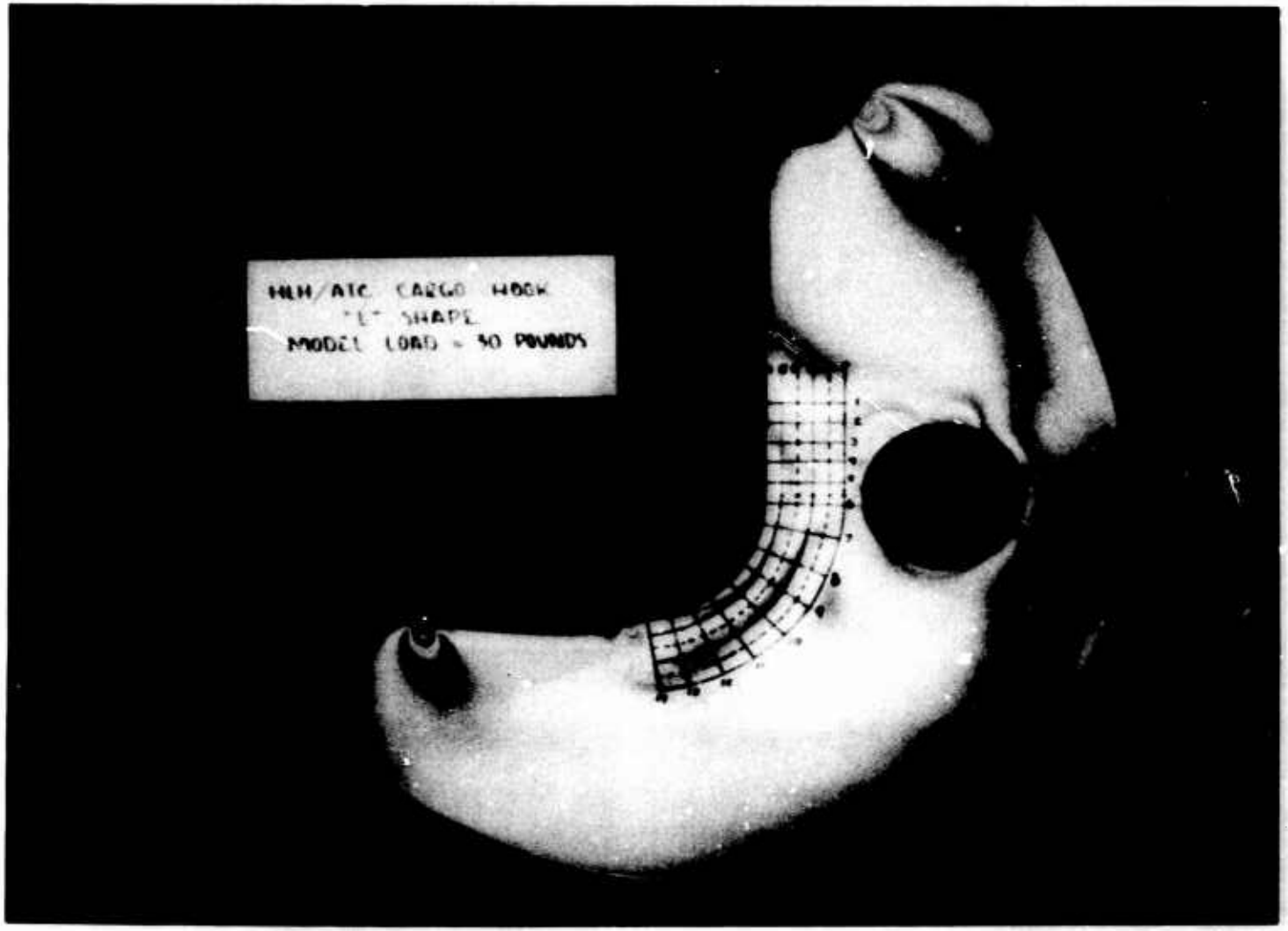

Figure 6. "L" Shaped Coupler Under 30-Pound Load.

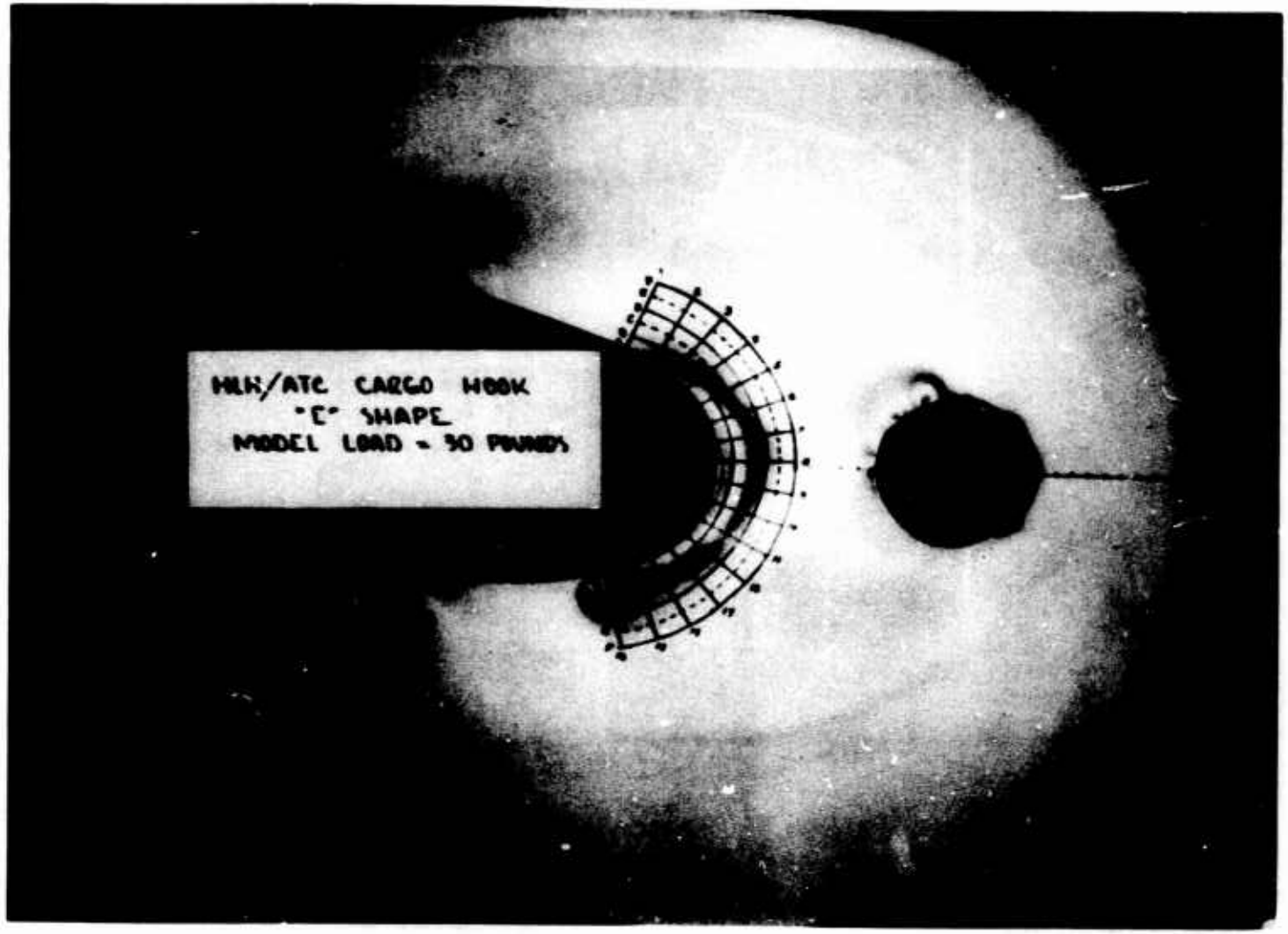

Figure 7. "C" Shaped Coupler Under 30-Pound Load.

TABLE I. "L" SHAPED COUPLER TEST DATA

ENGINEERING LABORATORY TEST REPORT | LABORATORY: EXP. MECH. | PAGE: of

EWO NUMBER: | TEST EVENT: TABLE I

TEST TITLE: HLH CARGO HOOK "L" SHAPE

SPECIMEN PART NUMBER: | SERIAL NUMBER: | SPECIMEN NO.: | AIRCRAFT MODEL: | DATE: 11/8/71

TEST ENGINEER: | WITNESSES: Brink

TEST MACHINE: Load - 30#

MANUF. MODEL SERIAL SENS. CABLE CAP.	POINT	FRINGE ORDER	∠ (DEG)	POINT	FRINGE ORDER	∠ (DEG)		POINT	FRINGE ORDER	∠ (DEG)		
	1A	2.14	+ 5	1B	1.82	+ 8		1C	1.46	+18		
	2A	2.36	+ 2	2B	1.98	+ 6		2C	1.67	+15		
	3A	2.53	0	3B	2.13	+ 5		3C	1.75	+13		
	4A	2.66	0	4B	2.28	+ 3		4C	1.87	+12		
	5A	2.79	0	5B	2.32	+ 4		5C	1.91	+12		
	6A	2.94	+ 6	6B	2.33	+ 7		6C	1.78	+14		
	7A	3.11	+14	7B	2.29	+15		7C	1.53	+23		
	8A	3.13	+27	8B	2.25	+27		8C	1.45	+34		
	9A	3.08	+38	9B	2.17	+40		9C	1.37	+48		
	10A	3.00	+48	10B	2.19	+50		10C	1.42	+55		
	11A	2.90	+61	11B	2.02	+62		11C	1.30	+66		
	12A	2.63	+71	12B	1.83	+71		12C	1.28	+64		
	13A	2.27	+81	13B	1.47	+75		13C	1.34	+64		
	14A	2.79	+81	14B	1.89	+64		14C	1.69	+65		

FORM 39240 (7/68)

TABLE II. "C" SHAPED COUPLER TEST DATA

ENGINEERING LABORATORY TEST REPORT	LABORATORY: EXP. MECH.	PAGE: OF
EWO NUMBER:	TEST EVENT: TABLE II	
TEST TITLE: HLH CARGO HOOK "C" SHAPE		
SPECIMEN PART NUMBER:	SERIAL NUMBER:	SPECIMEN NO.: / AIRCRAFT MODEL: / DATE: 11/9/71
TEST ENGINEER:		WITNESSES: BRINK
TEST MACHINE:		

MANUF. MODEL SERIAL SENS. CABLE CAP.	POINT	FRINGE ORDER	∠ (DEG.)		POINT	FRINGE ORDER	∠ (DEG.)		POINT	FRINGE ORDER	∠ (DEG.)	
	1A	1.10	-68		1B	.86	-58		1C	.75	-53	
	2A	1.37	-56		2B	.95	-50		2C	.76	-42	
	3A	1.69	-49		3B	1.02	-43		3C	.79	-33	
	4A	1.85	-37		4B	1.11	-32		4C	.83	-25	
	5A	2.09	-27		5B	1.32	-29		5C	.93	-18	
	6A	2.23	-18		6B	1.50	-18		6C	.99	-12	
	7A	2.40	- 9		7B	1.59	-10		7C	1.01	0	
	8A	2.55	- 2		8B	1.69	0		8C	1.15	+ 7	
	9A	2.61	+ 7		9B	1.83	+ 8		9C	1.14	+10	
	10A	2.60	+20		10B	1.87	+21		10C	1.07	+15	
	11A	2.51	+32		11B	1.75	+32		11C	1.05	+26	
	12A	2.30	+44		12B	1.63	+44		12C	1.02	+29	
	13A	2.16	+53		13B	1.60	+52		13C	.99	+31	
	14A	2.08	+62		14B	1.32	+60		14C	.90	+37	
	15A	1.87	+72		15B	1.19	+60		15C	.97	+47	
	16A	1.30	+77		16B	1.69	+68		16C	1.30	+59	

FORM 38240 (7/68)

(see Figures 8, 9, 10 and 11). Stress trajectories were also plotted to show the stress flow around the contours (data is from Reference 2).

Use of the following data shown produced curves 1 and 2 of Figure 12.

Applied test load: 30 lb

E of model: 4.98×10^5 psi

Model thickness: .258 in.

Calibration: 305 μ in./in./fringe

Ultimate load: 210,000 lb

Proposed actual thickness at pivot point: 3.0 in.

Stress in the plastic model at 1st fringe order:
$E \times \varepsilon = .498 \times 10^6 \times 305 \times 10^{-6} = 152$ psi

Stress in actual hook at 1st fringe order:
$$\frac{210{,}000 \times .258}{30 \times 3.0} \times 152 = 91{,}500 \text{ psi}$$

Stress in actual hook: 91,500 x fringe order

The two models were equal in thickness but not in depth at equivalent sections. A correction was therefore applied to the "L" hook stress levels to compare them directly with "C" hook stresses. The results are shown on Curve 3 of Figure 12.

TASK CONCLUSIONS AND RECOMMENDATIONS

A comparison of Curve 3, Total Measured Stress in L Hook - Corrected, to Curve 2, Total Measured Stress - C Hook, indicates that the "L" shape is more efficient. This is explained by the fact that the peak stresses occur at the center of curvature and this point is closer to the applied load in the "L" shape than it is in the "C" shape.

Figure 13 presents an analytical curve of maximum bending stress based on a rectangular section at Section A-A. Comparison of the test point to the curve indicates that the analytical work is unconservative within the elastic range of the beam material.

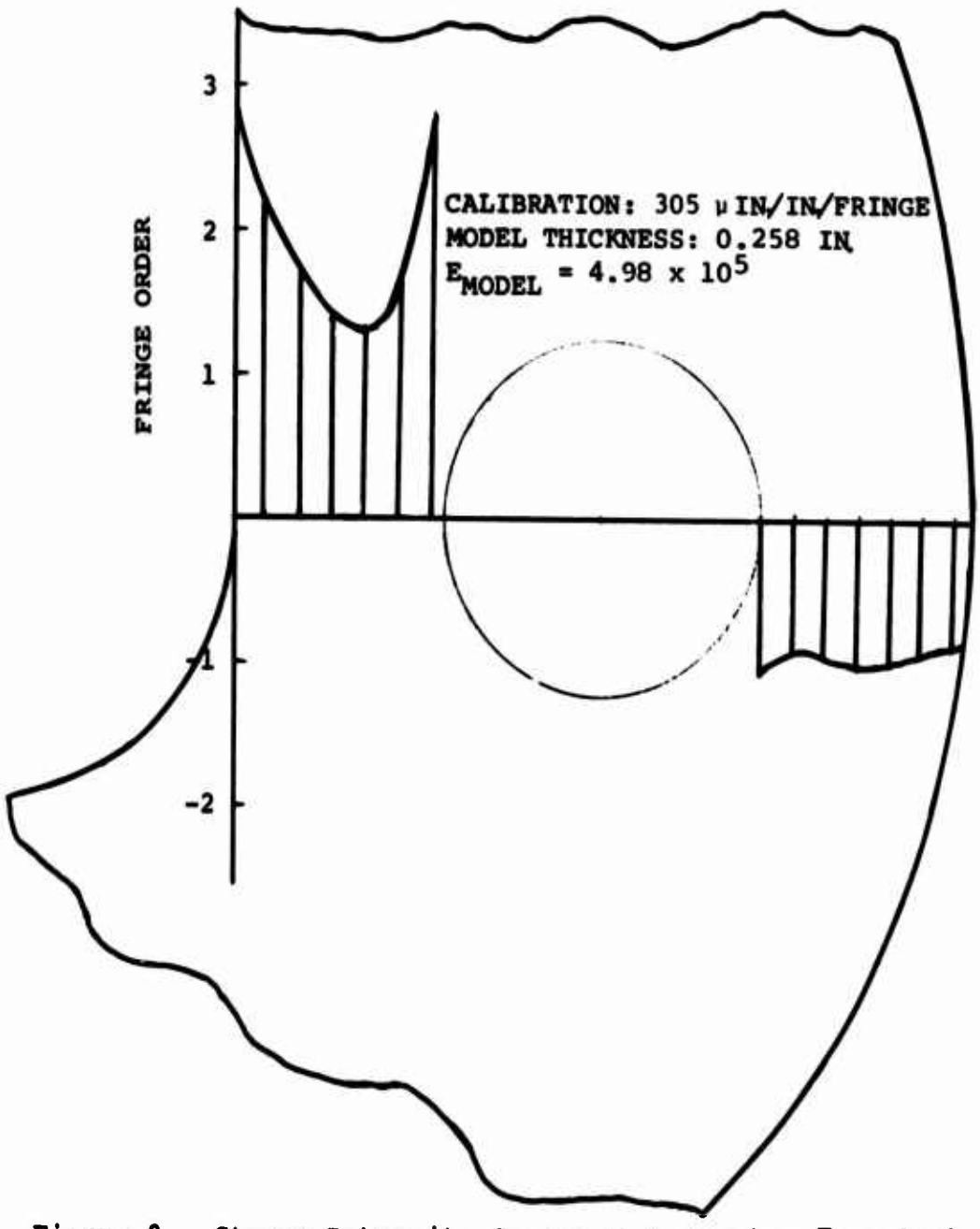

Figure 8. Stress Intensity Curves at a Section From Hook Throat Through Pivot Pin for "L" Shaped Load Beam Coupling Model.

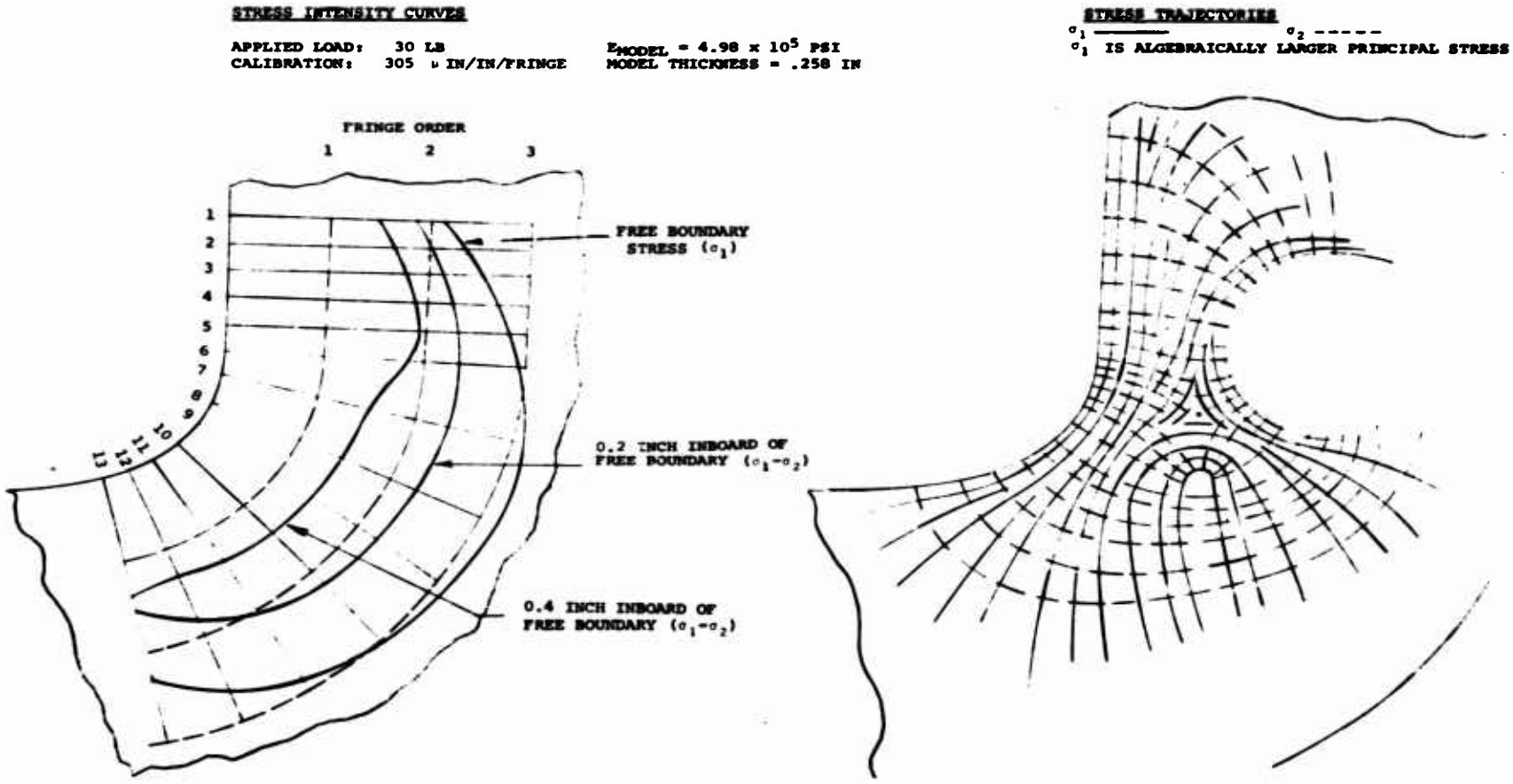

Figure 9. Stress Intensity Curves and Stress Trajectories for "L" Shaped Load Beam Coupling Model.

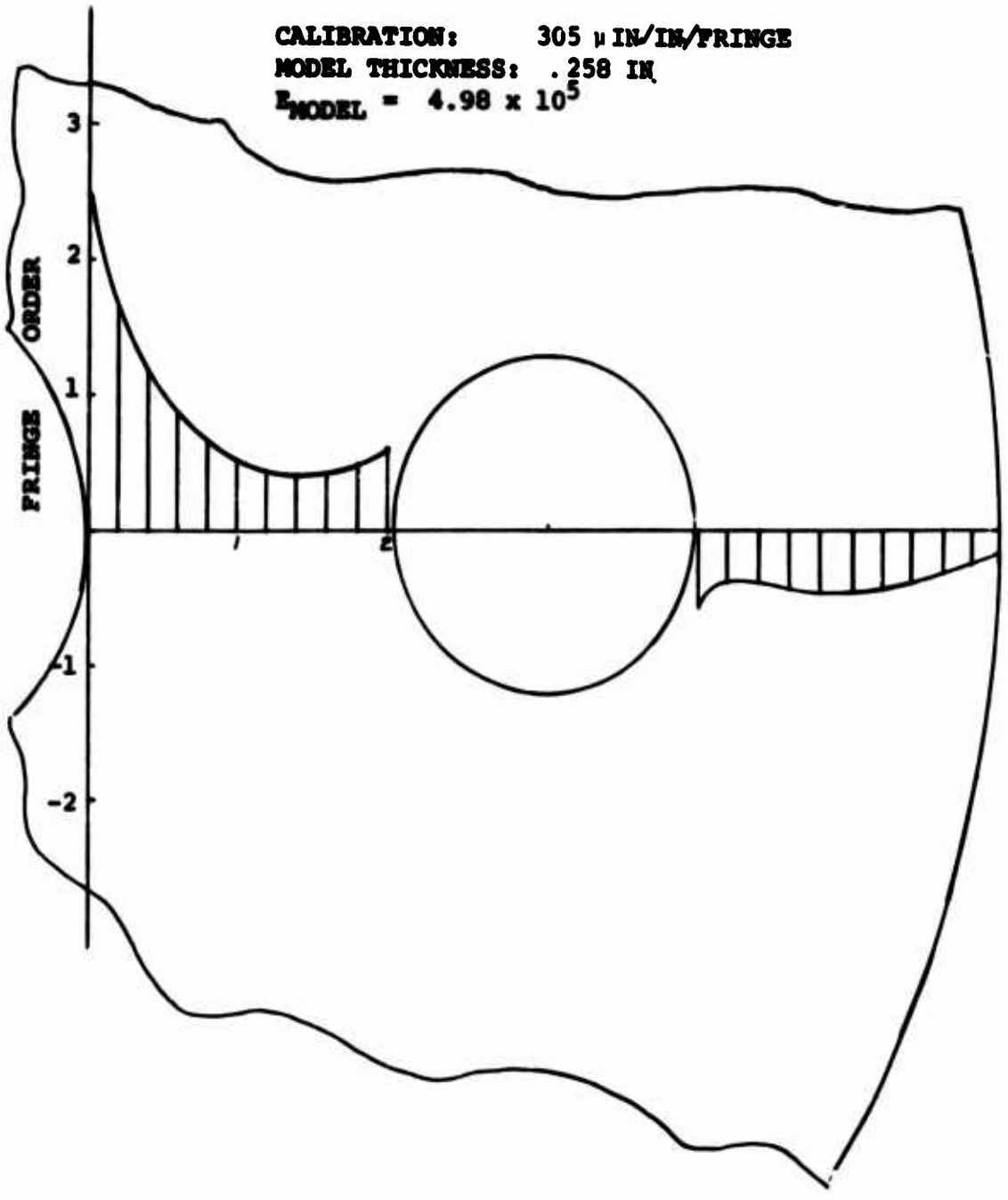

Figure 10. Stress Intensity Curve at a Section From Hook Throat Through Center of Pivot Pin for "C" Shaped Load Beam Coupling Model.

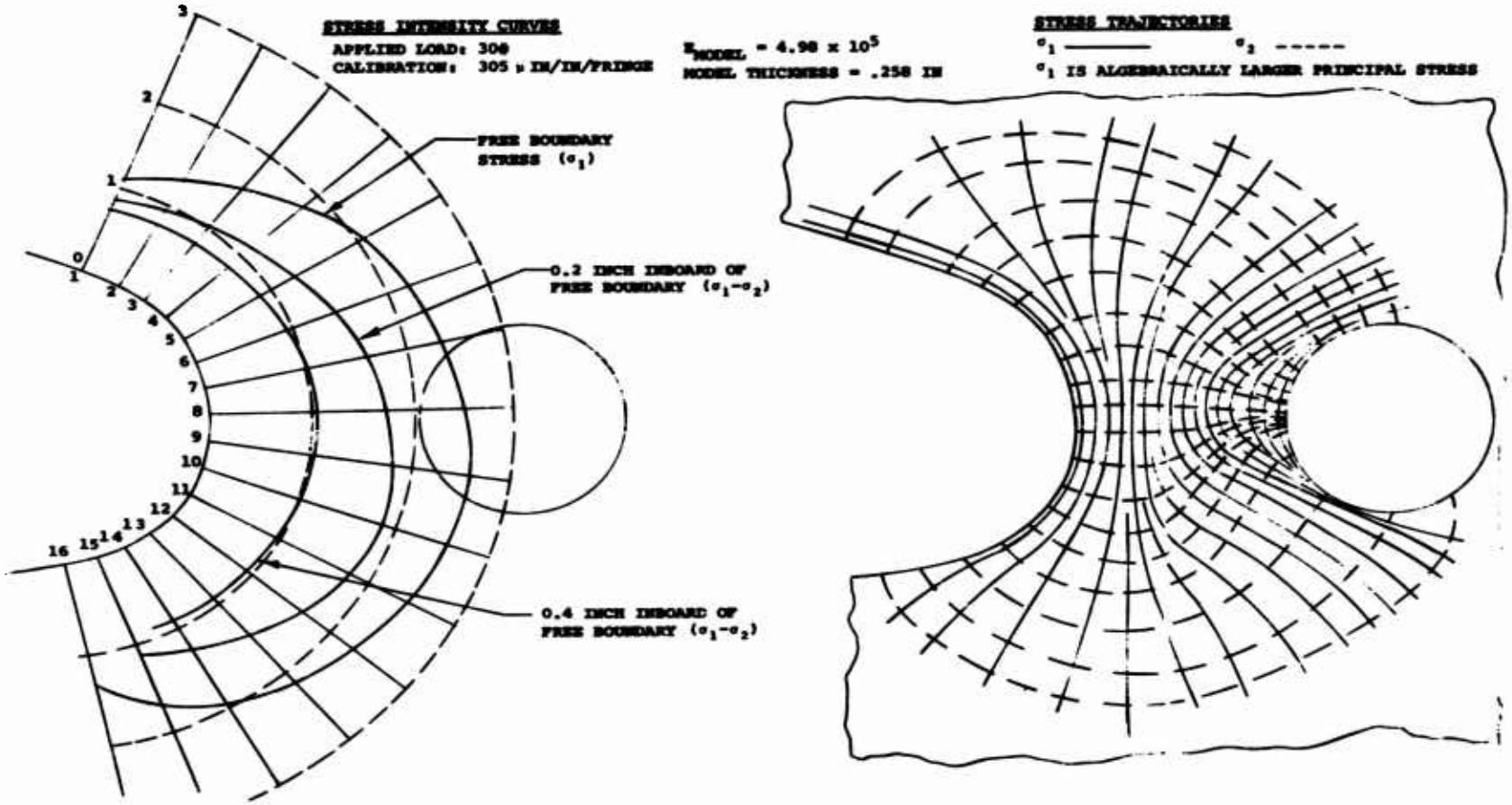

Figure 11. Stress Intensity Curves and Stress Trajectories for "C" Shaped Load Beam Coupling Model.

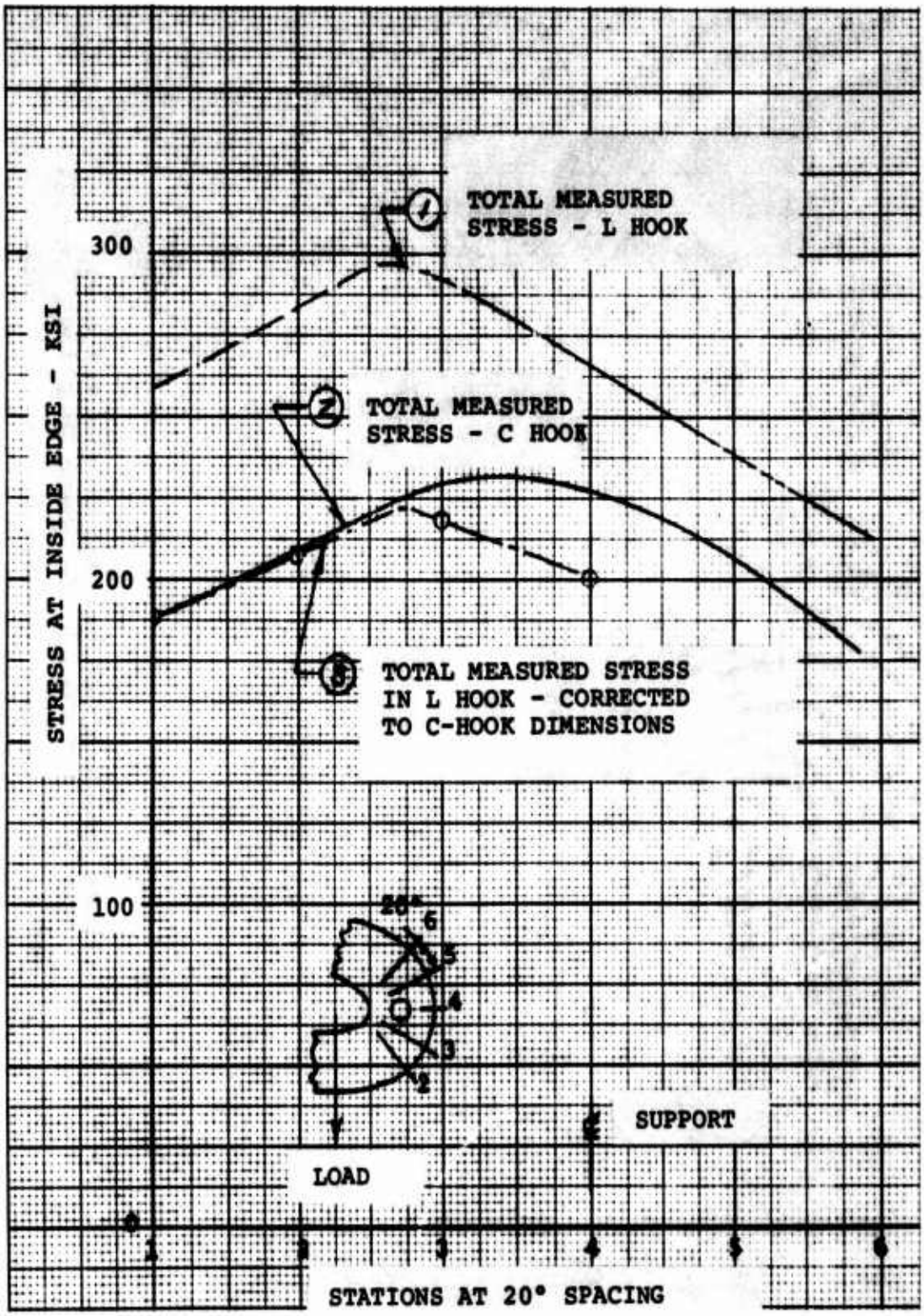

Figure 12. Photoelastic Model of HLH Cargo System Hook.

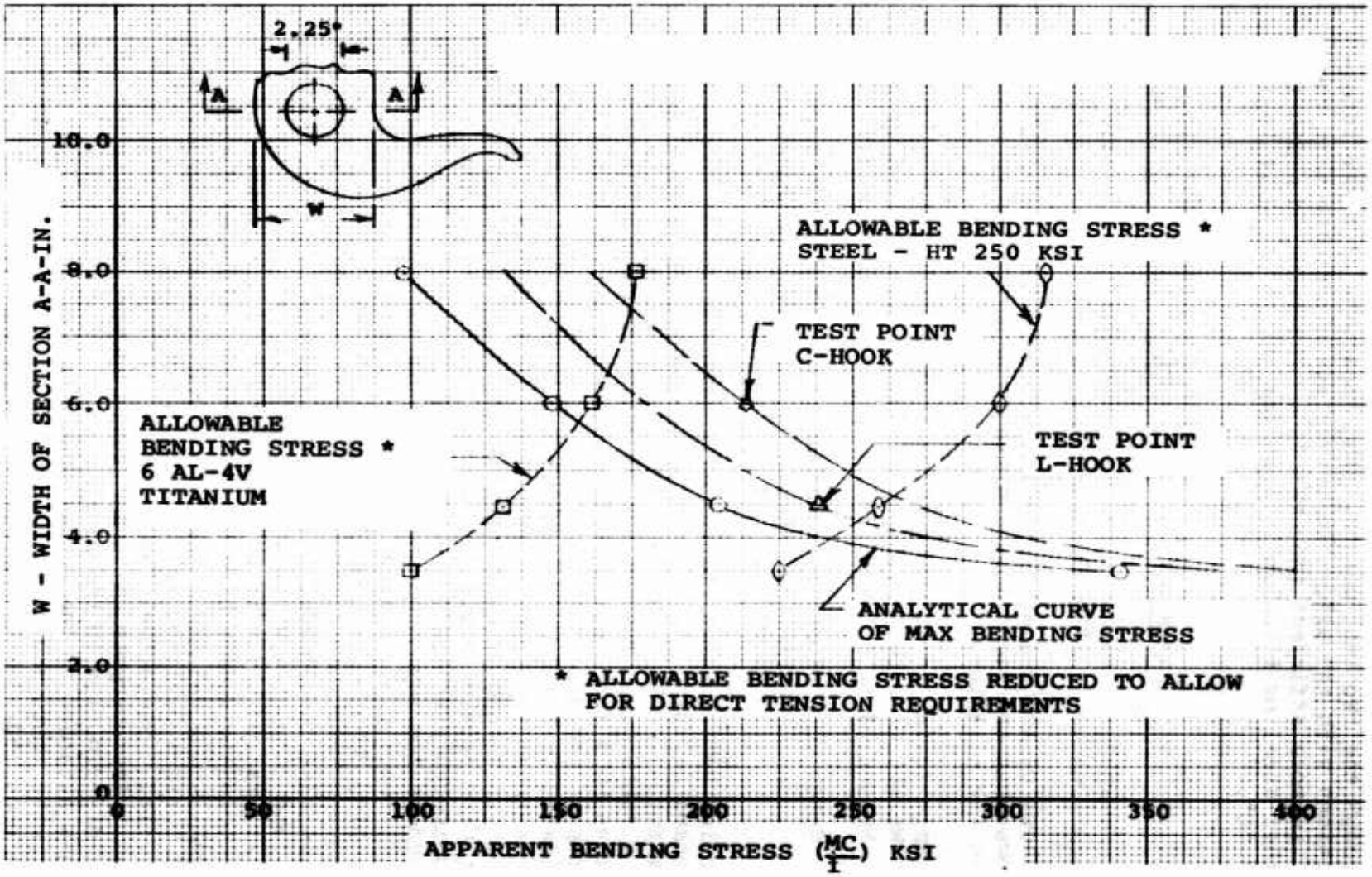

Figure 13. Photoelastic Model of HLH Cargo System Hook.

Curves of the same shape as the analytical curve are drawn through the two test points. The locations of their intersections with the allowable curves again indicate that the "L" is more efficient than the "C". The required width for either steel or titanium is less for the "L" than it is for the "C".

Material	Required Width (in.) "L" Shape	"C" Shape
Steel	4.2	4.6
Titanium	6.4	7.4

A check of the comparative weights of the two shapes also shows that the steel should prove to be a lighter material than the titanium.

Example (using an "L" hook and 3-inch thickness):
Weight of steel = .283 x 3.0 (4.2 - 2.25) = 1.66 lb/in.
Weight of titanium = .163 x 3.0 (6.4 - 2.25) = 2.03 lb/in.

Note: The properties used in the analysis were for Carpenter 455 steel (HT 250 ksi) and 6Al-4V titanium (Ftu = 140 ksi).

Section B-B shown in Figure 14 corresponds to the point of maximum measured stress on the "L" hook. The final shape on the actual hook at this section can be closely approximated by a rectangle. The analytical curve of maximum bending stress in a rectangular section is shown in the figure. A curve of the same shape is then drawn through the test point. Allowable bending stress curves for both steel and titanium rectangular sections are also shown. The location of the titanium allowable curve dictates that the dimensions of a titanium section would have to be greater than those considered practical; i.e., the required depth is 6.9 inches. Based on the foregoing conclusions, it is recommended that an "L" hook configuration be used and that the material selected be a high strength steel (HT 250 ksi).

It is also recommended that this series of tests be followed by (and completed with) strain-gaging of the actual hook configuration while it is undergoing ultimate test. The photoelastic models have been useful in determining relative capabilities but are limited in scope, since they will project the correct distribution only up the elastic limit of the material. The actual load beam is critical under ultimate load. Improvements in design could be more readily made if the distribution in the plastic range is determined. Strain gages attached to the actual load beam can be read during the ultimate test, and the data can be used where modifications are required.

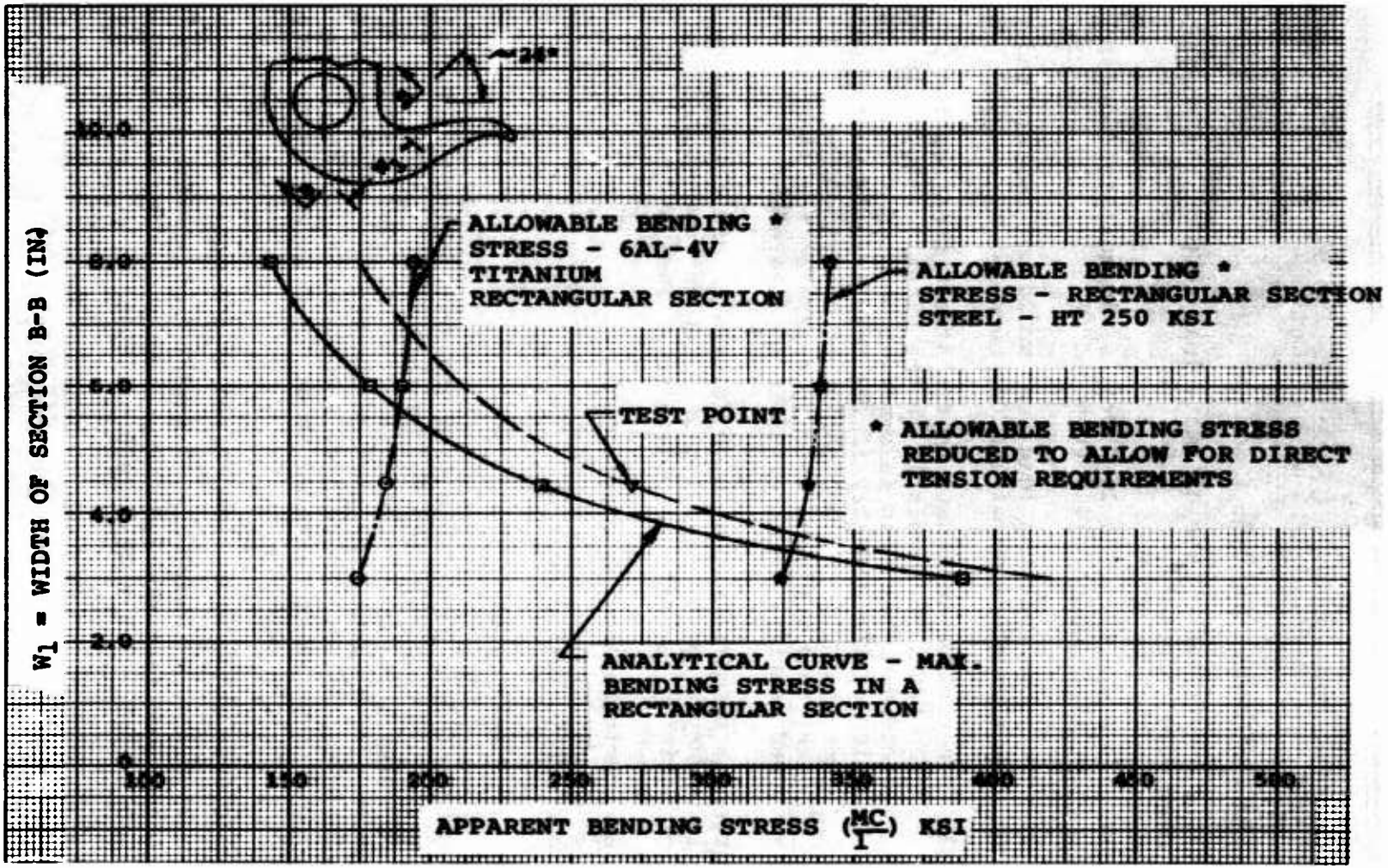

Figure 14. Photoelastic Model of HLH Cargo System Hook.

PART II. FIRST ULTIMATE TEST OF COUPLING LOAD BEAM

DISCUSSION

Task Objectives and Approach

The basic objectives of the ultimate load test on the coupling load beam were threefold:

1. To prove that the load beam would not yield under a limit load of 140,000 pounds.*

2. To prove that the load beam would not rupture under an ultimate load of 210,000 pounds.

3. To provide test data on the stress distribution in the beam, particularly in the plastic range. It was intended that this information be used for modification of the geometry if the test results warranted any changes. A combination of analytical work and test data would be used to determine the location and quantity of material to be altered.

The strength tests required in objectives 1 and 2 could be readily accomplished by a pull test. Methods considered for use in obtaining the data in objective 3 included:

a. Brittle lacquer coating

b. Photoelastic coating

c. Strain gages

The amount of data obtainable from the brittle lacquer method was judged to be too limited to use this method alone. It also appeared that the photoelastic readings would be hazardous to obtain during the latter part of the test, and the cost was considered excessive. Therefore, a combination of stress coat and strain gages was considered to be the best method to obtain the required information.

*The 140,000-pound figure is derived as follows:

System load at design gross weight = 28 tons
Limit load factor = 2.5
Limit load = 2.5 x 28 x 2000 = 140,000

Reviews and Trade-offs

Five steels were considered for the coupling load beam. The major features of each are described below. (Table III lists the mechanical properties.)

Custom 455

A precipitation hardening stainless steel with high strength, good ductility - and toughness. The alloy also has resistance to stress corrosion cracking at high stress levels and good resistance to atmospheric corrosion.

PH 13-8 Mo

The cleanliness of this stainless steel makes it ideal for corrosion-resistant forged parts. It has good strength and good fracture toughness.

Hy-Tuf

An alloy designed for use in the 220 and 240 ksi ultimate tensile strength range. It has good ductility, relatively high impact strength and hardness, and low notch sensitivity. Stress corrosion is not as good as PH 13-8 or Custom 455.

9 Ni-4Co-3C

This alloy has relatively high tensile yield strength, toughness, ductility, and fracture toughness at 220 to 240 ksi ultimate tensile strength. The fracture toughness is superior to other low-alloy steels.

4330M

A low-alloy, high-strength steel with relatively good ductility and good fatigue strength.

Specimen Selection

During use, the load beam will be subject to corrosive environments; consequently, the two stainless steels described above became the prime candidates.

The initial choice was Armco's PH 13-8 Mo. Boeing-Vertol had used the material before and had experienced no manufacturing or heat treating difficulties with it. In checking the availability of this material, it was found that the delivery of forged billets could not be achieved in less than 16 to 18 weeks. This frame did not fit into the

TABLE III. MECHANICAL PROPERTIES

ALLOY / MECH. PROP.	STAINLESS STEELS		LOW-ALLOY STEELS		
	ARMCO PH 13- 8 Mo.	Carpenter Custom 455	Crucible Hy-Tuff	4330 M	Republic 9 Ni-4Co- 3C
H.T. Level (KSI)	215/225	216/224	220/240	220/240	220/240
UTS (KSI)	2.5 Min.	220 Typ.	222 Typ.	220	230
YS (KSI)	200	205	193	185	210
% Elong.	10	9	14	8 (Est)	8 (Est)
% Red.Area	45	35	53	30	30
Endurance Limit (KSI)	105 (K_t =1.0) 40 (K_t =3.8)	94 (K_t = 1.0) 62 (K_t = 3.3)	85 (K_t=1.0) 45 (K_t= 2.5)	110 (K_t=1.0)	 60 (K_t = 25)
Stress Corrosion, K_{iscc} KSI $\sqrt{In.}$	83	58		51	

overall schedule for the coupling assembly. Subsequent investigation also indicated possible serious hydrogen embrittlement problems.

The second choice of material was Carpenter's Custom 455 which was also a stainless steel. Delivery of forged billets was 10 to 12 weeks which fitted into the overall program. Carpenter Custom 455, therefore, was chosen as the load beam material.

Specimen Design Details

The load beam configuration is depicted on Reference 3. Reference 1 defines the shape of the throat and also specifies that a cross section of the load beam in the throat area must be shaped with a 1.5-inch radius in order to minimize the wear with nylon-webbed slings. The cross section also had to be compatible with two 2.0- to 2.5-inch-diameter shackles. Figure 15 shows typical sections through the load beam in the throat area.

A 6.0-inch radius defines the shape of the tongue to minimize the sling wear and to provide a smooth transition as the loaded sling slides off the load beam during the release mode.

Because the material from which the load beam is made, Carpenter Custom 455, is considered to have a transverse strength equal to its longitudinal strength, the trunnion was made integral with the beam. There would have been a risk of loosening with a separate press-fitted shaft.

Keying the shaft to the beam would have introduced stress concentrations from the key way. The stress concentration in the fillet radius at the base of the trunnion was considered to be of lesser importance.

The width of the beam which fits within the side plate housing is machined to a 2.003/1.993 dimension for sealing purposes. For the same reason, the top end of the beam is machined to a 3.745/3.735 radius.

The face of the load beam which contacts the end of the internal lever was machined at an angle to the vertical to insure that the line of action of the reaction at this interface passes below the fulcrum of the internal lever, thus tending to keep the mechanism locked as the applied sling load increases.

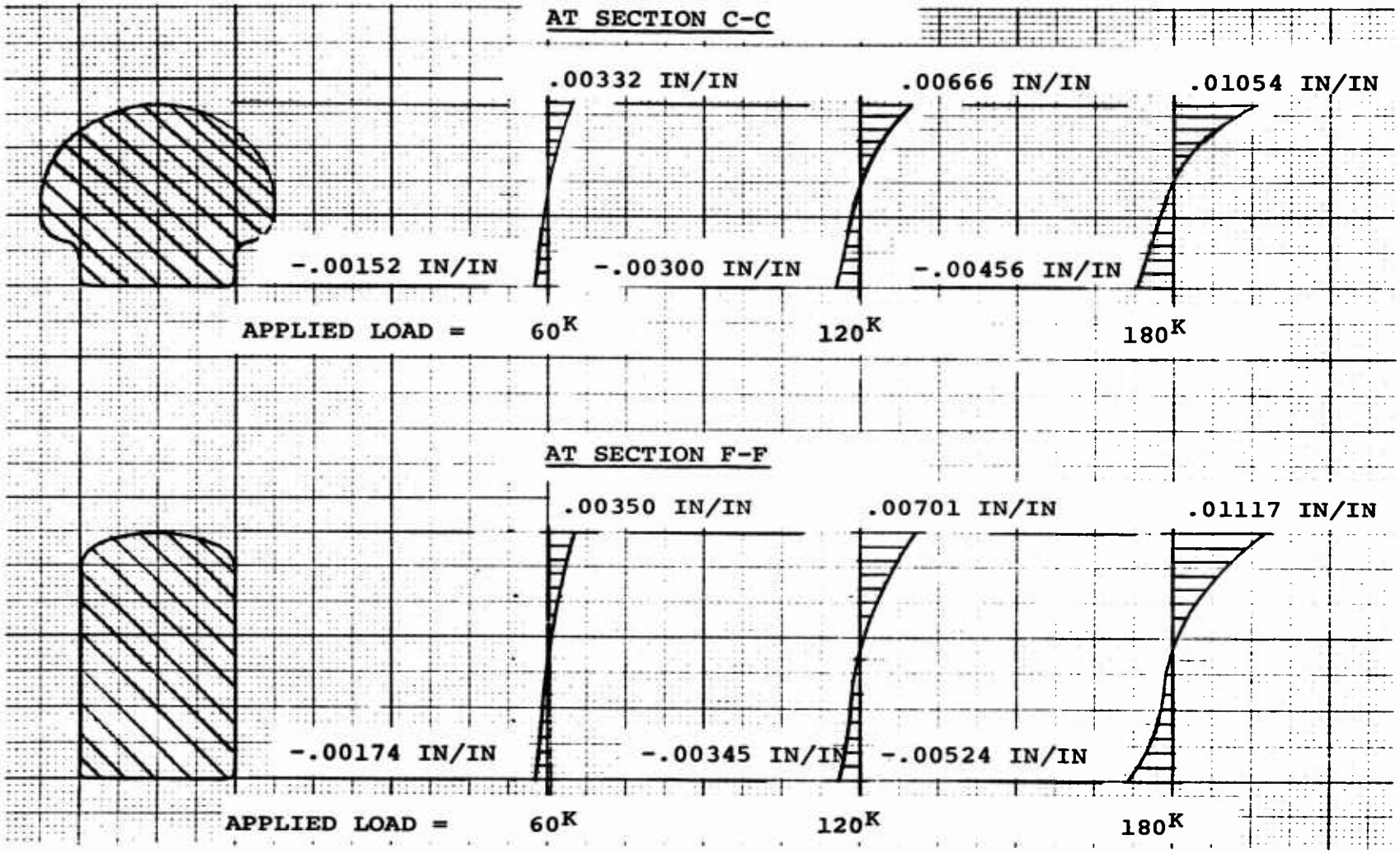

Figure 15. Section C-C.

Fabrication Details

The test load beam was machined from a billet forged by Rankin Forge Company, Braddock, Pennsylvania. The forging process included:

1. Heating to 1950-2200°F.
2. Forged reduction in billet cross section from 7½ x 8½ inches to 5½ x 7½ inches.
3. Reheating to 1950-2200°F.
4. Bending the billet to conform to hook contour.
5. Cooling to room temperature.
6. Annealing the billet at 1500°F for 1 hour and cooling with fans.

Eastern Rotorcraft Company performed a magnetic particle inspection on the billet and verified that the material hardness was not higher than Brinell 331 per AMS 5617.

Laneko Engineering Company, Ft. Washington, Pennsylvania, machined the load beam from the billet. The beam was rough-machined to within one-eighth of its finished contour and then aged per AMS-5617 by the Robert Wooler Company, Dresher, Pennsylvania. It was heated to 950°F, ± 10°, and was held at this temperature for 4 hours and air-cooled.

Test bars were sawn from the billet in accordance with Reference 4 (as shown in Figure 16). These pieces were machined to .252-inch diameter by Eastern Rotorcraft and aged with the rough machine load beam.

After heat-treat, Laneko finish-machined the load beam as shown in Reference 3 (Rev. C). In order to expedite the manufacture, the vendor was requested to omit the retaining ring groove and spring retention slot in the shaft. This would have no effect on the test result.

TEST PROGRAM

Test Plans and Approach

The first two purposes of the test - proof of no yield at limit load and no failure at ultimate - would require a test machine of considerable capacity but relatively simple instrumentation. The third purpose, that of obtaining a stress distribution across the load beam, required a larger number of strain gages.

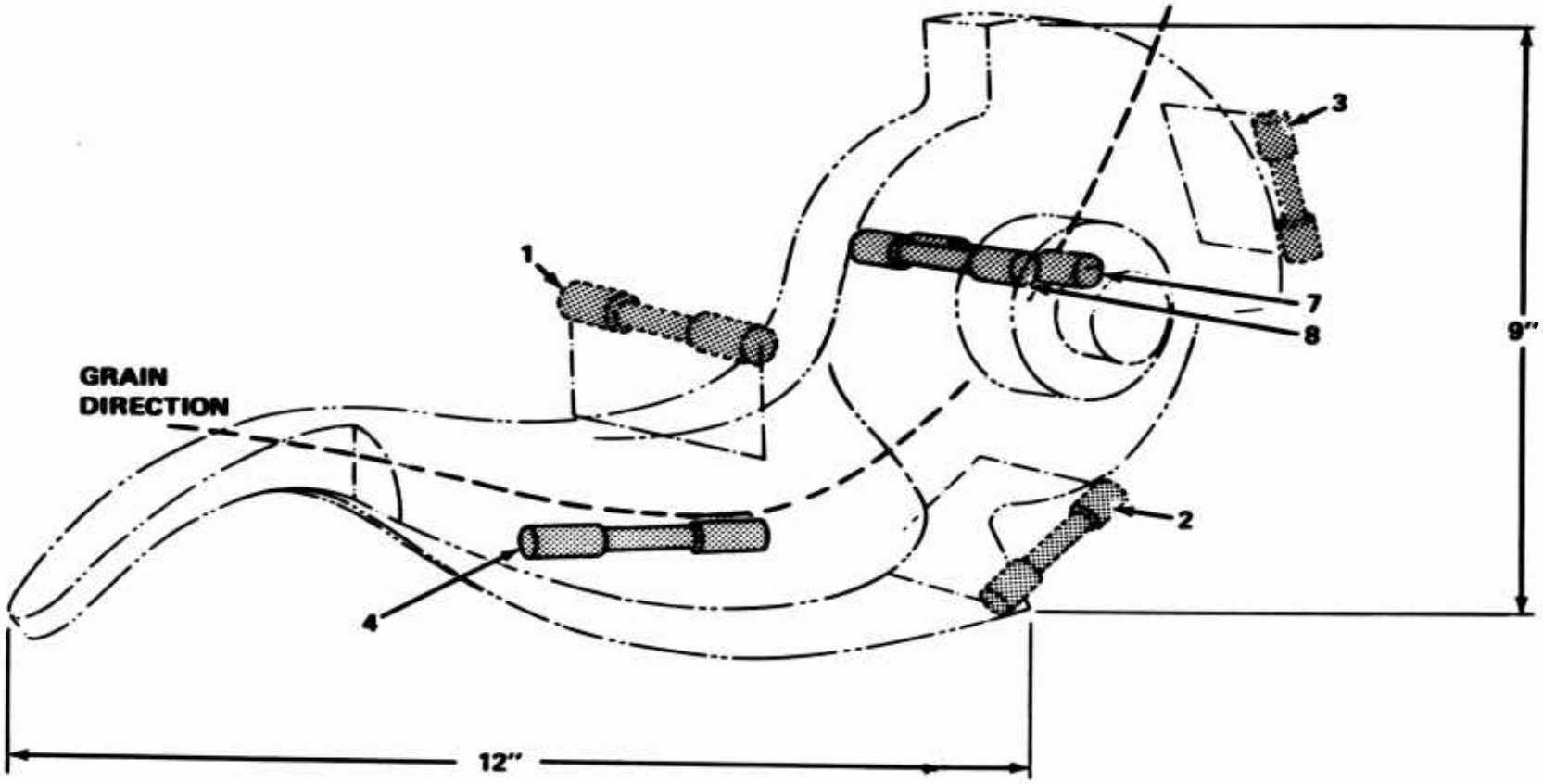

NOTE: 1, 2 AND 3 ARE EXTERNAL SPECIMENS
MADE FROM THE EXCESS BILLET MATERIAL

Figure 16. HLH Coupling Load Beam No. 1 and Tensile Specimens.

The gages were located as shown in Figure 17. Post yield gages were located in areas which were expected to be strained beyond the yield point. Gages were mounted symmetrically on both sides of the beam in several locations (7, 8, 9 and 10) so that unintentional lateral bending would be detected by comparison of the readings.

Prior to the application of strain gages for the main part of the test, stress coat was applied to the load beam and a preliminary test run was made. This was undertaken to verify the analytical location of critical sections and the placing of strain gages.

The three load levels planned for use in the test procedure were as follows, in order of application:

1. 1 "G" level of 56,000 pounds
2. Limit load level of 140,000 pounds
3. To failure, with the required level of 210,000 pounds

A dial gage was to be used to record the deflection at a point on the tongue of the beam. These deflections were to be plotted throughout the limit load test in order to detect yielding. Load was to be applied in the following manner:

1. Establish zero (1000 pounds) for the instrumentation.
2. Gradually apply load to 8000 pounds.
3. Record strains and deflections.
4. Increase load in 8000-pound increments to 56,000 pounds.
5. At each increment of load, record the strains and deflections.
6. Plot deflection curves.
7. Remove load in increments of 8000 pounds.
8. Record strains and deflections at each loading.
9. Repeat this until the whole load is removed.
10. Check deflection curve for permanent set.
11. Gradually apply load in 8000-pound increments to 56,000 pounds.

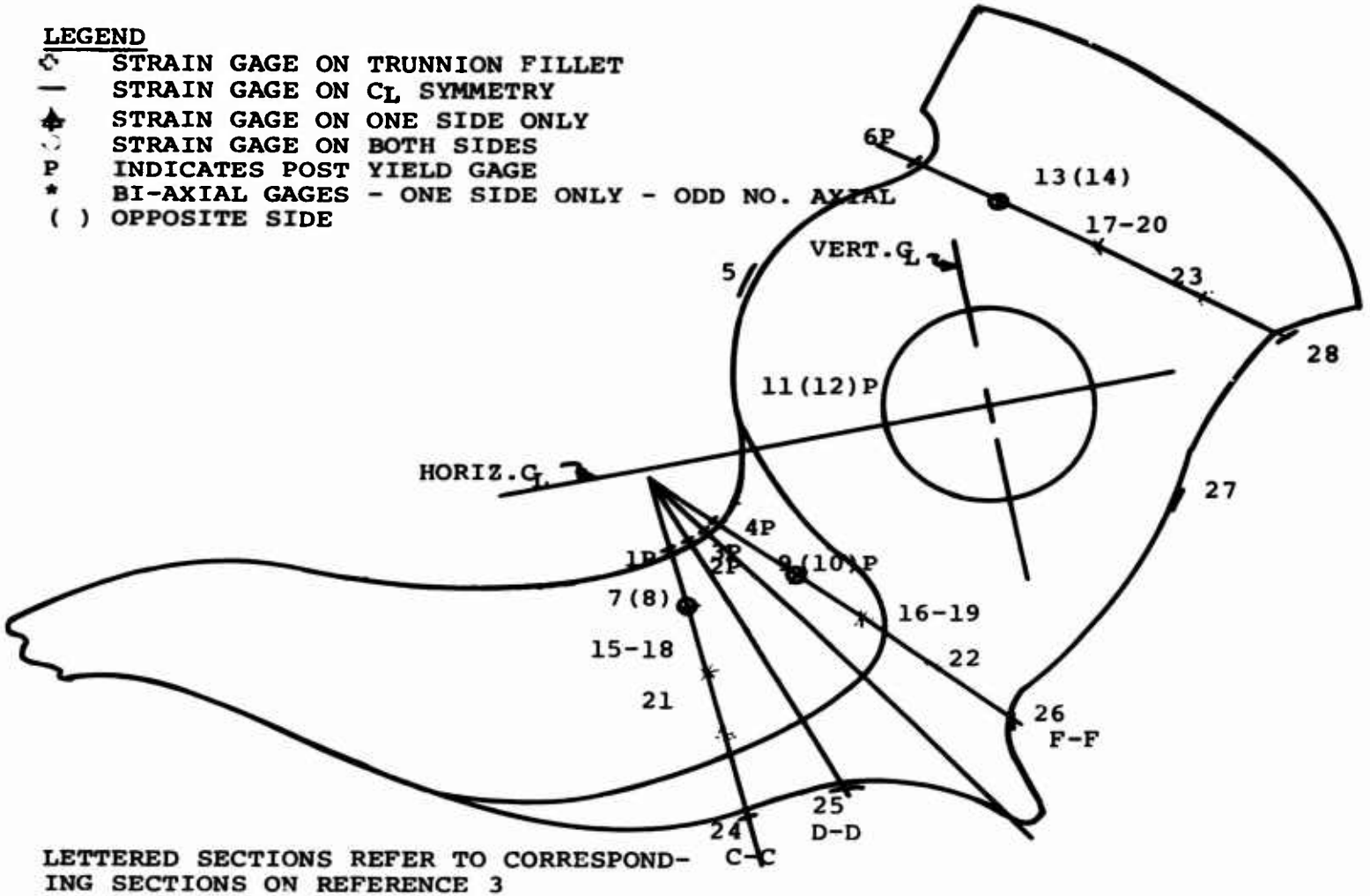

Figure 17. Strain Gage Location.

12. Record strains and deflection at each increment of loading.

13. Plot deflection for each increment of loading.

14. Apply load to 60,000 pounds.

15. Repeat steps 12 and 13.

16. Gradually apply load in 10,000-pound increments to 140,000 pounds.

17. Repeat steps 12 and 13.

18. Remove load in the reverse order.

19. Record strains and deflection at each increment of loading.

20. Check deflection curve for permanent set.

21. Gradually apply load in 8000-pound increments to 56,000 pounds.

22. Record strains and deflection at each increment of loading.

23. Plot deflection for increment of loading.

24. Apply load to 60,000 pounds.

25. Repeat steps 22 and 23.

26. Gradually apply load in 10,000-pound increments to 140,000 pounds.

27. Continue to failure in increments of 10,000 pounds.

28. Record failure point.

Testing Facilities and Instrumentation

The load beam test was performed using a Baldwin-Lima-Hamilton testing machine with a 600,000-pound capacity. A direct readout for the resistance strain gages was provided by a Magnaflux GA-100 strain indicator. Multiple Magnaflux GB-100 switch and balancing units were used to provide a method of observing the output of ten separate installations with the GA-100 strain indicator.

Prior to strain gaging, the initial test was run with the load beam coated with ST-80 stress coat approximately 0.007 inch thick. The ST-80 coating will crack or have a threshold sensitivity when exposed to 500 microinches per inch. This is equivalent to approximately 15,000 psi on the load beam surface.

Test Data Collection, Processing and Analysis

The first run was made to a load level of 56,000 pounds in 8000-pound increments with only the stress coating applied to the beam. The load was held at 56,000 pounds for approximately 15 minutes and then reduced gradually to zero. The beam was removed from the fixture and the crack pattern in the stress coat was observed. The results were satisfactory and the crack intensity confirmed that the critical areas determined by analytical methods were correct. The stress coat was removed, the strain gages were applied, and the load beam was again placed in the fixture. The 28-step test program previously described was then followed.

The final strain gage data was recorded at 180,000 pounds. The load was increased to 190,000 pounds and held for approximately 15 seconds when failure occurred.

The load beam fracture surfaces are shown in Figures 18, 19 and 20. The strain gage readings taken during the last run are listed in Table IV.

Tensile test coupons of the load beam were tested prior to and subsequent to the ultimate test. Data obtained from these coupons are tabulated in Table V. Coupons 1, 2, and 3 were taken from the same forged billet from which the load beam was manufactured and subjected to the same heat treat procedure. Coupons 4, 7 and 8 were cut from the remaining sections of the fractured load beam. The locations from which the test specimens were taken are shown in Figure 16.

Load strain diagrams for the six tensile specimens developed from the tensile coupon tests are shown in Figures 21 and 22. The material was designated to meet AMS specification 5617. The specification requirements for the longitudinal specimens are as follows:

F_{tu} = 220,000 psi minimum

F_{ty} = 205,000 psi minimum

Percentage elongation = 10% minimum

Percentage reduction in area = 40% minimum

Figure 18. Load Beam Fractures.

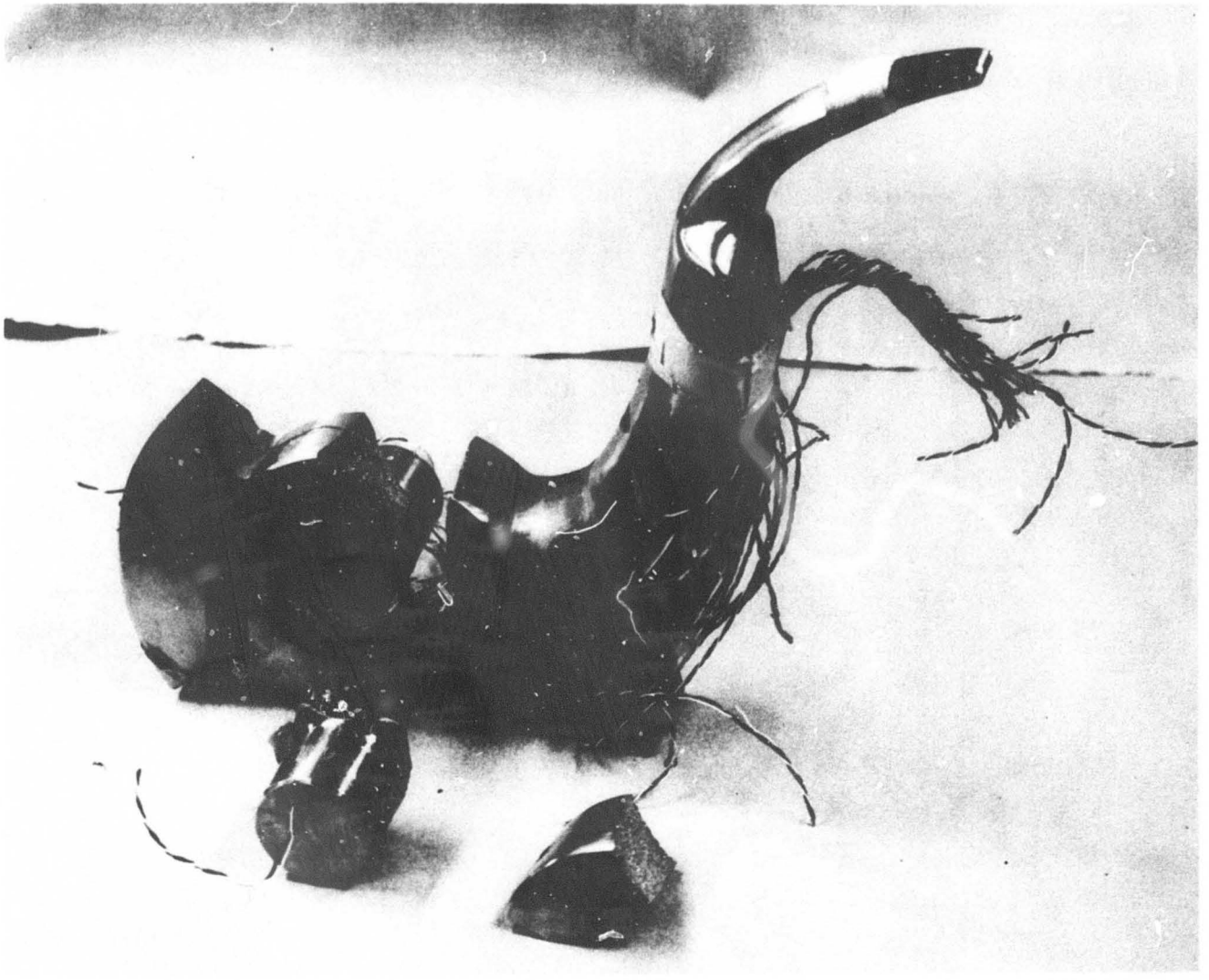

Figure 19. Load Beam Fractures.

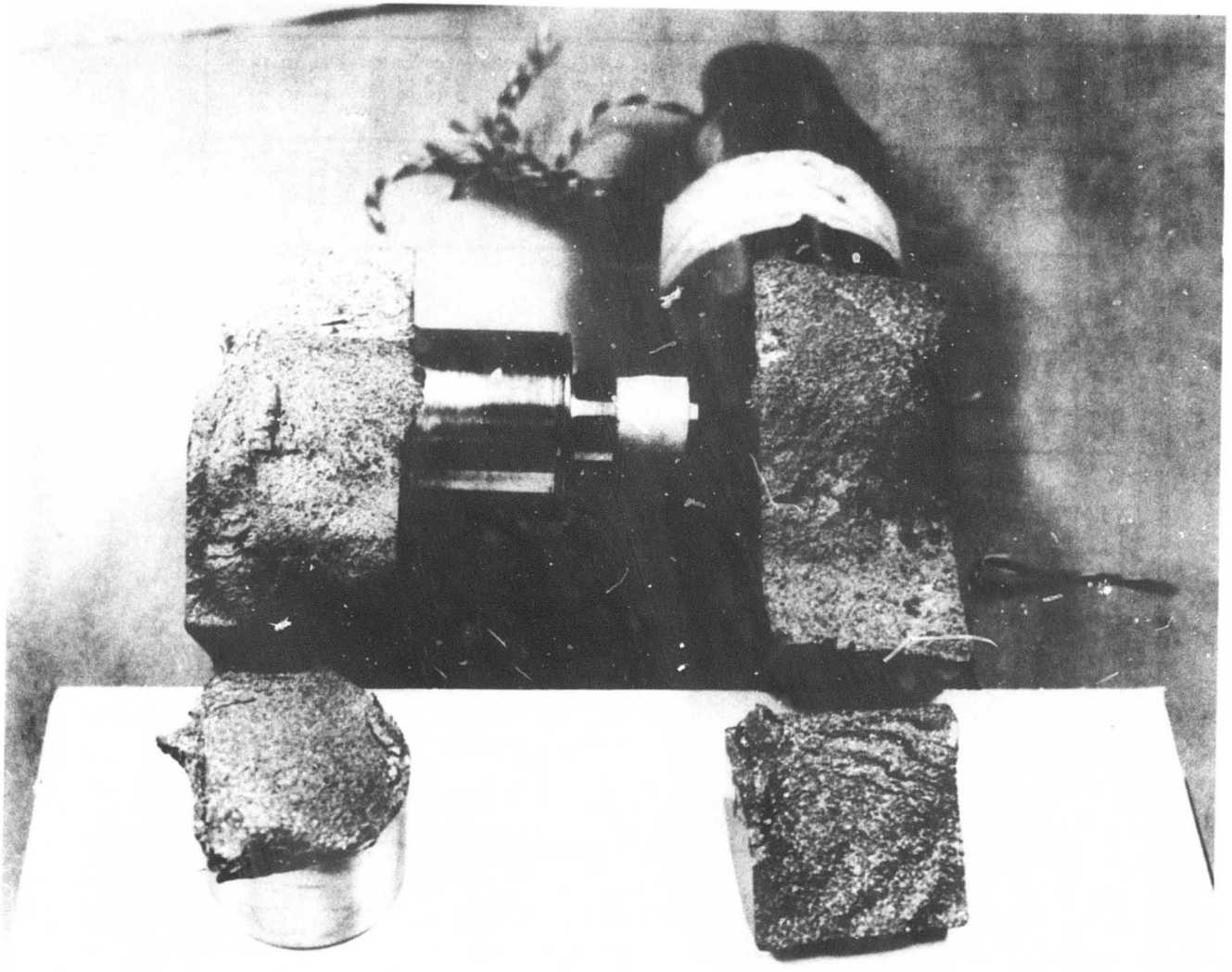

Figure 20. Load Beam Fractures.

TABLE IV. STRAIN GAGE READING IN MICROINCHES PER INCH

GAGE NO.	APPLIED LOAD "P" - FIG. 27 (KIPS)								
	1	8	16	24	32	40	48	56	60
1	0	396	844	1300	1745	2210	2650	3105	3320
2	↑	425	914	1404	1887	2387	2866	3353	3586
3		442	953	1457	1959	2475	2978	3475	3725
4		420	904	1375	1843	2330	2797	3265	3500
5		100	213		416	518	618	720	772
6		145	452	1050	1627	2216	2756	3310	3566
7		82	193	295	404	515	622	730	788
8		132	272	408	545	685	818	956	1022
9		97	232	360	497	640	782	925	1000
10		181	370	555	733	917	1097	1276	1363
11		-284	-593	-855	-1121	-1392	-1658	-1923	-2055
12		-270	-560	-800	-1047	-1302	-1557	-1814	-1942
13		79	157	195	233	271	308	345	362
14		90	167	205	239	272	306	345	362
15		- 27	- 57	- 88	- 115	- 143	-170	- 195	- 207
16		61	130	195	257	322	382	444	475
17		20	37	32	30	27	23	18	16
18		15	30	45	62	79	94	108	117
19		- 51	- 98	-147	- 190	- 232	-274	- 314	- 334
20		- 20	- 38	- 32	- 20	- 12	- 1	5	9
21		-110	-232	-350	- 470	- 588	-705	- 821	- 880
22		- 96	-200	-299	- 395	- 492	-588	- 684	- 729
23		- 23	- 58	-107	- 152	- 197	-243	- 290	- 310
24		-183	-394	-600	- 805	-1012	-1218	-1420	-1520
25		-178	-385	-590	- 793	- 999	-1204	-1404	-1501
26		-206	-443	-682	- 915	-1156	-1390	-1621	-1735
27	↓	-187	-403	-621	- 832	-1048	-1263	-1473	-1576
28	0	-106	-245	-413	- 575	- 740	- 903	-1063	-1142

ELECTRICALLY BALANCED

TABLE IV - Continued

GAGE NO.	APPLIED LOAD "P" - FIGURE 27 (KIPS)							
	70	80	90	100	110	120	130	140
1	3880	4444	4980	5536	6100	6656	7226	7780
2	4195	4800	5400	5983	6605	7191	7802	8418
3	4350	4977	5595	6204	6852	7462	8100	8746
4	4085	4668	5245	5826	6418	7007	7573	8168
5	902	1030	1158	1287	1414	1542	1664	1792
6	4242	4896	5535	6174	6803	7418	8040	8660
7	926	1067	1205	1344	1484	1624	1766	1950
8	1192	1360	1521	1603	1849	2014	2178	2344
9	1184	1370	1555	1740	1940	2133	2330	2532
10	1582	1802	2014	2230	2452	2655	2868	3075
11	-2390	-2719	-3040	-3360	-3687	-4000	-4307	-4608
12	-2268	-2585	-2888	-3200	-3570	-3803	-4108	-4394
13	408	452	496	540	586	631	678	725
14	410	459	508	557	608	659	711	763
15	- 238	- 267	- 295	- 322	- 350	- 376	- 402	- 427
16	550	626	698	770	845	915	990	1062
17	10	6	2	- 4	- 6	- 8	- 10	- 14
18	135	154	171	186	205	225	240	257
19	- 380	- 426	- 470	- 512	- 552	- 591	- 628	- 669
20	20	30	43	56	70	81	92	104
21	-1025	-1170	-1308	-1446	-1587	-1727	-1862	-2010
22	- 850	- 970	-1077	-1190	-1303	-1415	-1520	-1632
23	- 367	- 424	- 477	- 530	- 584	- 637	- 685	- 740
24	-1770	-2022	-2263	-2510	-2757	-3000	-3240	-3487
25	-1752	-2002	-2244	-2489	-2735	-2976	-3218	-3464
26	-2030	-2320	-2596	-2882	-3171	-3446	-3725	-4010
27	-1841	-2106	-2360	-2620	-2878	-3133	-3386	-3640
28	-1341	-1538	-1727	-1919	-2111	-2296	-2484	-2670

TABLE IV - Continued

GAGE NO.	APPLIED LOAD "P" - FIGURE 27 (KIPS)				
	150	160	170	180	190
1	8390	9070	9785	10543	FAILURE AT 190K (AFTER APPROXIMATELY 15 SECONDS AT LOAD)
2	9134	9960	10842	11775	
3	9565	10526	11574	12700	
4	8822	9545	10340	11170	
5	1915	2040	2160	2282	
6	9346	10092	10875	11672	
7	2074	2245	2420	2606	
8	2520	2705	2895	3110	
9	2745	2972	3220	3480	
10	3300	3525	3770	4030	
11	-4873	-5110	-5355	-5600	
12	-4642	-4872	-5103	-5337	
13	773	825	886	946	
14	818	807	925	983	
15	- 451	- 475	- 500	- 520	
16	1140	1225	1311	1404	
17	- 15	- 20	- 17	- 15	
18	275	292	310	315	
19	- 705	- 740	- 775	- 806	
20	119	133	145	155	
21	-2155	-2305	-2462	-2615	
22	-1745	-1860	-1983	-2100	
23	- 792	- 847	- 900	- 952	
24	-3740	-4010	-4283	-4565	
25	-3716	-3985	-4256	-4542	
26	-4300	-4610	-4917	-5244	
27	-3896	-4162	-4423	-4690	
28	-2866	-3064	-3259	-3454	

TABLE V. RESULTS IN TENSILE SPECIMEN TESTING

Specimen No.	UTS (KSI)	YTS (KSI)	% Elong.	% RA	Grain Dir.	Remarks
1	225	218	1.5	5.6	T	For
2	225	215	3.5	10.8	L	Specimen
3	225	216	1.0	2.4	T	Location
4	234	220	2	4.2	L	see Fig. 16
7	234	228	5	12	T	
8	235	228	5	8	T	

NOTES

L - Longitudinal

T - Transverse

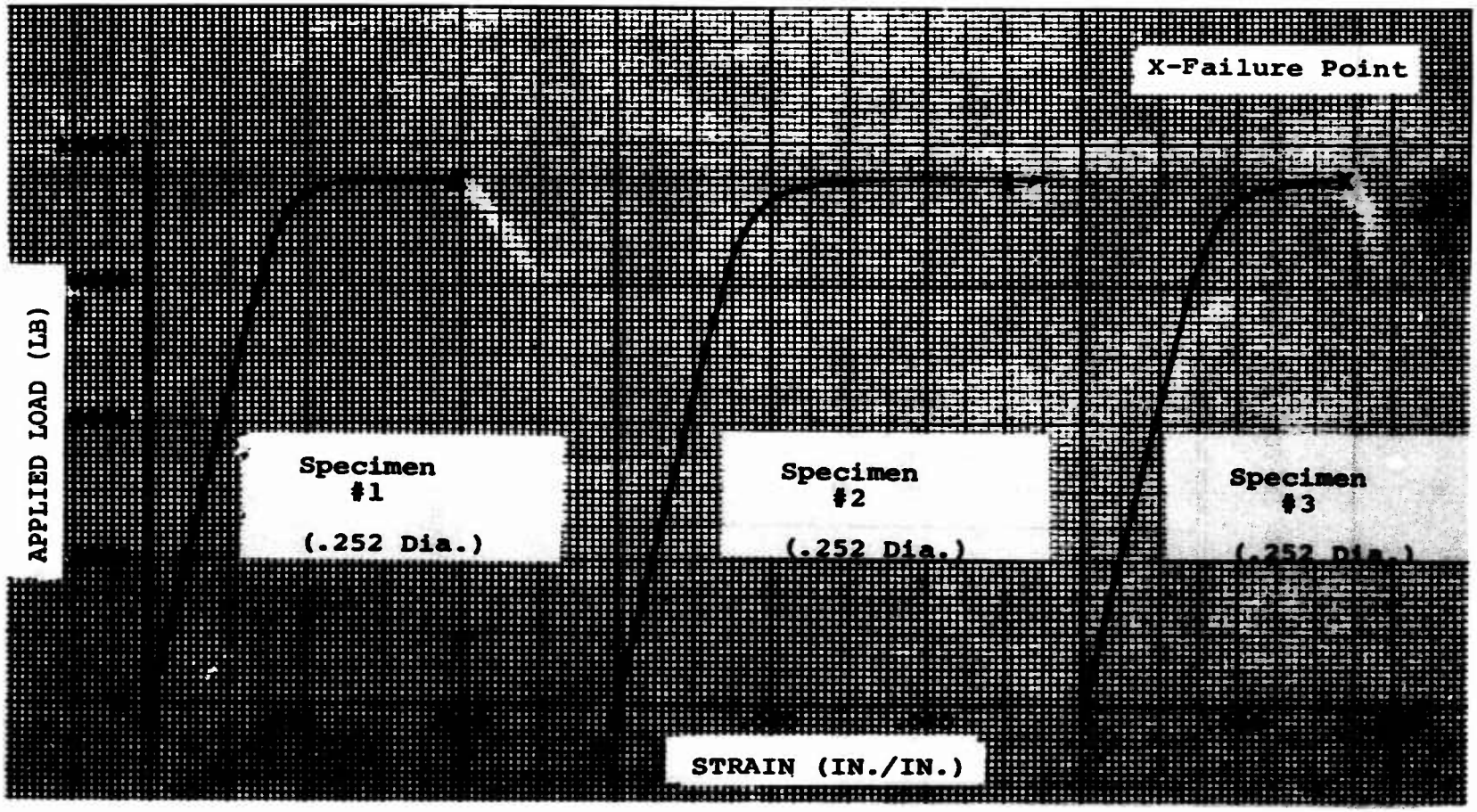

Figure 21. Test Specimen Load-Strain Curves for Specimens No. 1, 2 and 3.

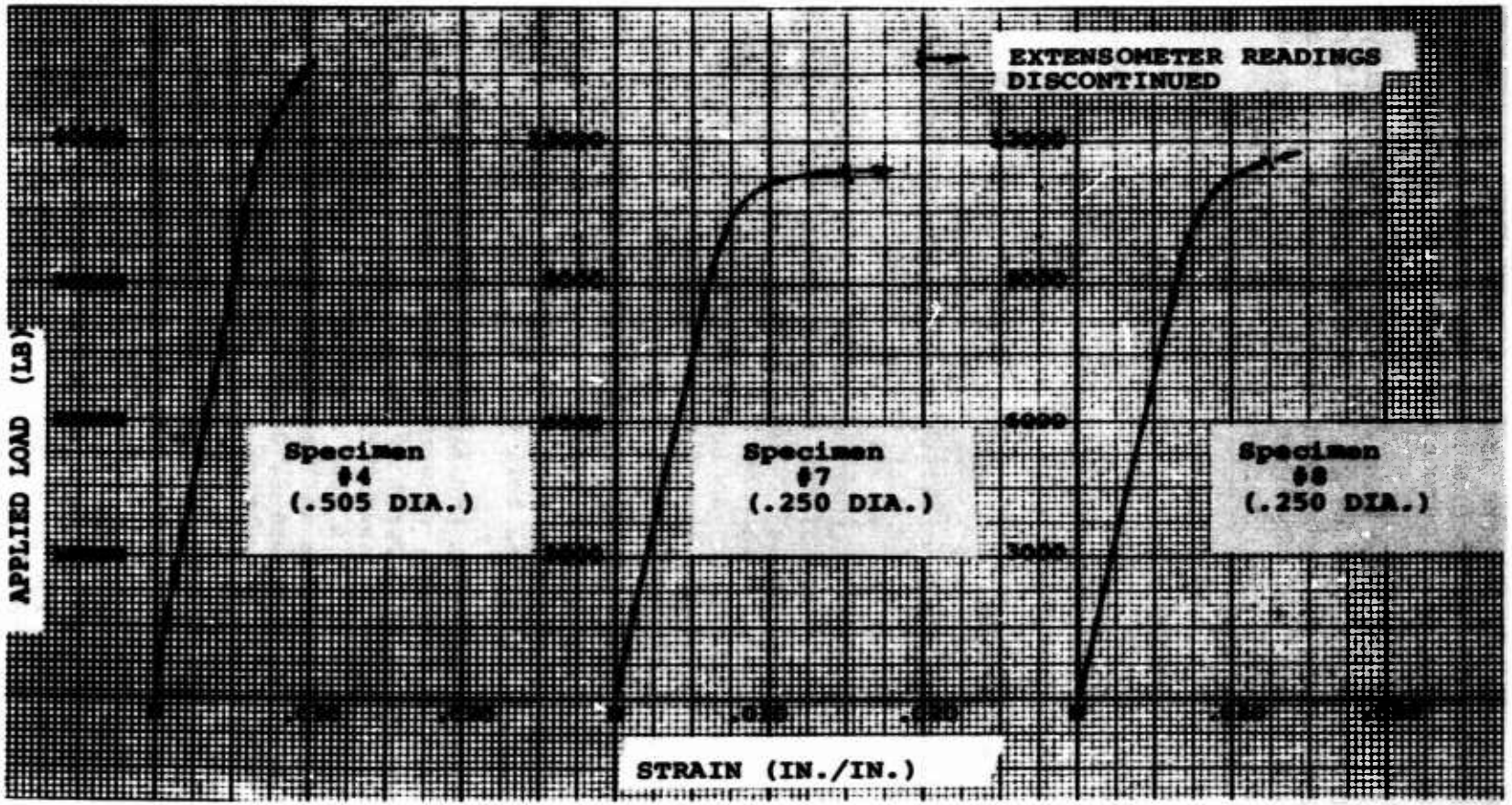

Figure 22. Test Specimen Load-Strain Curves for Specimens No. 4, 7 and 8.

All of the specimens met the preceding strength requirements, but none of the specimens met the stipulated percentage elongation or percentage reduction in area.

The ductility of the load beam was therefore considerably less than expected. The amount of necking down at failure on Specimens 3 and 7 is compared visually with a dimensionally similar steel specimen (Specimen A) in Figure 23. Specimen A was cut from a 4340 steel forging with the following physical properties:

F_{tu} = 152,000 psi

F_{ty} = 140,000 psi

Percentage elongation = 12

Percentage reduction in area = 31.3

The points of fracture on all three specimens are indicated by arrows.

Plots of extreme fiber stress versus load are shown in Figures 24 to 26. None of the locations show a strain level which would be high enough to precipitate a failure in a normal ductile steel specimen; i.e., the maximum strain gage reading at any gage at an applied load of 180,000 pounds was .0127 in./in. (gage 3). This corresponds to an elongation of 1.27 percent.

The strain distributions across Sections C-C and F-F (Figure 17) are shown in Figure 15. The interior (concave) surfaces of both sections show some plasticity, but failure at the trunnion prevented this effect from fully developing.

Boeing fracture analysis indicated a fracture origin in the trunnion fillet radius. All other cracks in the load beam were secondary to this point of initiation. This conclusion is substantiated by an examination of strain gage readings. Figure 27 shows that at a load magnitude of 180,000 pounds the strain gage readings increase from gage 1 to 2 to 3 and then start to decrease at gages 4 and 5. Fracture points A and B (Figure 27) between gages 4 and 5, and 5 and 6, respectively, are at lower stress levels than other surface areas and are therefore not the initial fracture points.

Destructive metallurgical examination revealed an ASTME 112 grain size of 1 to 2 at the fracture surface. Normal grain size expected for this corrosion-resistant steel is an average of No. 5. The large grain is detrimental to both notch tensile strength and fracture toughness.

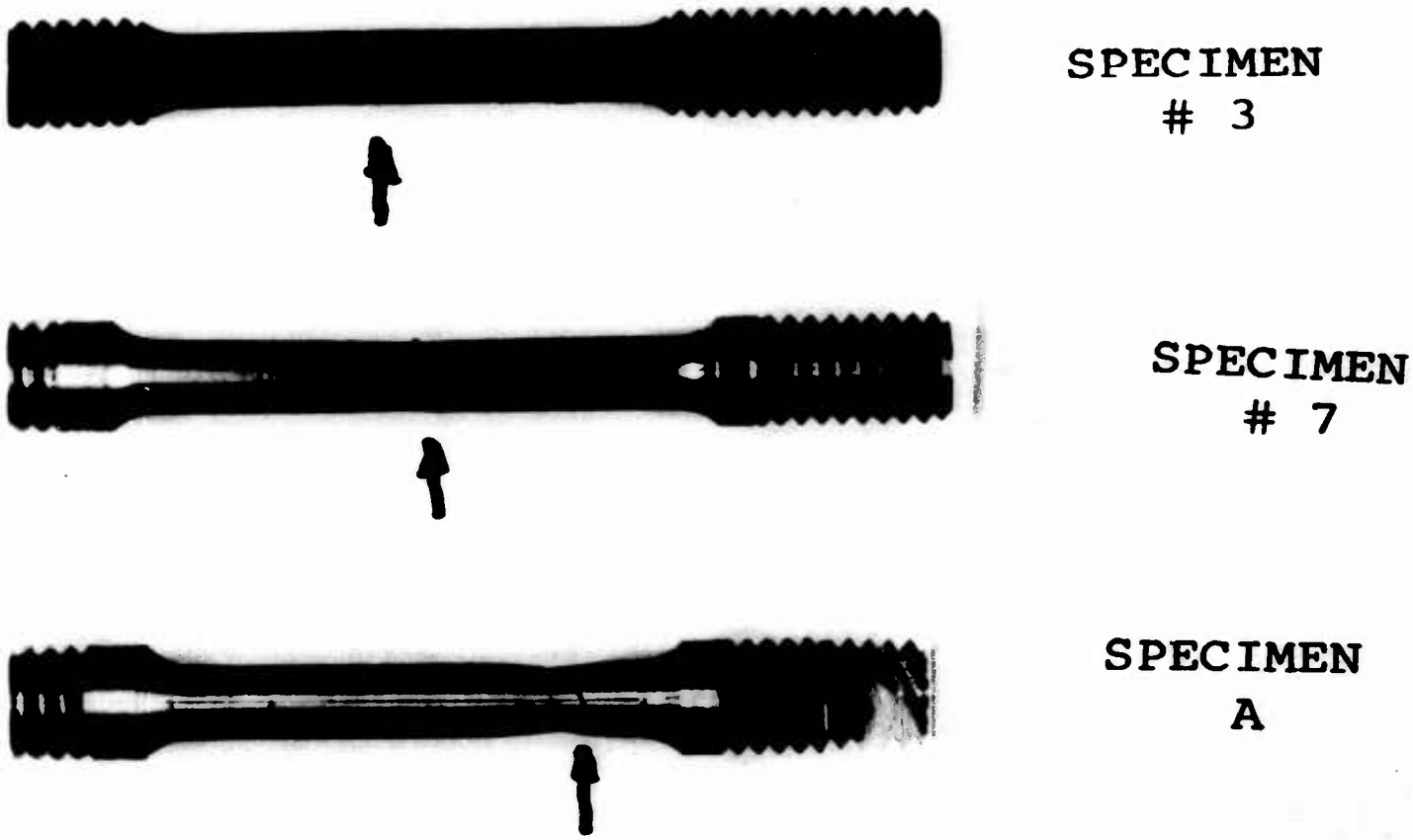

Figure 23. Necking Down at Failure.

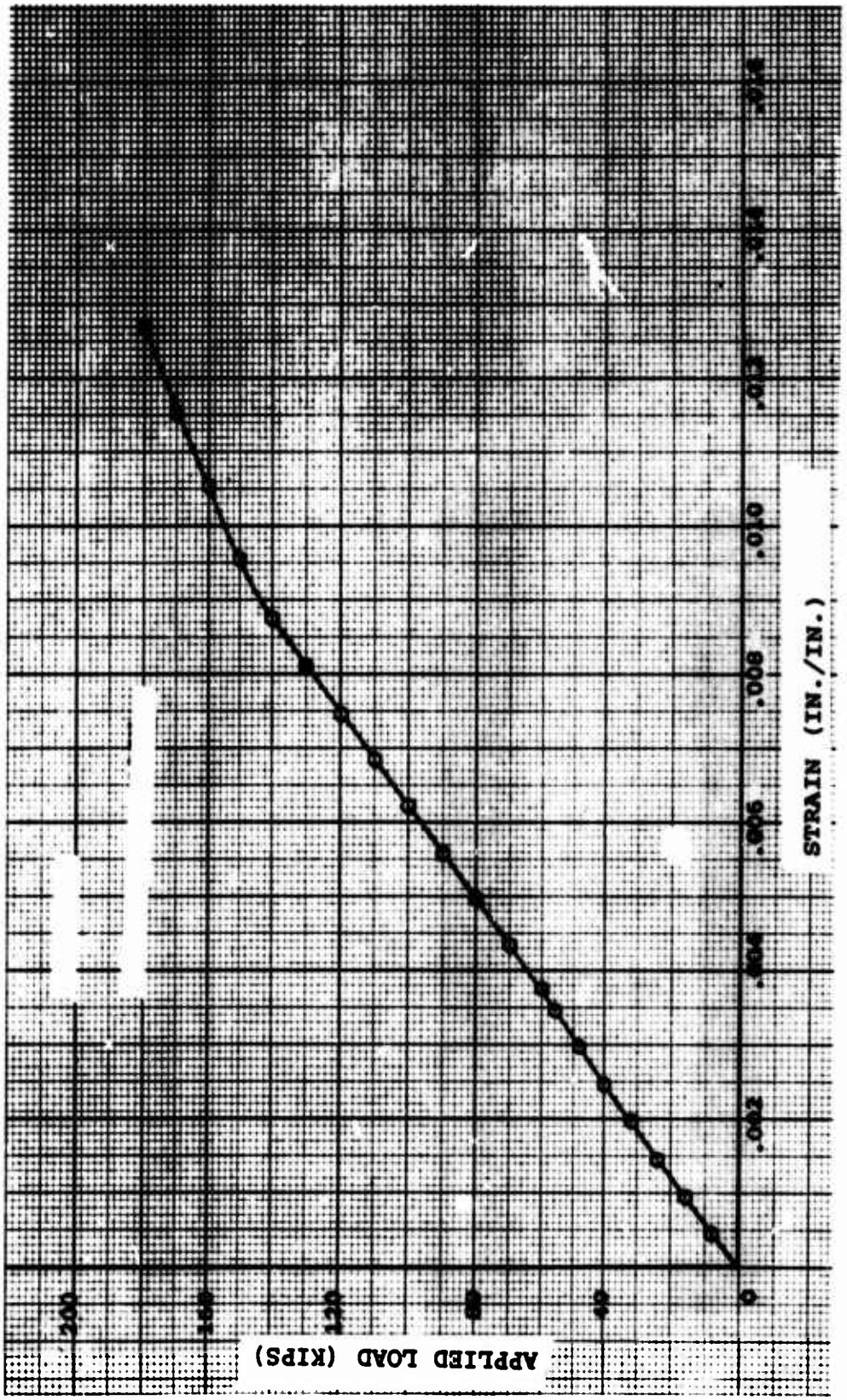

Figure 24. Load Versus Strain (Gage No. 3).

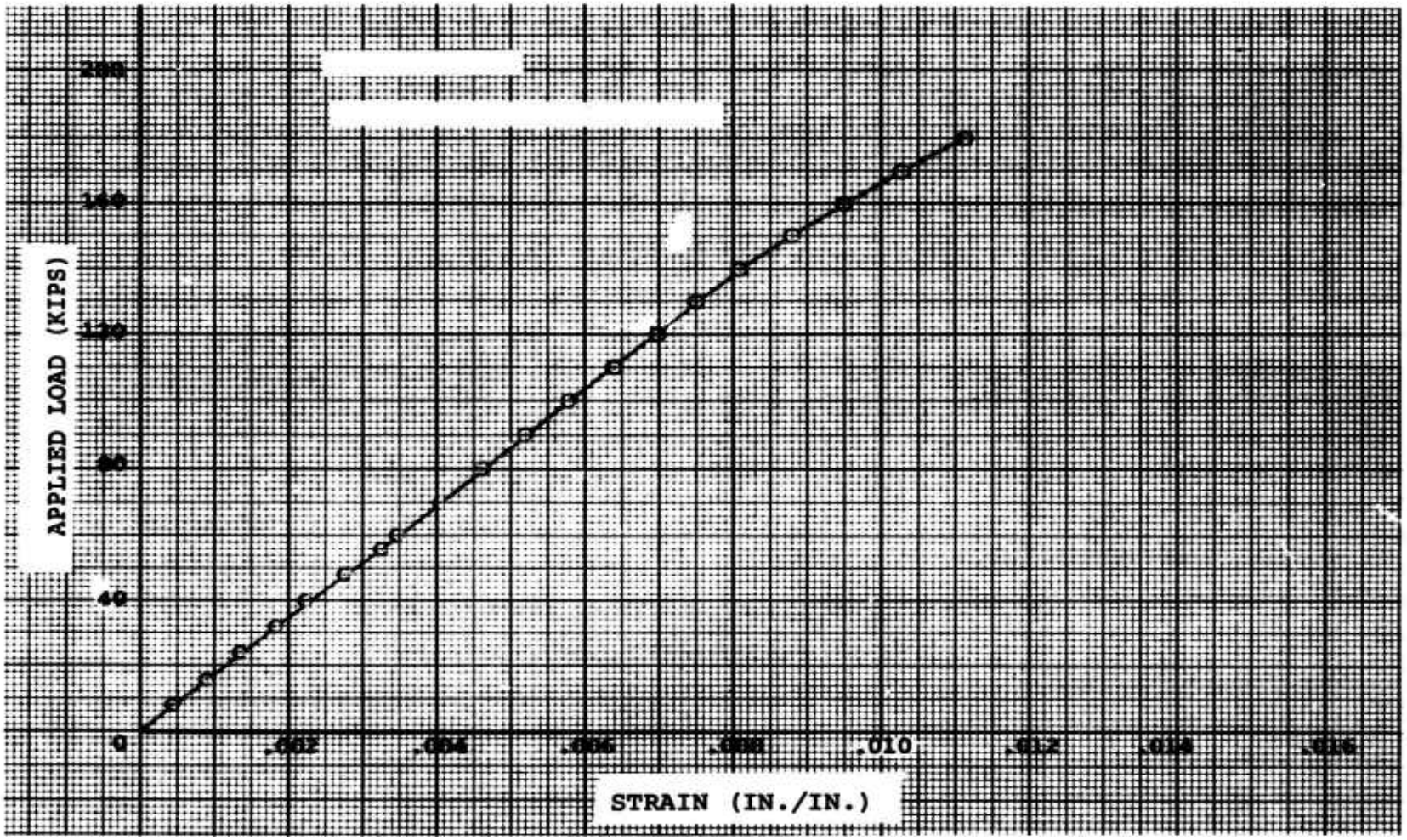

Figure 25. Load Versus Strain (Gage No. 4).

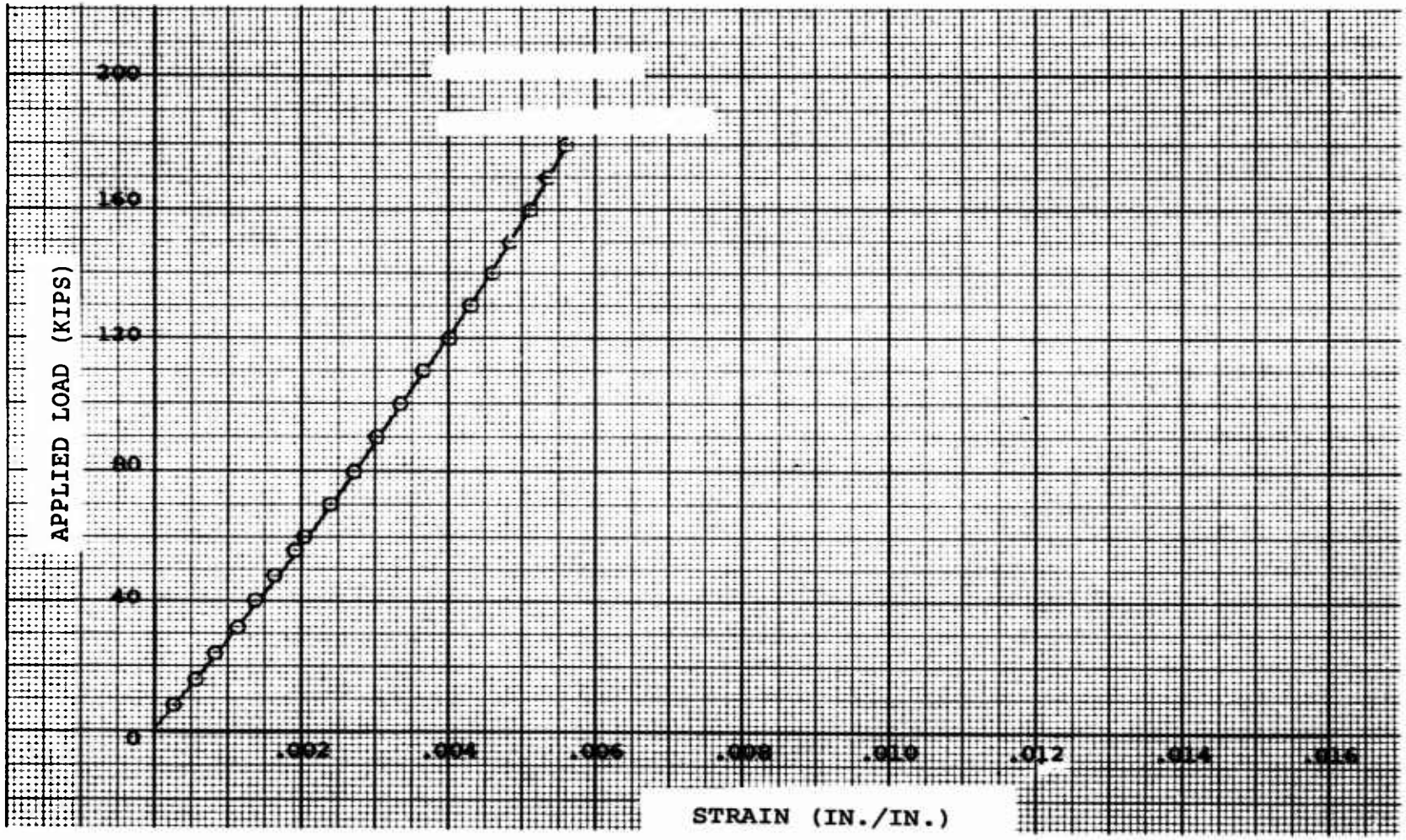

Figure 26. Load Versus Strain (Gage No. 11).

GAGE NO.	ϵ at P = 180^K (IN/IN.)
1	.010543
2	.011775
3	.012700
4	.011170
5	.002282
6	.011672

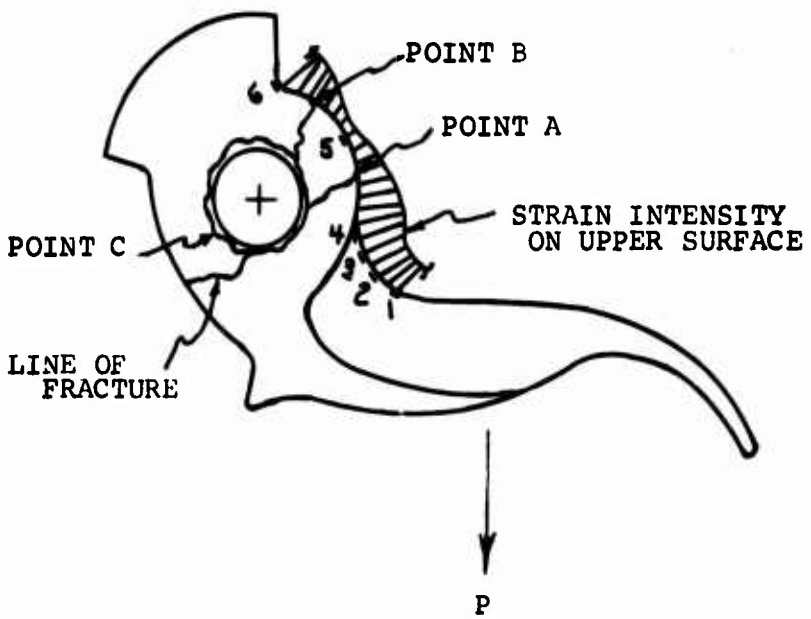

Figure 27. Fracture Points.

Test strain gage readings on Gage No. 11 at 180,000 pounds load equals .0056 in./in. (see Table IV).

This corresponds to a stress level of 150,000 psi based on the test results of Specimen No. 2, and also correlates with the calculations shown on Figure 28.
From Reference 5, based on the geometry shown on the previous page, $K_t = 1.95$.

This factor is not normally used in an ultimate analysis. It does, however, indicate the factor by which the nominal stress is increased due to the change in section. If the material is not ductile enough to redistribute the stress by local yielding, then the stress level would be high enough to precipitate a failure,

$$f_t = 1.95 \times 150{,}000 = 293{,}000 \text{ psi}$$

At a meeting held at Eastern Rotorcraft Company on September 12, 1972, representatives of the following companies were present:

Boeing-Vertol
Eastern Rotorcraft
(Responsible to Boeing for overall design of coupling)
Cartech
(Supplier of basic steel in ingot form)
Wooler
(Responsible for heat treatment of materials)
Rankin-Forge
(Responsible for forging)

It was concluded by the representatives of these companies that the loss of ductility and the improper grain size were due to incorrect forging procedure. As previously described, the forging vendor had reheated the billet subsequent to the bending operation, contrary to recommended practice, and had not met the minimum reduction in cross-sectional area of 2 to 1 following the final heating.

TASK CONCLUSIONS AND RECOMMENDATIONS

Conclusions

Based on the coupon testing, load beam strain gage readings, metallurgical examination and analytical procedures described in the (Part II) Test Program Section, it is concluded that the low ductility of the material was the most important factor in the inability of the load beam to reach its ultimate design load.

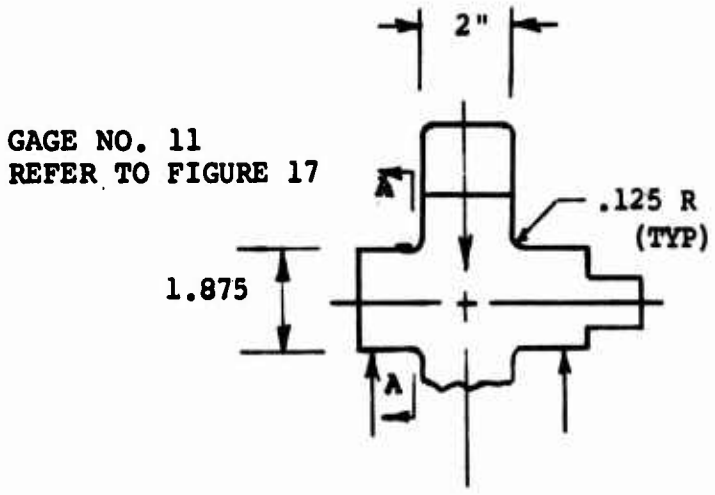

Section at
Trunnion

From Ref 6, Appendix III, Page 10
When hook load = 210,000 lb
f_b at A-A = 184 ksi
(No concentration factor used)

When hook load = 180,000 lb
f at A-A = $\frac{180}{210}$ x 184 = 157 ksi

Figure 28. Section at Trunnion.

Recommendations

It is recommended that new billets and load beams be obtained using the correct forging procedure and that Specification BMS 7-213 be used instead of Specification AMS 5617 in the call-out for the material. The BMS specification is more stringent and guarantees cross-grain properties as well as longitudinal properties.

It is also recommended that the stress concentration at the junction of the trunnion and load beam body be reduced and that a maximum acceptable grain size be stipulated on the drawing.

PART III. SECOND ULTIMATE TEST OF COUPLING LOAD BEAM

DISCUSSION

Task Objectives and Approach

An improved material and a new configuration were to be tested, with objectives almost identical to the first ultimate test:

1. To prove that the modified design could sustain a limit load of 140,000 pounds without yielding
2. To prove that the modified design could sustain an ultimate load of 210,000 pounds without rupture
3. To obtain sufficient information on the stress distribution in the new load beam so that any necessary modifications could be made

The approach used was that the new test specimen must be proved to be satisfactory but that needless repetition of data would be avoided. Strain gages were again chosen for obtaining data, but the number of gages was reduced considerably and no stress coat was applied. As the initial test plan had proved to be satisfactory, it was used again.

Reviews and Trade-offs

As recommended in Part II of this report, the material specification was changed from AMS 5617 to BMS 7-213. A comparison of the minimum physical properties attained by use of the two specifications is shown in Table VI. The strength and ductility properties in the longitudinal direction are the same under both specifications, but the advantage gained by using BMS 7-213 material is that reasonable properties are also guaranteed in the long transverse direction. Although neither specification guarantees properties in the short transverse direction, applied stresses to the load beam along this axis are considered to be low enough to present no problem.

The design of the initial load beam utilized a trunnion which was an integral part of the beam. The premature failure of this beam was shown to have been primarily due to a combination of the poor ductility along the axis of the trunnion and the stress concentration at the base fillet radius. Changing the design to include a separate trunnion shaft would result in the advantages of having superior longitudinal physical properties along the axis of the trunnion as well as removal of the fillet concentration. It would, however, also reduce the

TABLE VI. COMPARISON OF PHYSICAL PROPERTIES -- SPECIFICATIONS AMS 5617 AND BMS 7-213

PROPERTIES \ SPECIFICATION	AMS 5617			BMS 7-213 (H 950)		
	L.	L.T.	S.T.	L.	L.T.	S.T.
Ftu (ksi)	220	▲	▲	220	220	▲
Fty (ksi)	205			205	205	
% Elongation	10			10	5	
% Reduction in Area	40			40	20	

L = Longitudinal
L.T. = Long Transverse
S.T. = Short Transverse
▲ = Minimum properties in this direction are not stipulated

basic bending section of the beam in a section through the trunnion and therefore weaken this area.

Analytical work indicated that the basic section would be sufficiently strong with the center area removed, and it was therefore decided to make the trunnion a separate shaft as shown in Figure 29.

Specimen Design Details

The configuration of the load beam was essentially the same as had been used on the previous design. The major change was in the trunnion area. The trunnion was made into a separate shaft which was now pressed into the main load beam with a .001/.002 interference fit. The ℄ of the new shaft was retained in the same location as the previous trunnion so that the components of the release mechanism could also remain the same.

Fabrication Details

The billet was forged to BMS Specification 7-213, Grade 1 by Carpenter Technology Corporation, Reading, Pennsylvania.

The beam was rough machined to within 1/8 inch of its finished contour and the shaft to within 1/32 inch of finished size. Both parts and the three tensile specimens shown in Figure 30 were solution heat treated to 1525°F ±25° and soaked for 2 hours after reaching this temperature and then rapidly force cooled in a nitrogen atmosphere to room temperature. They were then aged in air to 955°F ±5° for 4 hours. The finished hardness was Rockwell C44 to C48. After a magnetic particle inspection, the load beam was finished machined to the dimensions of Reference 9 and the shaft to the dimensions of Reference 7.

After inspection, the load beam was heated to 180°F and the shaft cooled to -40°F. The shaft was then pressed into the beam.

TEST PROGRAM

Test Plans and Approach

The test plan from the first ultimate test was repeated with runs of increasing load intensity to:

a.	1 "G"	- 56,000 lb	
b.	Limit Load	- 140,000 lb	
c.	Failure Load	- 210,000 lb	required

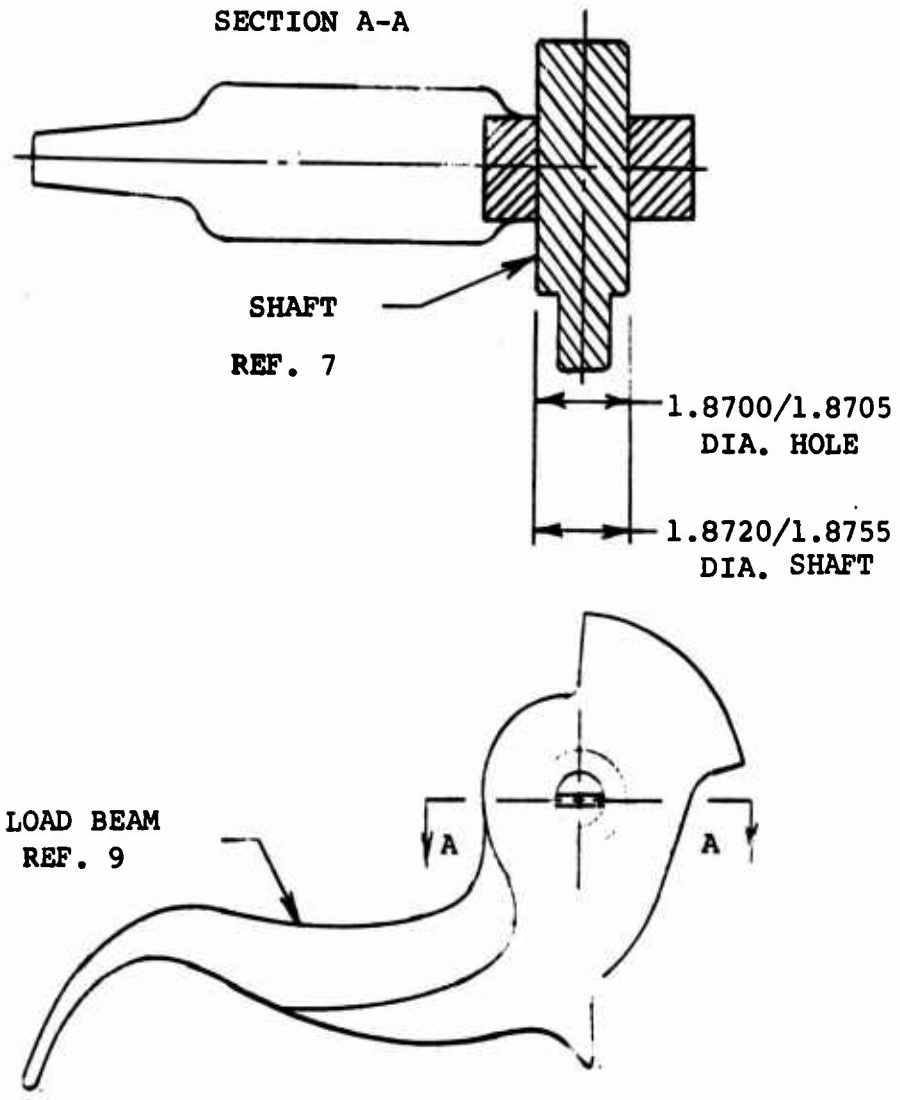

Figure 29. Load Beam Assembly - Second Ultimate Test.

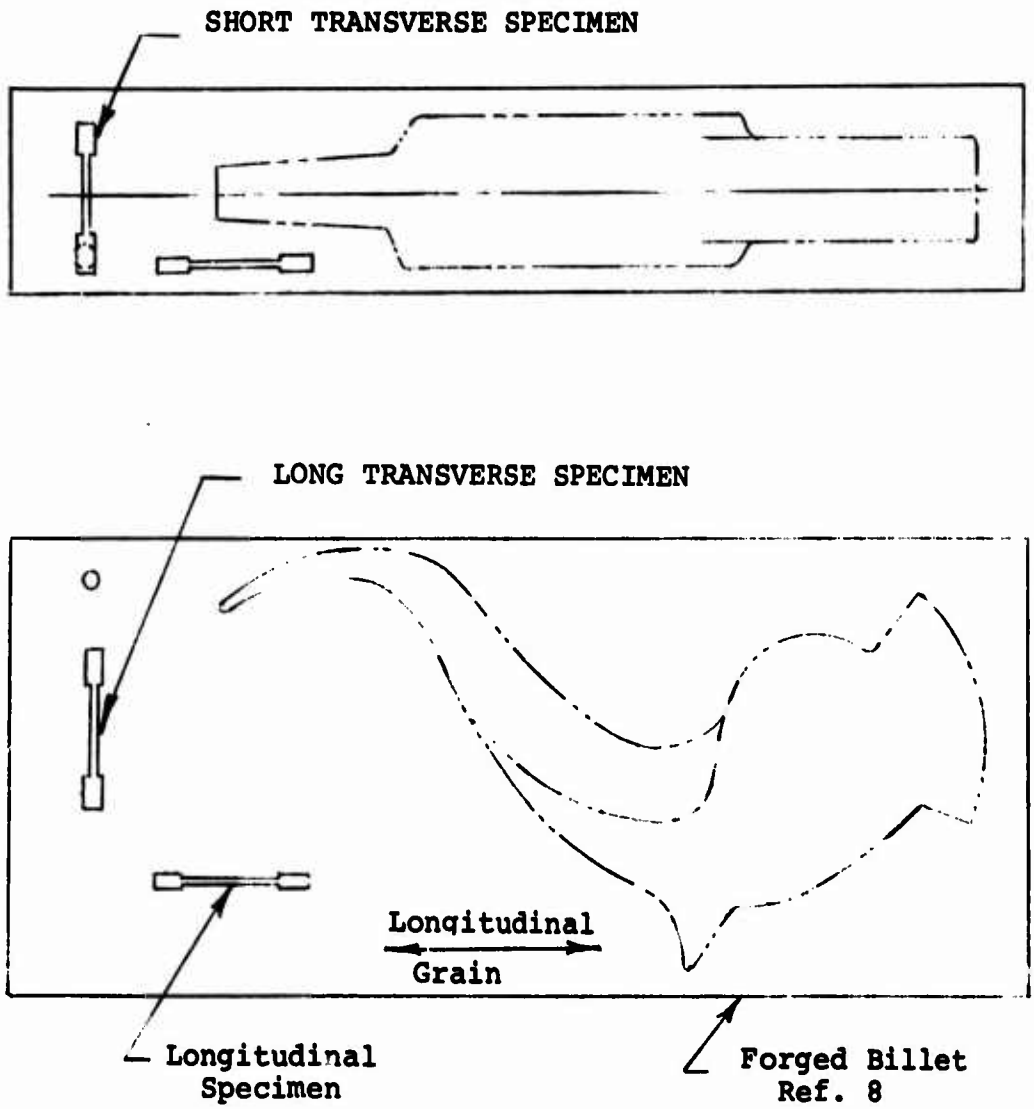

Figure 30. Location of Load Beam and Tensile Specimens in Forged Billet - Second Ultimate Test.

The gages used on the initial ultimate test provided relatively complete coverage of the specimen. Gage requirements on the second were not as elaborate but were intended t supply sufficient information on the redesigned area and correlation with the original test. The gage locations are shown on Figure 32.

Load was applied in the following manner:

1. Establish zero (1,000 lb) for the instrumentation.
2. Gradually apply load to 8,000 lb.
3. Record strains and deflections.
4. Increase load by 8,000-lb increments to 56,000 lb.
5. At each increment of load, record the strains and deflections.
6. Plot deflection curves.
7. Remove 8,000 lb of load.
8. Record strains and deflections.
9. Repeat steps 7 and 8 until the total load is removed.
10. Check deflection curve for permanent set.
11. Gradually apply load in 8,000-lb increments to 56,000 lb.
12. Record strains and deflection at each increment of loading.
13. Plot deflection for each increment of loading.
14. Apply load to 60,000 lb.
15. Repeat steps 12 and 13.
16. Gradually apply load in 10,000-lb increments to 140,000 lb.
17. Repeat steps 12 and 13.
18. Remove load in the reverse order.
19. Record strains and deflection at each increment of loading.

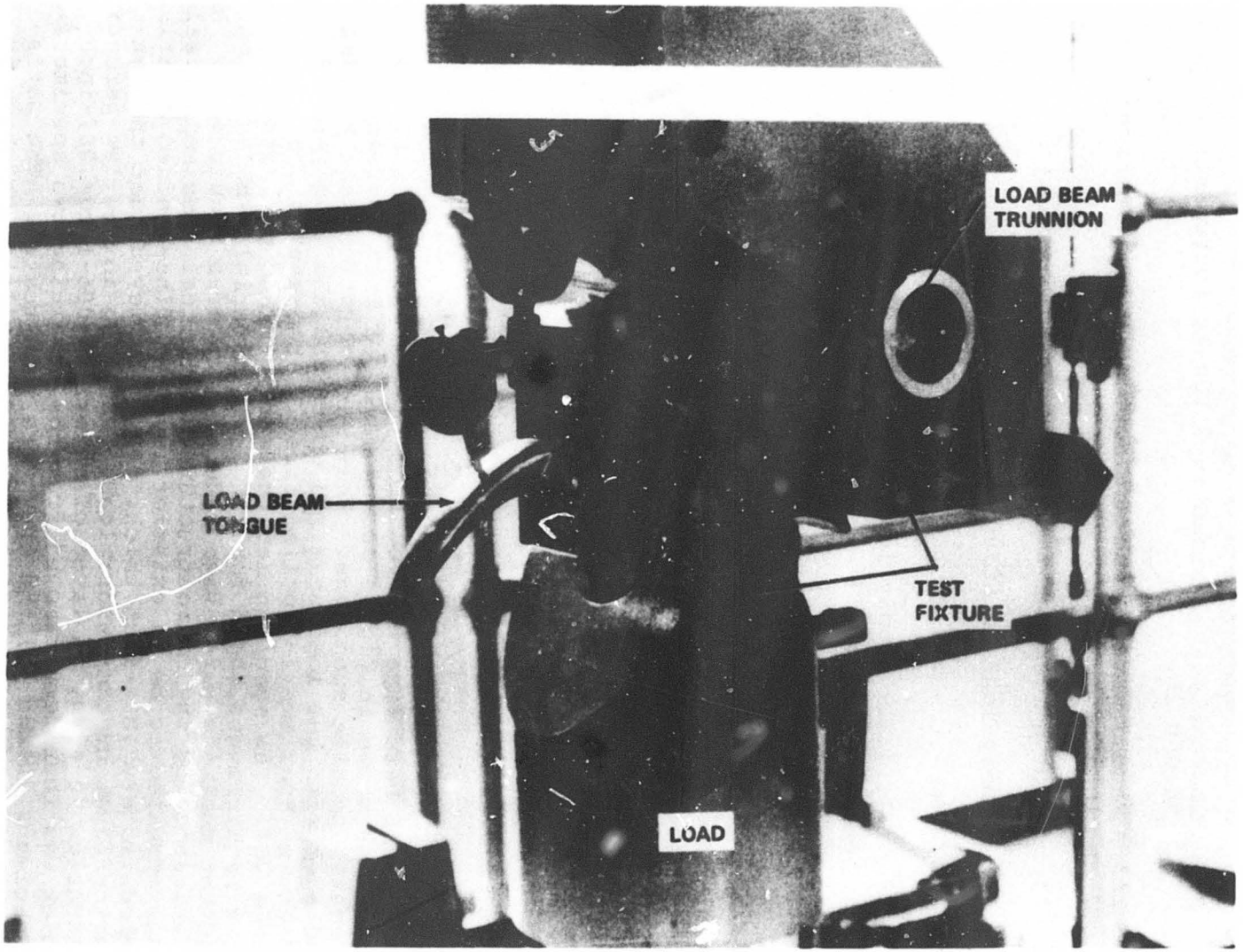

Figure 31. HLH Load Beam Fixture and Specimen.

20. Check deflection curve for permanent set.

21. Gradually apply load in 8,000-lb increments to 56,000 lb.

22. Record strains and deflection at each increment of loading.

23. Plot deflection for increment of loading.

24. Apply load to 60,000 lb.

25. Repeat steps 22 and 23.

26. Gradually apply load in 10,000-lb increments to 140,000 lb.

27. Continue to failure in increments of 10,000 lb.

28. Record failure point.

Testing Facilities and Instrumentation

The test was performed using the same 600,000-pound-capacity testing machine and test rig as utilized in the first test and shown in Figure 31. Readout of the resistance strain gages was again provided by the Magnaflux GA 100 strain indicator.

Test Data Collection, Processing and Analysis

Coupon Testing

Three test bars were removed from the forged billet at the locations shown in Figure 30 and machined into .252-inch-diameter tensile specimens. They were solution heat treated and aged with the load beam and shaft and the long transverse specimen (Specimen #9) pulled first. The results are shown in Table VII. The specimen met the strength and percentage elongation requirements shown for BMS 7-213 material (Table VI) but did not meet the percentage reduction in area requirement. An examination of the microstructure of the test specimen revealed what appeared to be an exterior layer of fine-grained material approximately .006-inch thick. It is believed that this exterior layer cracked under load, resulting in the low percent reduction in area. A layer of material .005-inch/.007-inch thick was therefore removed from the remaining two specimens (Specimens 10 and 11) and they were then tested. The satisfactory results of both strength and ductility are shown in Table VII.

TABLE VII. RESULTS IN TENSILE SPECIMEN TESTING - SECOND ULTIMATE TEST

PHYSICAL PROPERTIES	SPECIMEN #9 L.T.	SPECIMEN #10 L.	SPECIMEN #11 S.T.
U.T.S. (ksi)	229	233	220
Y.T.S. (ksi)	226	231	218
% Elongation	6.0	12.0	5.5
% Reduction in Area	7.3	49.0	2.2

L = Longitudinal
L.T. = Long Transverse
S.T. = Short Transverse

The exterior layer was originally thought to have been case hardening caused by the nitrogen used in the heat treatment process. Studies by both Boeing-Vertol and Cartech Metallurgical Laboratories, however, indicated that no nitrogen was present and that the hardness of the case was the same as the matrix. They believe that the condition may have been the result of cold working of the overage material during the lathe turning operation, followed by solution treatment and aging.

The finish machining operation on the load beam and shaft will remove any layer which may have been found during the rough machining and heat treatment. As a further precaution, the heat treatment cycle was changed to include an argon backfill rather than nitrogen to eliminate the possibility of nitriding the surface of the load beam and shafts.

Beam Testing

In accordance with the test plan, three load excursions were made.

The first,to 56,000 pounds, produced no permanent deformation at any of the gages.

The second, to 140,000 pound limit load, resulted in some permanent deformation being registered at gages 3, 4 and 6 and at the dial gage mounted on the tongue of the beam.

All of the strain gages registered strains well below the permissible .2% offset yield value,however. The beam is therefore capable of sustaining limit load without yielding. A small amount of permanent deformation registered at the dial gage, but the quantity is not considered to be detrimental to the function of the part.

The third run was to failure with a required capacity of 210,000 lb. The load sequence was as stipulated in the test plan, and failure occurred at 243,500 pounds. Data points from all strain gages are shown in Table VIII,and the load-strain curves are shown in Figure 32. The location of the failure is shown in both Figures 33 and 34.

TABLE VIII. STRAIN GAGE AND DIAL GAGE READINGS - LOAD RUN TO FAILURE

APPLIED LOAD (KIPS)	GAGE #31	GAGE #32	GAGE #33	GAGE #34	GAGE #35	GAGE #36	GAGE #37	DIAL GAGE
1 ⚠2	- 6	- 13	+1386	+1326	- 50	+ 406	0	.962
8	+ 190	- 187	+ 168	+ 158	+ 94	+ 459	+ 204	.930
16	+ 376	- 405	+ 450	+ 420	+ 206	+ 979	+ 416	.897
24	+ 606	- 616	+ 780	+ 719	+ 324	+1500	+ 658	.867
32	+ 856	- 827	+1145	+1050	+ 447	+2032	+ 912	.838
40	+1111	-1034	+1522	+1538	+ 573	+2570	+1173	.811
48	+1366	-1238	+1896	+1828	+ 702	+3115	+1423	.784
56	+1613	-1430	+2283	+2219	+ 834	+3638	+1668	.759
60	+1743	-1518	+2476	+2406	+ 910	+3890	+1788	.748
70	+2067	-1750	+2984	+2912	+1094	+4554	+2104	.717
80	+2375	-1978	+3495	+3423	+1273	+5200	+2400	.687
90	+2682	-2197	+4000	+3934	+1444	+5824	+2690	.658
100	+2988	-2425	+4521	+4470	+1623	+6493	+2992	.629

⚠1 Strain gage readings are in microinches/inch. Dial gage reading is in inches.
⚠2 Gages were rebalanced at 1,000 pounds.

TABLE VIII. (CONTINUED)

APPLIED LOAD (KIPS)	GAGE #31	GAGE #32	GAGE #33	GAGE #34	GAGE #35	GAGE #36	GAGE #37	DIAL GAGE
110	+3290	-2646	+5040	+5000	+1798	+7156	+3286	.600
120	+3584	-2864	+5560	+5540	+1970	+7813	+3575	.572
130	+3895	-3097	+6102	+6120	+2151	+8492	+3880	.543
140	+4220	-3324	+6690	+6760	+2330	+9213	+4192	.512
150	+4577	-3568	+7718	+7785	+2495	+10110	+4540	.478
160	+4956	-3849	+9150	+9211	+2633	+11167	+4910	.438
170	+5338	-4160	+10938	+10974	+2752	+12366	+5295	REMOVED DIAL GAGE AT 160K
180	+5696	-4486	+12982	+12956	+2843	+13641	+5670	
190	+6056	-4872	+15770	+15632	+2900	+15016	+6050	
200	+6398	-5335	+19630	+19343	+2890	+16726	+6428	
210	+6696	-5907	+25628	+25288	+2864	+18448	+6770	
215	+6862	-6213	+30583	+30170	+2838	+19490	+6930	
220	+7023	-6795	--	--	+2813	+20654	+7093	
225	+7188	-7436	--	--	+2795	+21886	+7264	

TABLE VIII. (CONTINUED)

APPLIED LOAD (KIPS)	GAGE #31	GAGE #32	GAGE #33	GAGE #34	GAGE #35	GAGE #36	GAGE #37	DIAL GAGE
230	+7365	-8366	Strain exceeding range of gages #3 & #4.		+2800	+23210	+7452	REMOVED
235	+7582	-9860			+2931	+24900	+7682	DIAL
240	+7854	-13200			+3652	+26810	+7990	GAGE
243	--	F A I L U R E			--	31260	--	AT 160K

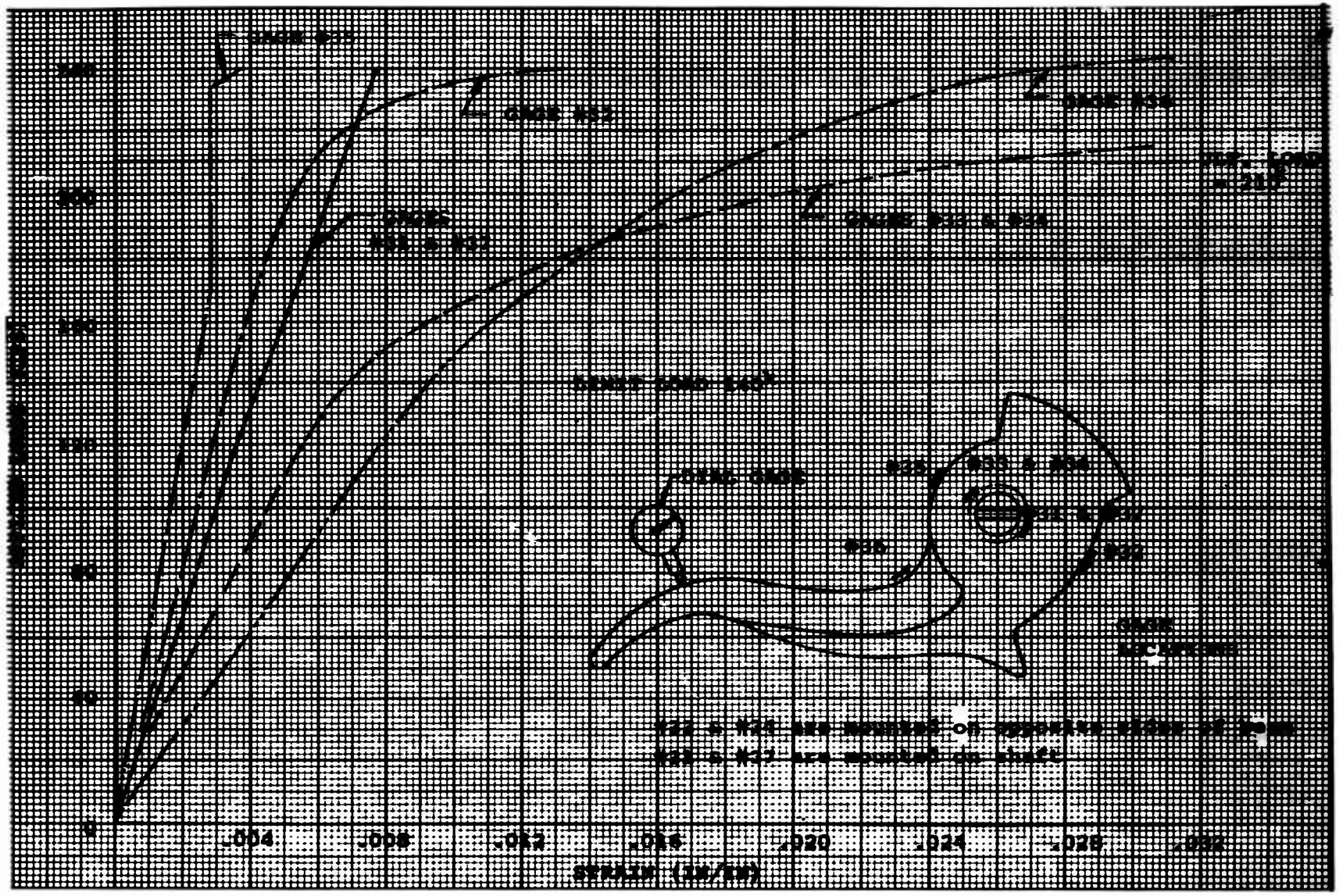

Figure 32. Load Versus Strain - Second Ultimate Test.

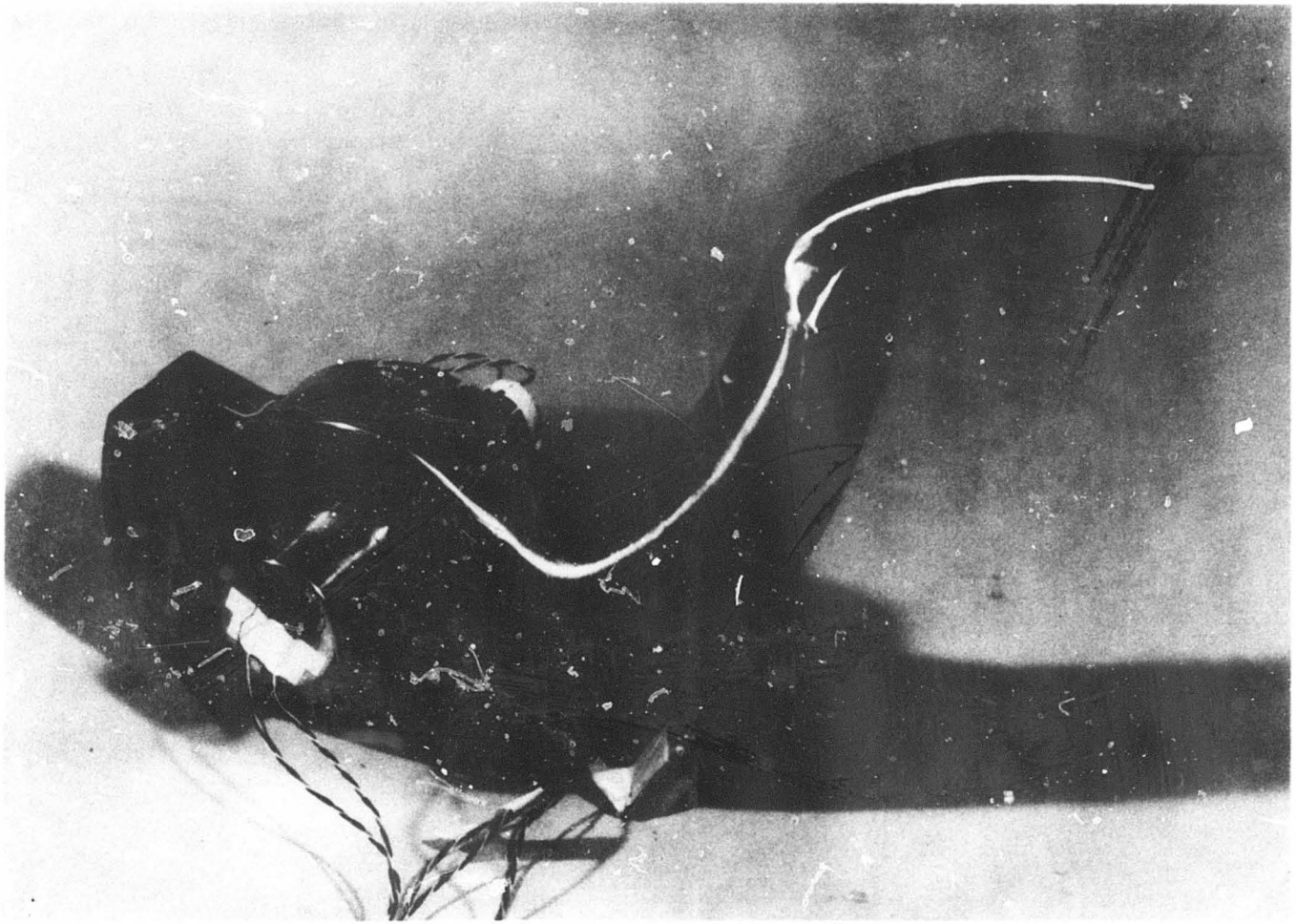

Figure 33. Load Beam Fracture - Second Ultimate Test.

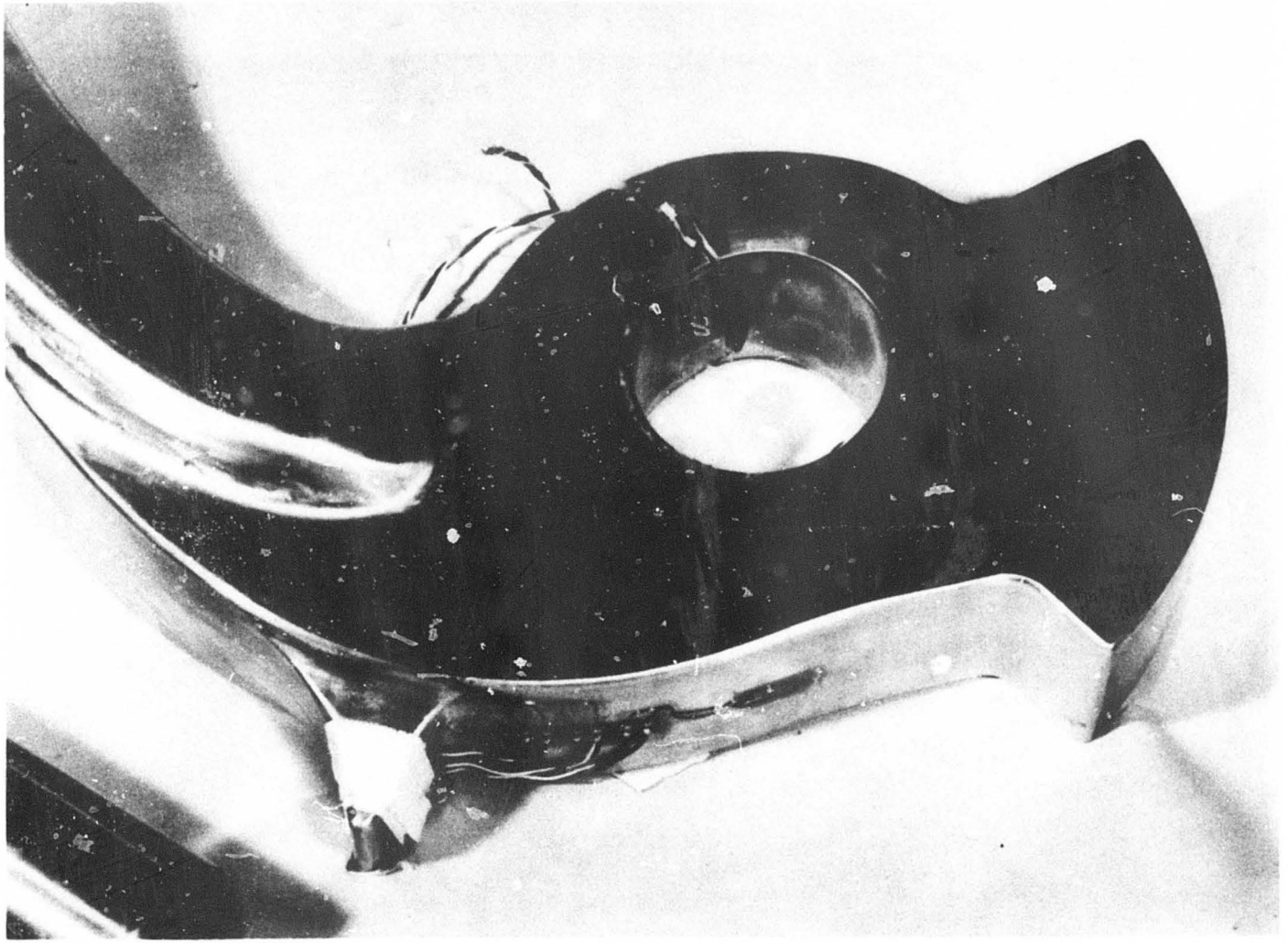

Figure 34. Load Beam Fracture - Second Ultimate Test.

TASK CONCLUSIONS AND RECOMMENDATIONS

Conclusions

The load beam specimen has sustained the limit load without yielding and the ultimate load without rupture. The material and design are therefore structurally acceptable.

Recommendations

One improvement which has been suggested by the results of the test is the installation of a mechanical pin which will prevent the rotation of the shaft with respect to the beam. The shaft is now pressed into the beam with a .001/.002 interference fit. Comparatively large strain gage readings in the vicinity of the shaft under high loads indicate the possibility of relative rotation between the two parts. Although this would cause no structural damage, it would interfere with the function of the part. The change will be made on Revision B of Reference 9, by locating the pin in an area of the beam where the stress levels are at a minimum.

LITERATURE CITED

1. ENVELOPE, Drawing No. 301-10231, The Boeing Company, Vertol Division, Philadelphia, Pennsylvania.

2. HLH ATC LOAD BEAM COUPLING MODEL, Engineering Test Lab Report SL-0512, The Boeing Company, Vertol Division, Philadelphia, Pennsylvania.

3. LOAD BEAM - HLH COUPLING, Drawing No. 17102, Eastern Rotorcraft Corporation, Doylestown, Pennsylvania.

4. TEST SPECIMENS - LOCATION IN FORGED BILLET, HLH LOAD BEAM, Drawing No. 17103, Eastern Rotorcraft Corporation, Doylestown, Pennsylvania.

5. Peterson, R. E., STRESS CONCENTRATION DESIGN FACTORS, John Wiley and Sons, New York, New York, 1953.

6. TEST REPORT OF THE LOAD BEAM ULTIMATE TEST, Report No. T425, Eastern Rotorcraft Corporation, Doylestown, Pennsylvania.

7. SHAFT - HLH LOAD BEAM, Drawing No. 13405, Eastern Rotorcraft Corporation, Doylestown, Pennsylvania.

8. FORGED BILLET - HLH LOAD BEAM, Drawing No. 14273, Eastern Rotorcraft Corporation, Doylestown, Pennsylvania.

9. LOAD BEAM ASSEMBLY - HLH COUPLING, Drawing No. 17122, Eastern Rotorcraft Corporation, Doylestown, Pennsylvania.